2008

Regional Infiltration of Meteoric Water into the Mira Terrane: a Stable Isotope Study of the Avalonian Huntington Mountain Pluton and Related Rocks, Cape Breton Island, Canada

Duane C. Petts
Western University

Regional Infiltration of Meteoric Water into the Mira Terrane: a Stable Isotope Study of the Avalonian Huntington Mountain Pluton and Related Rocks, Cape Breton Island, Canada

(Spine title: Infiltration of Meteoric Water into the Mira Terrane)

(Thesis format: Monograph)

by

Duane C. Petts

Graduate Program in Geology

Thesis submitted in partial
fulfillment of the requirements for the
degree of Master of Science

The School of Graduate and Postdoctoral Studies
The University of Western Ontario
London, Ontario, Canada

THE UNIVERSITY OF WESTERN ONTARIO
The School of Graduate and Postdoctoral Studies

CERTIFICATE OF EXAMINATION

Supervisor	Examiners
Dr. Fred Longstaffe	Dr. Roberta Flemming
Supervisory Committee	Dr. Sandra Barr
Dr. Joanne Potter	Dr. Wayne Nesbitt
Dr. Roberta Flemming	

The thesis by

Duane Christopher Petts

entitled:

Regional Infiltration of Meteoric Water into the Mira Terrane: a Stable Isotope Study of the Avalonian Huntington Mountain Pluton and Related Rocks, Cape Breton Island, Canada

is accepted in partial fulfillment of the
requirements for the degree of
Master of Science

Date_____

_____
Chair of the Thesis Examination Board

Abstract

The Avalonian Mira terrane of Cape Breton Island, Nova Scotia, Canada is composed mainly of late Proterozoic volcanic-plutonic-sedimentary rocks that formed in an evolved magmatic arc along the margin of Gondwana. The purpose of this study is to determine the source(s) and timing of the ^{18}O-depletion that has affected the 620 Ma Huntington Mountain pluton and East Bay Hills volcanic suite of the Mira terrane.

Plutonic and volcanic rock samples have oxygen-, hydrogen- and carbon-isotope values of –6.3 to +14.3‰, –93 to –56‰, and –7.4 to +0.1‰, respectively. These values likely signal the interaction of meteoric-dominated hydrothermal fluids with the Huntington Mountain pluton and East Bay Hills volcanic suite. The occurrence of widespread, pervasive propylitic alteration and the absence of a localized pattern of oxygen-isotope anomalies suggest that the ^{18}O-depletion arose during initial rifting of the Mira terrane from Gondwana, ca. 575-560 Ma.

Keywords: Avalon Zone, Carbon-isotope, Hydrogen-isotope, Hydrothermal, Meteoric Water, Mira Terrane, Northern Appalachian Orogen, Oxygen-isotope, Plutonic, Volcanic.

Acknowledgments

I would like to first thank my supervisor Fred Longstaffe for the opportunity to investigate this magnificent project. Fred is also thanked for his wonderful guidance and patience throughout the project. My advisor, Joanne Potter, is thanked for her guidance and mentoring, and for her assistance during sample collection and in the application of stable isotope analytical techniques. Fred and Joanne are both thanked for their very insightful discussions over the past three years.

I am grateful to Kim Law and Li Huang for their assistance in the application of stable isotope analytical techniques. Desmond Moser and Alexandre Aubin are also thanked for their assistance during the application of mineral separation techniques.

Sam Russell is thanked for his assistance during sample collection and for unknowingly mentoring me throughout this project. Sandra Barr and Chris White contributed greatly by assisting during sample collection and by helping to understand the geology in Cape Breton Island.

I appreciate the support of family and friends, including Jeff Petts and Tom Yee. I would also like to recognize the support received from fellow graduate students in the Department of Earth Sciences and members of the Laboratory for Stable Isotope Science. Norm Duke is thanked for his stimulating discussions regarding hydrothermal ore deposits. Finally, I would like to acknowledge the funding received by NSERC and the University of Western Ontario.

TABLE OF CONTENTS

LIST OF TABLES

LIST OF FIGURES

LIST OF APPENDICES

Chapter 1. Introduction

1.1 Outline of the Problem

The Avalon zone, which forms a fragmented belt along the eastern margin of the northern Appalachian orogen (Fig. 1.1), provides a record of the complex tectonic history of an evolving late Proterozoic magmatic arc that formed proximal to Gondwana (Murphy et al., 1990; O'Brien et al., 1996; Barr et al., 1998). Similar to the other terranes in the Avalon zone, the Mira terrane of southeastern Cape Breton Island is composed mainly of late Proterozoic volcanic-plutonic-sedimentary belts that are overlain by younger sedimentary cover sequences (Fig. 1.2). The tectonic history of the Mira terrane, especially in relation to the Bras d'Or and Aspy terranes of Cape Breton Island, is not clearly understood and has been the subject of debate for many years (e.g., Barr and Raeside, 1989; Murphy et al., 1990; Barr et al., 1998). Recently, oxygen-isotope studies of the northern Appalachian orogen have provided a means to resolve this ambiguity by showing the Mira terrane to be isotopically distinct from other non-Avalonian terranes in Cape Breton Island (Potter et al., 2008).

The previous oxygen-isotope studies of the Mira terrane have identified a large number of felsic volcanic and plutonic rocks with low $\delta^{18}O$ values (<+6‰), which were likely acquired though water-rock interaction with meteoric-dominated hydrothermal fluids (Ayuso et al., 1996; Potter et al., 2008). Because of the regional extent of volcanic and plutonic rocks with low $\delta^{18}O$ values, Potter et al. (2008) concluded that all Avalonian terranes underwent post-magmatic oxygen-isotope exchange with meteoric-dominated hydrothermal fluids, which infiltrated the crust during regional transtensional faulting associated with initial rifting of Avalonia from Gondwana, ca. 575-550 Ma.

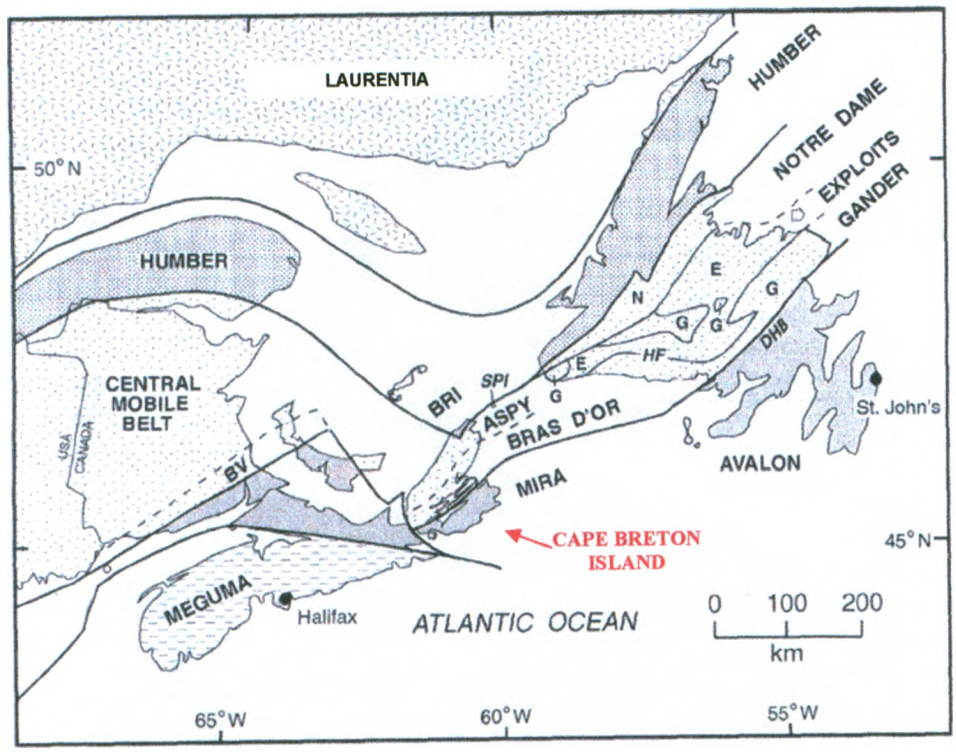

Figure 1.1. Terrane divisions of the northern Appalachian orogen. Abbreviations include, BRI - Blair River Inlier, BV - Brookville terrane, DHB - Dover – Hemitage Bay faults, E - Exploits, G - Gander, HF - Hermitage Flexture area, N - Notre Dame, SBI - St. Paul Island. Modified from Barr et al. (1998).

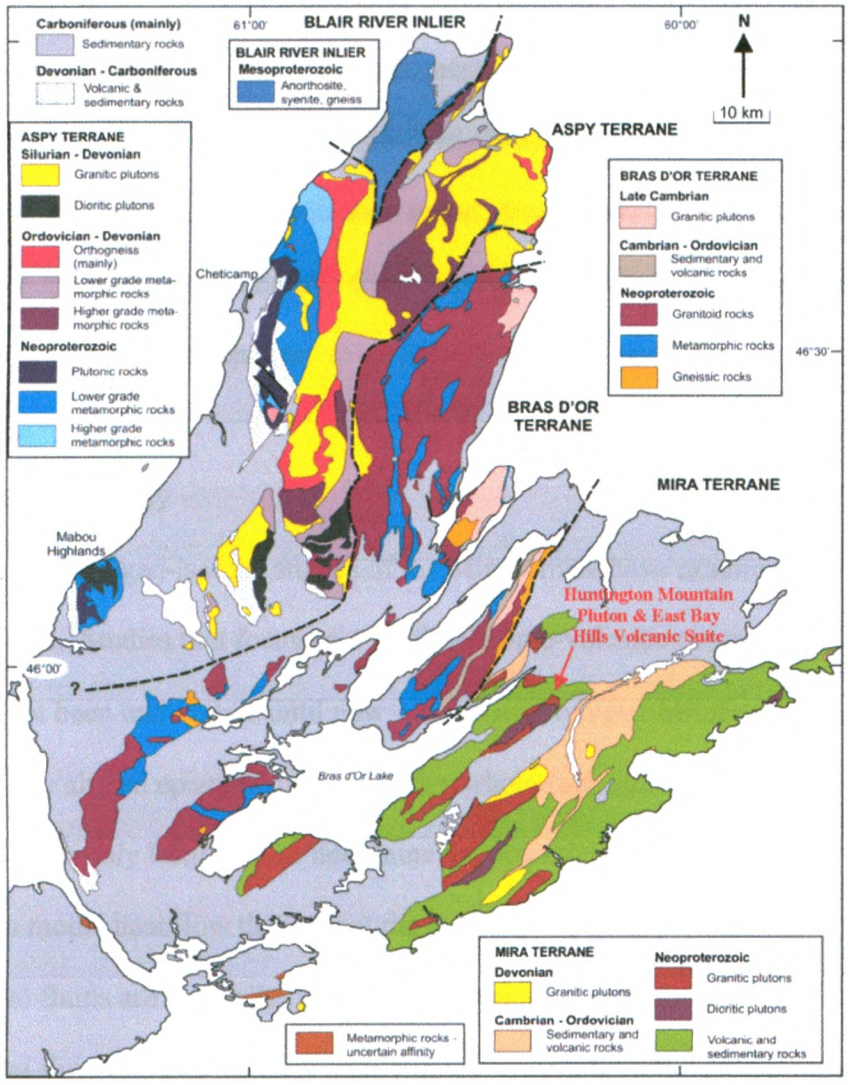

Figure 1.2. Geological map of Cape Breton Island. The terrane divisions of Barr et al. (1998) include the Blair River Inlier, the Apsy terrane, the Bras d'Or terrane and the Mira terrane. This study is centered on the Huntington Mountain pluton and East Bay Hills volcanic suite. Modified from Potter et al. (2008).

A number of locations in the Mira terrane and elsewhere on Cape Breton Island are currently being examined by industry as potential economic resources of Au, Cu, Pb and Zn. Typically, large base- and precious-metal deposits are associated with the movement of meteoric-dominated hydrothermal fluids, and have been invoked in models to explain the occurrence of mineralization in the Mira terrane (e.g., Kontak et al., 2003). An understanding of the hydrothermal fluid activity is important in any explanation of the formation of these mineral deposits.

1.2 Purpose of the Study

Previous oxygen-isotope studies of the Mira terrane have examined these rocks on a regional scale. Studies that focus on a single plutonic-volcanic complex in greater detail have not been undertaken until now. In classical oxygen-isotope studies of hydrothermally altered epizonal plutonic rocks, whole-rock and mineral oxygen-isotope ratios have commonly been used to determine the potential source(s) of the hydrothermal fluids and to model heat flow throughout the system. Typically, it was shown that hydrothermal fluids are generally dominated by meteoric-water and that these hydrothermal fluid movements were responsible for causing chemical and mineralogical changes within a rock, which include the formation of alteration minerals and ^{18}O-depletion of igneous rocks (e.g., Sheppard et al., 1971; Taylor, 1971, 1974; Criss and Taylor, 1986).

This study reports on the oxygen- and hydrogen-isotope isotope ratios of mafic and felsic rocks from the 620 Ma Huntington Mountain pluton and associated East Bay Hills volcanic suite from the Mira terrane, Cape Breton Island, Nova Scotia, Canada (Fig.

1.2), with the purpose of determining the source(s) and timing of hydrothermal fluid movement that has affected these and other late Proterozoic volcanic and plutonic rocks of the Mira terrane. The source(s) of such hydrothermal fluids, and the timing of their movement, are important to understanding the tectonic history of the Mira terrane.

1.3 Location, Physiography and Access

The East Bay Hills volcanic suite and Huntington Mountain pluton form a 7 km x 27 km belt located along the south shoreline of Bras d'Or Lake in southeastern Cape Breton Island, Nova Scotia (Fig. 1.3). Southeastern Cape Breton Island is defined by high-relief belts, formed by resistant felsic volcanic and plutonic rocks, separated by bog-rich lowlands, underlain mainly by sedimentary and volcanic rocks. The area is extensively covered by glacial till, with a trend of greater till accumulation towards the Atlantic Ocean shoreline. Access is mainly achieved via logging roads and all-terrain vehicle trails. Additionally, an electrical power-line that traverses the length of the pluton provides access to a large portion of the Huntington Mountain area. In most areas of southeastern Cape Breton Island, rock exposure is limited generally to road-cuts, areas of high elevation, stream and river banks and beds, and coastlines. Because of the large amount of logging in the area, rock exposure can also be found within cleared areas and along logging roads. Generally, access and exposure in the chosen study area is better than in most areas of southeastern Cape Breton Island.

1.4 The Geology of Southeastern Cape Breton Island

Williams (1979) subdivided the northern Appalachian orogen into five distinct zones, the Humber, Dunnage, Gander, Avalon and Meguma zones, on the basis of their structural and stratigraphic contrasts, as well as paleotectonic interpretations. In this definition of the Appalachian orogen, all of Cape Breton Island was defined as part of the Avalon zone, on the basis that it was composed mainly of late Precambrian volcanic and sedimentary rocks, of the same age, with similar lithological analogues found in the Avalon zone of Newfoundland (Fig. 1.1). However, subsequent mapping and petrological studies showed the rocks of southeastern Cape Breton Island to be distinct from the rocks of northern Cape Breton Island, and led to reclassification of the island's zones (Fig. 1.2). In this definition of Cape Breton Island, the Avalon zone, which was termed the Mira terrane, encompasses the area of southeastern Cape Breton Island, whereas the rest of Cape Breton Island was divided into the Bras d'Or terrane, the Aspy terrane and the Blair River Inlier. Some of the criteria that led to this rezoning include the following: tectonostratigraphic and geochemical variations between each zone (Barr and Raeside, 1986, 1989; Barr, 1993, Barr et al., 1998), reliable dates for volcanic and plutonic rocks from each zone (Barr et al., 1990; Bevier et al., 1993), differing magmatic and metamorphic thermal histories (Barr and Raeside, 1989; Barr et al., 1990; Raeside and Barr, 1990; Ayuso et al., 1996), contrasting Pb and Nd-Sm isotopic ratios from each zone (Barr and Hegner, 1992; Ayuso et al., 1996; Barr et al., 1998) and recently, reports of the widespread occurrence of low-^{18}O igneous rocks in southeastern Cape Breton Island and other Avalonian terranes, which are generally absent from other areas of Cape Breton Island (Ayuso et al., 1996; Potter et al., 2008).

1.4.1 The Mira Terrane

The Mira terrane of southeastern Cape Breton Island is composed mainly of volcanic and plutonic rocks that form linear northeast-southwest trending belts separated by regional-scale faults and younger sedimentary cover sequences (Fig. 1.3). In the original work of Weeks (1954), the majority of the volcanic-sedimentary rocks of southeastern Cape Breton Island were assigned to the Fourchu Group, a characterization based largely on radiometric dating using isotopic systems that had been disturbed by subsequent geological events (e.g., Cormier, 1972). Further mapping (e.g., Barr et al., 1996) and U-Pb age dating (Barr et al., 1990; Bevier et al., 1993) of volcanic and plutonic rocks revealed that the Fourchu Group only represents the 575-560 Ma volcanic-dominated rocks of the Coastal Belt, which also includes the dominantly epiclastic sedimentary rocks of the Main-á-Dieu group. The remaining volcanic rocks, originally assigned to the Fourchu Group, were found to be associated with the 620 Ma plutonic rocks mainly located along the southeastern coast of Bras d'Or lake. The volcanic rocks of the Stirling Group were originally inferred to be of Cambrian age, based on their pristine appearance and association with interbedded sedimentary rocks. However, a rhyolitic porphyry unit of the Stirling Group was later dated at 680 Ma, and is interpreted to be the representative age of the entire Stirling Group (Bevier et al., 1993). The majority of the rocks in the Mira terrane can be subdivided into four magmatic units: the 680 Ma Stirling Group, the 620 Ma volcanic-plutonic groups, which include the East Bay Hills volcanic suite and Huntington Mountain pluton, the 575-560 Ma Coastal Belt, and the ~380 Ma Devonian plutons.

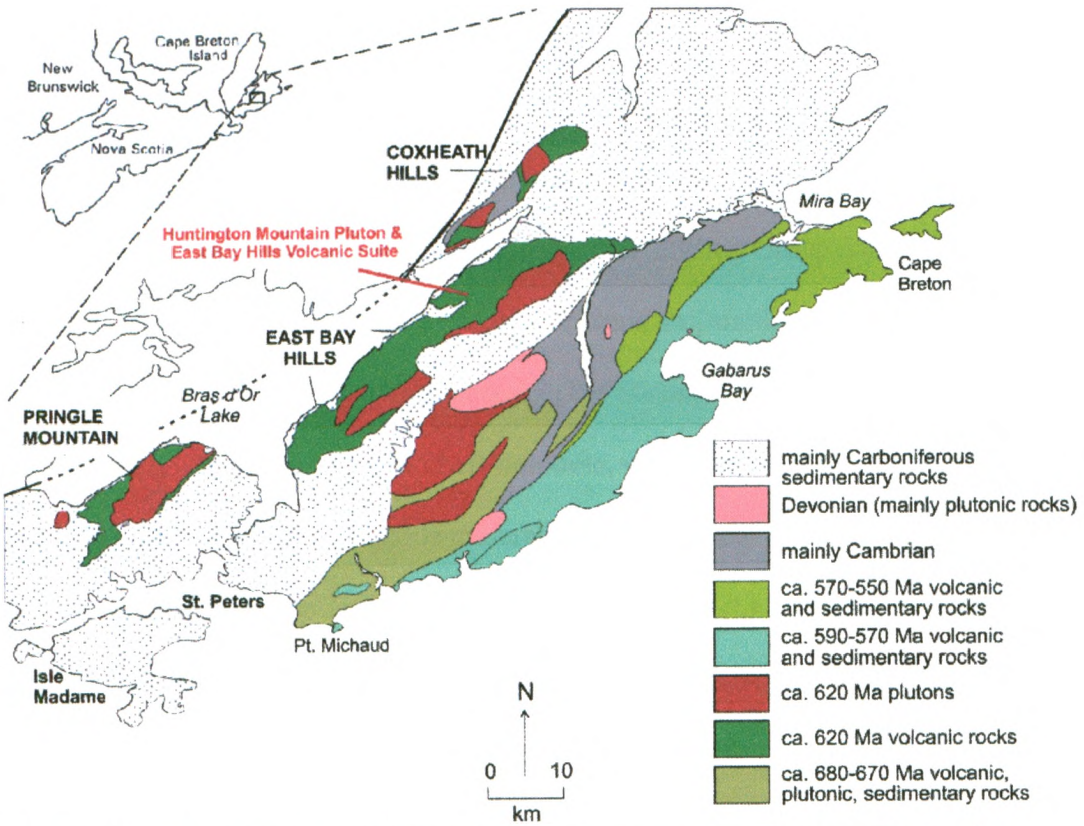

Figure 1.3. Geological map of the Mira terrane, Cape Breton Island. The reader should refer to the appropriate text for a description of the rock units and localities of interest to this study. Modified from Barr et al. (1996).

The 680 Ma Stirling Group

The oldest unit of the Mira terrane, the Stirling Group, consists of 680 Ma volcanic-sedimentary sequences that are primarily composed of andesitic to basaltic lapilli tuff with interbeds of tuffaceous arenite and laminated siltstone. Because of the abundance of volcaniclastic and clastic sedimentary rocks, and the apparent absence of structural breaks between these units, the rocks of the Stirling Group are interpreted to have formed in an extensional basin within a volcanic arc, similar to modern-day Japan (Barr, 1993; Barr et al., 1996). Also present in the Stirling Group are zones of pyrite-rich, laminated litharenite-siltstone-chert-dolomite, which are interpreted to represent exhalative volcanic massive sulphide mineralization, and were an important host for the now abandoned Mindamar Zn-Pb-Cu-Ag-Au deposit (Barr et al., 1996). Similar ca. 680 Ma rocks occur east of the Hermitage Bay fault in the Avalon terrane of Newfoundland. They consist mainly of felsic volcanic flows and volcaniclastic rocks and carbonate sedimentary rocks, which are interpreted to have been formed in an extensional volcanic arc setting (O'Brien et al., 1996). Other analogues to the Stirling Group have not been reported elsewhere in the northern Appalachian orogen.

The 620 Ma Volcanic-Plutonic Groups

The 620 Ma Coxheath Hills, East Bay Hills (which includes the study area for this project), Pringle Mountain and Chisholm Brook plutonic suite form volcanic-plutonic-sedimentary belts that are composed mostly of granitic-granodioritic rocks and andesitic-rhyolitic tuffs and flows. These rocks are high-K, calc-alkaline in composition, and are interpreted to have formed in a subduction-related convergent margin setting (Barr, 1993;

Barr et al., 1996). The U-Pb and $^{40}Ar/^{39}Ar$ results available for volcanic and plutonic rocks from each group all yield dates of 620 Ma (within error) (Barr et al., 1990; Keppie et al., 1990; Bevier et al., 1993), which suggests that these rocks formed on top of one continuous subduction zone (Barr et al., 1996). Similar ca. 620-600 Ma calc-alkaline volcanic and plutonic rocks exist in other Avalonian terranes and are also interpreted to represent subduction-related arc settings. Examples of these include the Connaigre Bay Group and the Simmons Brook intrusive suite of the Avalon terrane in southeastern Newfoundland (O'Brien et al., 1996), the Debert River pluton of the Cobequid Highlands and the Georgeville Group of the Antigonish Highlands in northern mainland Nova Scotia (Murphy et al., 1990; Pe-Piper et al., 1996), the Broad River Group of Caledonian Highlands in southern New Brunswick (Barr and White, 1988, 1996) and southeastern New England (Hermes and Zartman, 1992). Mineralization within these rocks consists of sporadic Cu-Ag-Au anomalies in the Pringle Mountain Group and vein-hosted Cu-Mo-Au in the Coxheath Hills Group. Previous studies of the Coxheath Hills Group have shown that the nature of ore mineralization and alteration assemblage has similarities to large porphyry-epithermal deposits, which has led to classifying the deposit as a large tonnage, low-grade porphyry deposit (Lynch and Ortega, 1997). The discovery of extensive pyrophyllite alteration in the volcanic rocks of Coxheath Hills has led to reclassification of the deposit as a high-level, linked porphyry-epithermal system (Kontak et al., 2003).

The 574-560 Ma Coastal Belt

The volcanic-sedimentary sequences of the 575-560 Ma Coastal Belt are subdivided into the Fourchu Group and the Main-á-Dieu Group, a subdivision which is largely based on contrasts in rock type (Barr et al., 1996). The Fourchu Group consists mainly of dacitic tuffs and flows, with minor basaltic-rhyolitic tuffs and flows and tuffaceous sedimentary rocks, and is interpreted to represent a volcanic-arc setting. The Main-á-Dieu Group consists mainly of tuffaceous sedimentary and epiclastic rocks, with minor basaltic and rhyolitic flows, and is interpreted to have formed in an intra-arc extensional setting (Barr, 1993; Barr et al., 1996). Because of the strong stratigraphic association of these two groups, the Fourchu Group and the Main-á-Dieu Group are inferred to represent facies equivalents in the same tectonic environment (Barr et al., 1998). Similar volcanic and sedimentary rocks are exposed in the 560-550 Ma Coldbrook Group of the Caledonia terrane, New Brunswick, and the 580-570 Ma Belle Rivière group of the Avalon terrane, Newfoundland, and are similar to the Coastal Belt in representing a volcanic arc evolving into an extensional tectonic setting (Barr et al., 1996). No analogues to the Coastal Belt have been recognized in the Cobequid and Antigonish highlands of northern mainland Nova Scotia or in the Boston terrane of southeastern New England.

The Devonian Plutons

The Devonian plutons, which are primarily composed of granite to granodiorite, include the 384 Ma Deep Cove pluton and the 378 Ma Lower St. Esprit pluton in the Coastal Belt, the 380 Ma Salmon River Porphyry in the Stirling belt and the 384 Ma

Gillis Mountain pluton that intrudes Cambrian sedimentary rocks (Barr et al., 1996). These Devonian plutons have been shown to have affinities to those of typical I-type granites in previous petrochemical studies (Barr and Macdonald, 1992). However, based on tectonic models for the northern Appalachian orogen, which indicate that the region was in the final stages of terrane amalgamation and given the absence of other evidence for Devonian subduction in the Mira terrane, the Devonian plutons are interpreted to have formed in an anorogenic, within-plate setting (Barr and Macdonald, 1992).

Sedimentary Cover Sequences

An important stratigraphic unit in the Mira terrane is the late Neoproterozoic-Cambrian clastic sedimentary rocks, which were deposited in a stable platform shelf environment. These rocks contain distinctive Acado-Baltic fauna that are unique to the Avalon terrane, which also link the Avalon to Gondwana geographically (e.g., Landing, 1991; Barr et al., 1996). A section of red clastic sedimentary rocks, the Bengal Road formation, which overlies the Main-á-Dieu Group, has been correlated to similar units exposed in other Avalonian cover sequences (Landing, 1996; Barr et al., 1998). Unconformably overlying, or in faulted contact with these units are the Devonian-Carboniferous sedimentary rocks of the Horton, Windsor, Canso, Riversdale and Morien groups, which form widespread cover sequences throughout most of the northern Appalachian orogen.

Chapter 2. Methods

2.1 Sample Collection and Preparation of the Samples

A total of 65 rock samples were collected from the Huntington Mountain pluton and East Bay Hills volcanic suite for petrographic description and oxygen- and hydrogen-isotope analysis. All of the rocks in the study area are characterized by some degree of alteration. However, an effort was made to collect a representative range of slightly to moderately altered volcanic and plutonic rocks, on the basis of turbid feldspar, veining and the identification in hand sample of possible alteration minerals (e.g., chlorite, epidote, quartz, calcite, pyrite and ilmenite). A secondary focus of sample collection was to obtain a large spatial density of samples in order to test for localized patterns in the distribution of $\delta^{18}O$ values, and low-^{18}O anomalies, in particular, in the Huntington Mountain pluton and East Bay Hills volcanic suite.

Preparation for oxygen- and hydrogen-isotope analysis began by using a standard jaw crusher with a ~1 cm plate spacing to obtain chip- to coarse-sand sized pieces of the rock samples. A small fraction of these pieces were set aside for mineral separation, while the remainder was powdered using a milled steel pulverizer. The pieces set aside for mineral separation were sieved and the 0.105 to 0.063 mm grain fraction was collected. However, depending on the average grain size of the minerals in the samples and the amount of material collected on the optimal sieve fractions, additional crushing was performed by utilizing a hand mortar and pestle.

Highly magnetic materials, such as magnetite and iron filings from the crushing procedure, were isolated using a hand-magnet. Initial separation of ferrimagnetic minerals (e.g., ilmenite and hematite) and any remaining magnetite was performed using

a Frantz isodynamic magnetic separator with a 15° side tilt and a 25° forward slope, and an amperage setting of 0.2A, while paramagnetic minerals (e.g., amphibole, chlorite and biotite) were separated from diamagnetic minerals (e.g., quartz, feldspar and sericite) using an amperage setting of 0.8A. A final magnetic separation of the paramagnetic mineral fraction was performed at 0.4A using the paramagnetic mineral fraction to separate chlorite and biotite (more magnetic fraction) from amphibole (less magnetic fraction). Amphibole was purified further by using an amperage setting of 0.6A, in order to remove epidotized and sericitized feldspar. In some instances (e.g., dioritic rocks) pure chlorite was difficult to obtain, requiring additional magnetic separation with incremental increases in amperage, e.g., 0.25 to 0.5A increments within the range of 0.3 to 0.55A.

In order to isolate the diamagnetic mineral fraction and purify the paramagnetic minerals, specific gravity separation techniques were then applied using the heavy liquid sodium polytungstate (SPT), which has an optimal specific gravity of up to 2.95 and can be diluted to the desired specific gravity by addition of distilled water. The samples were added to SPT of an appropriate specific gravity in a 50 ml Nalgene tube and left overnight for separation. Upon complete separation, the lower half of the Nalgene bottle was immersed into liquid nitrogen, which froze the heavier mineral fraction and facilitated decanting of the light mineral fraction into a funnel lined with filter paper. The heavy mineral fraction was then warmed and also decanted into a funnel lined with filter paper. Both mineral fractions were then rinsed with distilled water and dried overnight. Typically, a specific gravity of 2.8 was chosen to separate amphibole, sericitized feldspar and minor amounts of epidote (SG ~2.80 - 3.40) from chlorite and biotite (SG ~2.60 -

2.80). Plagioclase from dioritic plutonic rocks and most volcanic rocks (SG 2.62 - 2.75) were separated from sericitized and epidotized feldspar using a specific gravity of 2.76. For granitic rocks, Na- and K-feldspar (SG 2.58 - 2.65) was isolated from quartz and sericitized feldspar using a specific gravity of 2.64, while pure quartz was generally isolated from Na- and K-feldspar using a specific gravity of 2.66, which is slightly unusual for quartz as it typically has a specific gravity of 2.65.

The purity of mineral separates was determined using X-ray diffraction. These analyses were performed on randomly oriented samples using a Rigaku rotating anode diffractometer with CoKα radiation and set at 160 kV and 45 mA. If necessary, mineral separation procedures were repeated until a >90% purity was achieved for most samples and >95% purity for quartz samples.

2.2 Stable Isotope Analysis

The oxygen-, hydrogen- and carbon-isotope values for whole-rock and mineral samples are reported in the δ-notation relative to VSMOW (Vienna Standard Mean Ocean Water) for oxygen and hydrogen and VPDB (Vienna Pee Dee Belemnite) for carbon. The δ-notation is defined by McKinney et al. (1950) as:

Eq. 2.1

$$\delta = \left(\frac{R_x - R_{std}}{R_{std}}\right) \times 1000$$

where R represents the ratio of the heavy isotope over the light isotope of various elements (e.g., $^{18}O/^{16}O$, D/H, and $^{13}C/^{12}C$), for a sample x and a standard *std*, reported in the standard 'per mill' notation (‰).

2.2.1 Oxygen-isotope Analysis

The techniques used for extracting oxygen from whole-rock and mineral samples follow the conventional method of Clayton and Mayeda (1963), as modified by Borthwick and Harmon (1982) for use with ClF_3. Samples were weighed out (between 8-10 mg) and placed under vacuum overnight at 150°C in order to remove absorbed water. The samples were then dried under vacuum for 2 hours at 300°C. Oxygen was liberated from the silicate mineral structure by reacting the dried samples with ClF_3 at 550°C in sealed Ni reaction vessels overnight. The released oxygen gas was then quantitatively converted to CO_2 over a red-hot carbon rod and yields were measured to evaluate whether the conversion had gone to completion. Oxygen isotopic ratios were then measured using a dual-inlet DeltaPlus XL mass spectrometer. The $\delta^{18}O$ values of ORX (internal laboratory standard quartz), NBS-30 (biotite) and NBS-28 (quartz) were +11.4 ± 0.2‰, +5.1 ± 0.1‰ and +9.7 ± 0.3‰, respectively, which compares well with their accepted $\delta^{18}O$ values of +11.5‰, +5.1‰ and +9.6‰. Reproducibility of the $\delta^{18}O$ values for standards and samples was generally better than ±0.2‰.

2.2.2 Hydrogen-isotope Analysis

Hydrogen was extracted from whole-rock and mineral samples following the methods of Bigeleisen et al. (1952), as modified by Vennemann and O'Neil (1993) for

use with Zn as the reducing reagent. Samples were weighed (~80 mg for mineral separates and ~180 mg for whole-rock powders) and absorbed water was removed from mineral surfaces by evacuating under vacuum at 200°C for 2 hours. In order to release the structural water from hydrous mineral phases the samples were then heated to 1200°C using an oxygen-methane torch. The released hydroxyl groups were immediately converted to H_2O by reacting with copper oxide at 400–600°C, and trapped with liquid nitrogen, after which non-condensables were pumped away. Any CO_2 was then released and pumped away using an ethanol slurry at ~ –80°C. The purified H_2O was then quantitatively reduced to H_2 over Cr at 900°C, and the yield was measured to evaluate whether the conversion had gone to completion. Hydrogen isotopic ratios were measured using a dual-inlet Prism mass spectrometer and standardized using four in-house water standards, which have been calibrated against VSMOW and VSLAP. Throughout the study the δD value of KGa-1 (internal laboratory kaolinite) was –55 ± 5‰, which compares well to its accepted δD value of –57‰. Reproducibility of the δD values for standards and samples was generally better than ±5‰.

2.2.3 Oxygen- and Carbon-isotope Analysis of Calcite

Samples were assessed for their carbonate mineralogy and abundance using standard petrographic techniques and X-ray diffraction. Samples were then weighed out according to their abundance of calcite (~0.1 to 5.2 mg), placed in reaction vials and then dried in a furnace at 60°C for 12 hours. A septum-lined cap was screwed onto the dried sample vials, which were then loaded onto a GV MultiPrep autosampler. Orthophosphoric acid was introduced into the sample vials and reacted with the samples

for 10 minutes at 90 °C to produce pure CO_2 gas. The oxygen- and carbon-isotope ratios of the CO_2 gas were then measured using a dual-inlet VG Optima mass spectrometer. The $\delta^{18}O$ and $\delta^{13}C$ values were determined by following the method of Coplen (1996) by calibrating against NBS-18 and NBS-19, for oxygen-isotope ratios, and NBS-19 and Suprapur, for carbon-isotope ratios. Throughout this study the calcite standard WS-1 had $\delta^{18}O$ and $\delta^{13}C$ values of +26.2 ± 0.1‰ and +0.7 ± 0.1‰, which compares to its accepted values of +26.2‰ and +0.8‰, respectively. Reproducibility of the $\delta^{18}O$ and $\delta^{13}C$ values for standards and samples was generally better than ±0.1‰.

Chapter 3. Petrography and Petrogenesis of the Huntington Mountain Pluton and East Bay Hills Volcanic Suite

3.1 Previous Studies

The Huntington Mountain pluton is located west of the Mira River and intrudes into the northeast portion of the East Bay Hills volcanic suite. The pluton consists of diorite to syenogranite, but is largely dominated by diorite. The silica content (SiO_2) of the pluton ranges from 46 to 59% for dioritic rocks and 70 to 77% for monzogranite, leucogranite and syenogranite (Barr et al., 1996). Cross-cutting age relations in the pluton indicate that the diorite was intruded by the leucogranite, and the leucogranite was intruded by the syenogranite, which is inferred to be the youngest unit of the pluton. In the southwestern portion of the pluton, leucogranite and syenogranite dykes are present within the granodiorite. No cross-cutting relationships have been observed for the monzogranite (Barr et al., 1996). On tectonic discrimination diagrams, samples from Huntington Mountain pluton plot within the volcanic-arc field, and are typical of I-type granitoid rocks that have formed along the continental margin of a subduction zone (Barr et al., 1996).

The East Bay Hills volcanic suite forms an elongate belt of volcanic rocks along the southeastern shore of Bras d'Or lake, and consists of basaltic to rhyolitic tuffs and flows, but is compositionally dominated by andesitic to dacitic rocks. A younging direction for the suite is difficult to establish given the rarity of contact exposures between rock units and the lack of evidence for volcaniclastic bedding structures. The silica content of the volcanic rocks ranges from 46 to 75% SiO_2. On tectonic discrimination diagrams, mafic volcanic rocks overlap the boundary between the volcanic-arc and the within-plate tholeiitic basalt fields, while felsic volcanic rocks plot

within the volcanic-arc field (Barr et al., 1996). Overall, the chemical compositions of the East Bay Hills volcanic suite define a calc-alkaline trend, which is consistent with their formation in a volcanic-arc setting (Barr et al., 1998). The volcanic rocks are interpreted to have formed in a sub-aerial setting, on the basis of flow-banding in rhyolitic rocks and abundant amygdules in basaltic rocks (Barr et al., 1996). The lack of evidence for subaqueous volcanism, such as pillowed flows and depositional bedding features, also supports this interpretation (Barr et al., 1996).

Overall, the Huntington Mountain pluton and East Bay Hills volcanic suite most likely represent cogenetic magmatism arising from a continental margin subduction zone. This interpretation is confirmed by U-Pb age dates of 619 Ma for the leucogranite (Barr et al., 1996) and 623 Ma from a flow-banded rhyolite (Bevier et al., 1993), and $^{40}Ar/^{39}Ar$ (hornblende) plateau ages of ca. 618 and 631 Ma for the diorite (Keppie et al., 1990).

Previous petrographic work by Potter et al. (2008) on felsic rocks from the Huntington Mountain pluton and East Bay Hills volcanic suite has shown that these igneous rocks underwent post-magmatic hydrothermal alteration. This is indicated by the presence of a typical propylitic alteration assemblage, consisting of turbid feldspar, epidote, chlorite, titanite and sericite, quartz-calcite-sericite alteration, and fractures that are typically filled with quartz, calcite, epidote, chlorite and titanite (Potter et al., 2008). Based on these findings, coupled with oxygen- and hydrogen-isotope results, Potter et al. (2008) concluded that the igneous rocks across the Mira terrane have been altered by post-magmatic, meteoric-dominated hydrothermal fluids, which infiltrated the crust during the late stages of extensional volcanism in the Coastal Belt, ca. 575-560 Ma.

3.2 Petrographic Descriptions of the Rock Suites

The rocks of Huntington Mountain pluton and East Bay Hills volcanic suite have been previously described and characterized in several geochemical and petrographic studies (e.g., Barr et al., 1996). The purpose of this section is to provide details of the alteration that has affected the rocks of Huntington Mountain pluton and East Bay Hills volcanic suite. The rock type classifications used here are adopted from the mapping and geochemical studies of Barr et al. (1996). A description of these rock types, and in particular their alteration mineralogy, is provided below, with sample number locations and lithologies referred to in Figures 3.1 to 3.5, and Appendix A. Given the lack of age constraints for the monzogranite, as well as its minor spatial extent and paucity of exposure, no samples of monzogranite were collected.

3.2.1 The Huntington Mountain Pluton

Diorite – Granodiorite

Diorite occurs mainly as a large exposure in the center of Huntington Mountain pluton (Fig. 3.1 - HHd), and granodiorite as smaller exposures along the margin of the pluton (Fig. 3.1 - HHg). Together, these rocks comprise approximately half of the total exposure of the pluton. Rocks from the diorite vary from fine- to coarse-grained, but are typically medium-grained. The diorite is generally grey in colour, subophitic to hypidiomorphic (Fig. 3.2A) and is dominated by plagioclase, hornblende and ilmenite,

Figure 3.1. Geologic map of the Huntington Mountain pluton and East Bay Hills volcanic suite, including sample localities for this study.

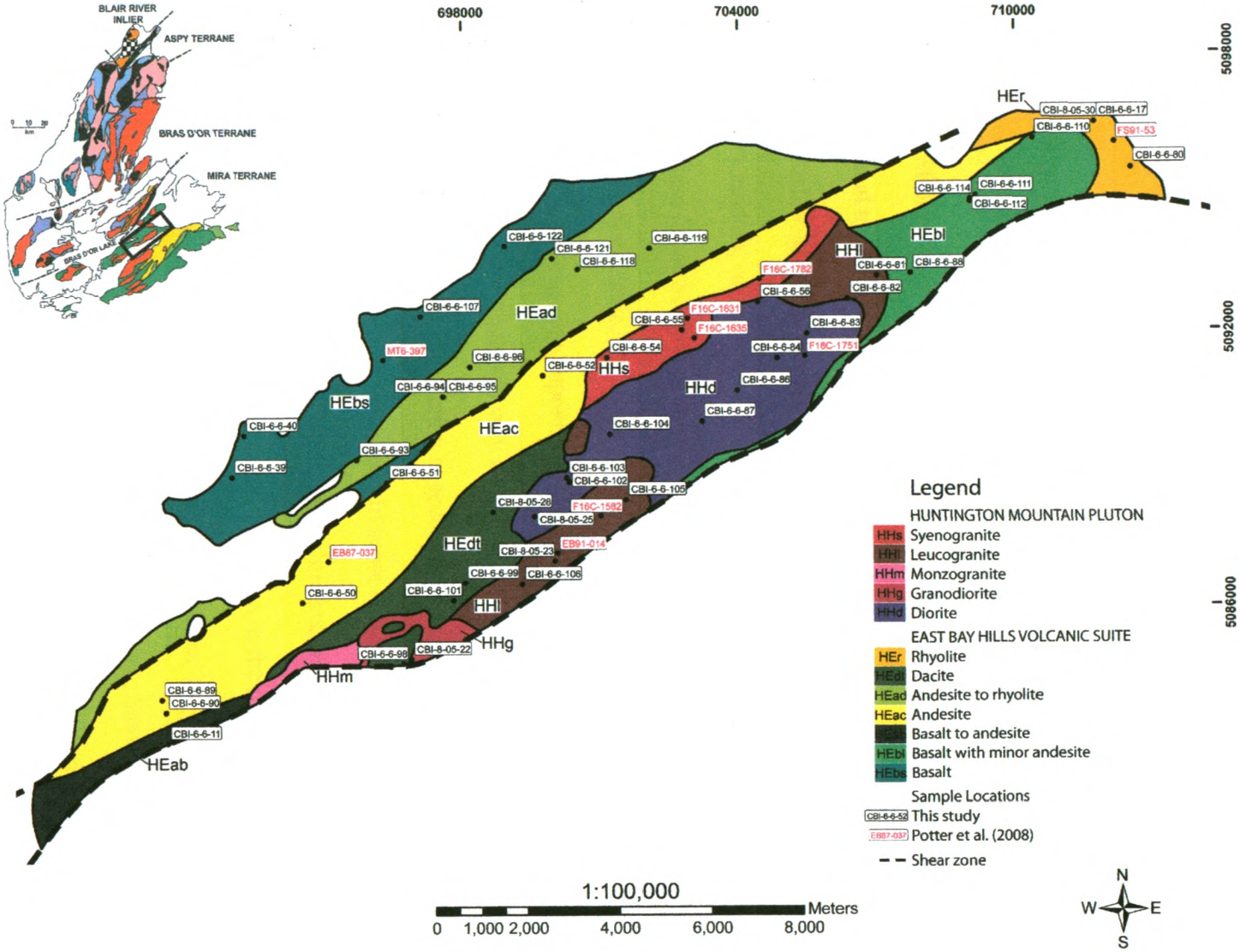
BLAIR RIVER INLIER
ASPY TERRANE
BRAS D'OR TERRANE
MIRA TERRANE
BRAS D'OR LAKE
698000
704000
710000
5098000
5092000
5086000
HEr
HEbl
HHl
HEad
HHs
HHd
HEbs
HEac
HEdt
HHg
HHm
HEab
CBI-8-05-30
CBI-6-6-17
CBI-6-6-110
FS91-53
CBI-6-6-80
CBI-6-6-114
CBI-6-6-111
CBI-6-6-112
CBI-6-6-122
CBI-6-6-121
CBI-6-6-119
CBI-6-6-118
F16C-1782
CBI-6-6-81
CBI-6-6-88
CBI-6-6-82
CBI-6-6-56
CBI-6-6-107
F16C-1631
CBI-6-6-55
F16C-1635
CBI-6-6-83
MT6-397
CBI-6-6-96
CBI-6-6-54
CBI-6-6-84
F16C-1751
CBI-6-6-52
CBI-6-6-94
CBI-6-6-95
CBI-6-6-86
CBI-6-6-87
CBI-6-6-40
CBI-6-6-104
CBI-6-6-93
CBI-6-6-39
CBI-6-6-51
CBI-6-6-103
CBI-6-6-102
CBI-6-6-105
CBI-8-05-26
F16C-1582
CBI-8-05-25
EB87-037
CBI-8-05-23
EB91-014
CBI-6-6-99
CBI-6-6-106
CBI-6-6-50
CBI-6-6-101
CBI-6-6-98
CBI-8-05-22
CBI-6-6-89
CBI-6-6-90
CBI-6-6-11
Legend
HUNTINGTON MOUNTAIN PLUTON
HHs Syenogranite
HHl Leucogranite
HHm Monzogranite
HHg Granodiorite
HHd Diorite
EAST BAY HILLS VOLCANIC SUITE
HEr Rhyolite
HEdt Dacite
HEad Andesite to rhyolite
HEac Andesite
Basalt to andesite
HEbl Basalt with minor andesite
HEbs Basalt
Sample Locations
CBI-6-6-52 This study
EB87-037 Potter et al. (2008)
Shear zone
1:100,000
0 1,000 2,000 4,000 6,000 8,000 Meters
N
W
E
S

with minor amounts of biotite and secondary chlorite and epidote (Fig. 3.3A). The alteration of plagioclase to epidote-sericite-chlorite has caused some rocks to attain dark grey to green hues (Fig. 3.2B). In sample CBI-8-05-25/26, secondary chlorite and epidote appear to be overprinted by later secondary quartz and calcite (Fig. 3.4). In one area (CBI-6-6-87), fine-grained plagioclase and hornblende define a weak foliation, which may be the result of contact metamorphism caused by emplacement of the nearby leucogranite. Strong alteration of the diorite to quartz, sericite and pyrite was also observed proximal to the dacite of the East Bay Hills volcanic suite (Fig. 3.3B). In sample CBI-6-6-104, secondary quartz, sericite and pyrite appear to be overprinted by later secondary epidote, sericite and chlorite (Fig. 3.5).

Plagioclase forms 50-65% of the diorite, and is represented by euhedral medium- or coarse-grained crystal laths, which range in composition from An_{13-90}, with the majority ranging from An_{20-60} (compositions determined by electron probe micro-analysis). Plagioclase grains are typically zoned, with Ca-rich cores that commonly demonstrate moderate to strong alteration to secondary sericite and epidote, and rims that generally do not show evidence of alteration. In some areas of the diorite, plagioclase grains aggregate to form moderate to strong spherulitic textures. Two samples (CBI-6-6-102 and CBI-6-6-103), from the southwest end of the pluton, have plagioclase grains that show moderate to complete replacement by quartz, sericite and pyrite. K-feldspar is rare throughout the diorite unit, but where present, tends to replace plagioclase, and in turn exhibits strong alteration to sericite and Fe-oxide. In one area of the pluton (CBI-6-6-82), K-feldspar partially overprints plagioclase, and both minerals display moderate to strong alteration to sericite, epidote and Fe-oxides (Fig. 3.3C).

Anhedral to euhedral hornblende forms 25-45% of the diorite and generally shows subophitic growth textures. Hornblende is commonly altered to actinolite, biotite and chlorite, and is typically associated with ilmenite and rare, medium- to coarse-grained epidote. In sample CBI-6-6-83, rare medium-grained clinopyroxene is present (Fig. 3.3D). Biotite is commonly found as an alteration product of hornblende, particularly in the areas adjacent to more felsic intrusive units or areas of abundant felsic dykes (e.g., CBI-6-6-82 and CBI-6-6-87), and may have formed as the result of post-magmatic metasomatism. Secondary mafic minerals comprise 10-20% of the diorite, and consist of subhedral to euhedral chlorite and ilmenite. Chlorite and ilmenite are fine-grained and usually form as an alteration product of hornblende. Commonly, ilmenite has alteration rims consisting of fine-grained anhedral titanite and leucoxene. In the dioritic samples proximal to felsic intrusions (e.g., CBI-6-6-87), chlorite and medium-grained ilmenite, which appear to be alteration products of biotite, form in a hornblende-poor zone dominated by secondary quartz (Fig. 3.3E).

The granodiorite is medium-grained, pink to dark red, and its crystals are allotriomorphic to idiomorphic in habit. It is comprised mostly of plagioclase, quartz and chlorite, with minor amounts of K-feldspar and ilmenite (Fig. 3.3F). Typically this rock unit displays moderate to strong alteration to sericite and epidote.

The granodiorite contains 65-70%, medium-grained euhedral plagioclase, which ranges in composition from An_{0-14} (compositions determined by electron probe micro-analysis). Plagioclase crystals tend to be zoned, with their core strongly altered to sericite and epidote, and their rim weakly altered to sericite. Strong, reddish Fe-oxide alteration is developed along the rim of most plagioclase grains. K-feldspar, which is interpreted to

comprise part of the primary mineralogy of the granodiorite, is sparse throughout the rock unit (1-2%), and consists of euhedral grains with strong sericite and iron-oxide alteration.

Quartz, which is also interpreted to comprise part of the primary mineralogy of the granodiorite, is generally anhedral, fine- to coarse-grained and forms 20-25% of the rock unit. Locally, coarser quartz grains are bleb-like and can form embayments into plagioclase (Fig. 3.3F). Quartz grains generally display strong undulose extinction, although coarse grains tend to be internally fractured, with varying extinction angles. In one sample (CBI-6-6-21), fine-grained quartz is commonly found partially embaying the margin of euhedral plagioclase.

Secondary mafic minerals compose 5-8% of the granodiorite and are dominated by chlorite and ilmenite. Chlorite appears to be the alteration product of rare primary biotite, and is generally associated with ilmenite, which is characterized by alteration rims consisting of fine-grained anhedral titanite and leucoxene.

Leucogranite

Leucogranite is present as three extensive exposures on either side of the main diorite (Fig. 3.1 - HHl). It varies from medium- to coarse-grained and is pink to brick-red (Fig. 3.2C). Leucogranite samples are dominated by perthitic feldspar, quartz and plagioclase with minor to moderate amounts of chlorite, ilmenite and epidote (Fig. 3.6A). These rocks typically vary from allotriomorphic to hypidiomorphic-granular in texture (Fig. 3.6B), although micro-granophyric textures are also common (Fig. 3.6C). In some areas (e.g., CBI-6-6-106), features of cataclasis are well developed, and consist of quartz

with strong undulatory extinction and bent feldspar laths. In sample CBI-6-6-105, rapakivi textures are prominent in thin section (Fig. 3.6D).

The leucogranite contains three phases of feldspar, perthite, plagioclase and K-feldspar, with perthite being the most abundant. Subhedral, medium- or coarse-grained perthitic feldspar forms 40-65% of the leucogranite unit. The composition of the perthite ranges from An_{1-5} for albitic bands and $\sim Or_{97}$ for K-feldspar bands (compositions determined by electron probe micro-analysis). In thin section, the bands of K-feldspar and albite in the perthite are clearly distinct from each other with the presence of secondary iron-oxide and minor sericite in the K-feldspar bands and secondary sericite and epidote in the albitic bands. Locally, the perthite exhibits moderate internal shearing, which is likely the result of cataclasis.

Discrete crystals of medium-grained subhedral to euhedral plagioclase and K-feldspar form 1-5% of the leucogranite. Given their paucity, compositions were difficult to determine. Typically, the plagioclase exhibits moderate to strong sericite alteration and weak to moderate iron-oxide staining, while the K-feldspar shows moderate to strong Fe-oxide staining. In one area (CBI-6-6-105), unaltered plagioclase forms distinctive micro-rapakivi textures around perthitic feldspar (Fig. 3.6D).

Quartz is fine- to coarse-grained, anhedral to subhedral and forms 25-40% of the leucogranite. Generally, quartz grains display strong shearing and are commonly internally fragmented, exhibiting varying extinction angles. In sample CBI-6-6-81, fine-grained quartz is associated with K-feldspar and forms micro-granophyric textures around perthitic feldspar. In some areas (e.g., CBI-8-05-23 and CBI-6-6-106), fine-

grained quartz occurs along the margins of perthitic feldspar and coarser grained quartz, and embays euhedral plagioclase and perthitic feldspar.

Mafic minerals form 2-5% of the leucogranite and consist of fine- or medium-grained, anhedral to subhedral secondary chlorite and ilmenite, which are typically in association with each other. Ilmenite is commonly rimmed by fine-grained secondary titanite and leucoxene. In one area (CBI-8-05-23), chlorite and ilmenite are associated with fine-grained quartz that embays euhedral plagioclase and perthitic feldspar.

Syenogranite

Syenogranite crops out as a large elongate exposure on the northeastern side of the dioritic intrusion (Fig. 3.1 - HHs). Syenogranite is commonly fine-grained and brick-red in colour. The most distinctive characteristic of the syenogranite is its strong micro-granophyric texture about euhedral feldspar, which produces the appearance of a porphyritic texture (Fig. 3.2D). The syenogranite consists mainly of K-feldspar, quartz and albite with minor amounts of secondary chlorite, epidote and ilmenite, and show very strong alteration to Fe-oxide (Fig. 3.6E).

The syenogranite contains 50-65% K-feldspar, which ranges from fine-grained anhedral to coarse-grained euhedral in size and shape. Fine-grained K-feldspar is generally associated with quartz, which together form the distinctive granophyric texture characteristic of the syenogranite (Fig. 3.6F). The majority of K-feldspar is heavily stained by Fe-oxide and exhibits only minor alteration to sericite. Because of the iron-staining, K-feldspar has a muddy appearance in thin section. Plagioclase is medium- or coarse-grained, subhedral to euhedral, and forms 10-15% of the syenogranite. The

composition of plagioclase is dominantly An_{0-15} (compositions determined by electron probe micro-analysis). Plagioclase grains exhibit minor alteration to sericite and strong Fe-oxide staining, although to a lesser degree than K-feldspar.

Fine- or medium-grained, anhedral quartz forms 20-35% of the syenogranite. As previously mentioned, the fine-grained quartz is generally associated with K-feldspar, which together form a distinctive granophyric texture. A small fraction of the quartz is medium-grained and anhedral to subhedral, and is also surrounded by fine-grained granophyre. In some cases, medium-grained quartz grains exhibit weak to moderate internal fractures, which are likely the result of weak cataclasis.

Mafic minerals form a minor portion of the syenogranite (5-7%) and consist of secondary chlorite, epidote and ilmenite, which are generally found in association with each other. In one area (CBI-6-6-55), fine- or medium-grained chlorite and fine-grained epidote and ilmenite comprise secondary alteration of euhedral hornblende.

3.2.2 The East Bay Hills Volcanic Suite

Basaltic Rocks

Basaltic rocks are the second most abundant rock type in the East Bay Hills volcanic suite (Fig. 3.1 - HEbs, HEbl and HEab). They crop out as two extensive elongate units along the shore of Bras d'Or Lake and adjacent to the leucogranite in the northeastern section of the study area, as minor dykes throughout the volcanic complex, and as a small unit in the southwestern section of the study area. They are generally aphanitic and massive, with weak to moderate porphyritic textures (Fig. 3.2E). Barr et al. (1996) reported an abundance of vesicles throughout these rocks, but only minor vesicles

were observed in the samples examined here, which were commonly filled by very fine-grained quartz, calcite, epidote and Fe-oxide. The basaltic rocks are dominated by fine-grained quartz and plagioclase microlites, with minor to secondary amounts of plagioclase phenocrysts, chlorite, epidote and ilmenite, and(or) pyrite (Fig. 3.7A). Two alteration assemblages were observed in these rocks: (1) weak to strong secondary chlorite, epidote, ilmenite and sericite (Figs. 3.7A & B), and (2) moderate to very strong secondary quartz, sericite, calcite and Fe-oxide (Fig. 3.7C).

The basaltic rocks are dominated by 65-75% aphanitic groundmass, which consists of fine-grained plagioclase and quartz microlites, with minor amounts of sericite and epidote. Plagioclase phenocrysts form 5-15% of the basaltic units, and are represented by medium-grained euhedral laths. Locally, these laths tend to be weakly to moderately altered to sericite, epidote and ilmenite, or moderately to strongly altered to quartz, sericite, calcite and Fe-oxide.

Secondary mafic minerals comprise 10-15% of the basaltic units, and consist of fine-grained chlorite and epidote, with lesser amounts of ilmenite. These phases commonly occur together and and tend to be alteration products of rare clinopyroxene, some of which remains present in some samples (Fig. 3.7A).

Dacite

Dacite occurs as a small exposure in contact with the diorite, leucogranite and monzogranite within the northwestern section of the Huntington Mountain pluton (Fig. 3.1 - HEdt). These rocks are generally fine-grained, grey to black, and aphanitic to weakly porphyritic. Dacite mainly consists of plagioclase, hornblende and quartz, with

minor amounts of chlorite, sericite, epidote and ilmenite (Fig. 3.7D). In some samples (e.g., CBI-6-6-101), ilmenite appears to be replaced by pyrite. The dacite typically exhibits moderate alteration to sericite and epidote, and proximal to the diorite of the Huntington Mountain pluton, intense alteration to quartz, sericite and pyrite. Although the dacitic unit tends to be composed mainly of dacite, minor amounts of basaltic to andesitic rocks also occur.

Plagioclase is fine-grained, euhedral and forms 40-65% of the dacite. The composition of plagioclase ranges from An_{0-18} (compositions determined by electron probe micro-analysis). Generally, plagioclase shows moderate alteration to sericite and epidote. In one area (CBI-8-05-28), plagioclase grains are highly embayed to completely overprinted by quartz, sericite and calcite.

Quartz forms 15-25% of the dacite and is generally fine-grained and anhedral to subhedral, although medium-grained quartz phenocrysts are also observed. Fine-grained quartz is typically associated with sericite and pyrite, and to a lesser extent epidote and chlorite, which comprise the dominant alteration minerals in the dacite. Like plagioclase, medium-grained quartz phenocrysts are highly fractured and appear to be filled by fine-grained quartz, sericite and pyrite.

The dacite consists of 10-15% hornblende, which is anhedral to subhedral and fine- or medium-grained. Hornblende commonly surrounds euhedral plagioclase grains to form subophitic textures. Generally, hornblende is moderately fractured and tends to be altered locally to chlorite, epidote and ilmenite.

Secondary mafic minerals form 8-12% of the dacite and consist of fine-grained chlorite, epidote and ilmenite, or in some areas (e.g., CBI-6-6-101), pyrite. These phases

are typically observed in association with each other and likely are the alteration products of hornblende. In one area (CBI-8-05-28), fine-grained alteration rims of leucoxene and titanite are present on ilmenite.

Andesite – Rhyolite

The most abundant lithology in the East Bay Hills volcanic suite consists of andesitic to rhyolitic rocks (Fig. 3.1 - HEac, HEad and HEr). These rocks are aphanitic to porphyritic and dominated by ash to lapilli crystal tuff, and to a lesser extent, flow-banded pyroclastic beds (Fig. 3.2F). They are generally comprised of fine-grained quartz, and feldspar microlites, with minor feldspar phenocrysts, epidote and chlorite (Fig. 3.7E). Weak to moderate alteration of the andesite is represented by secondary quartz, sericite, calcite, chlorite and ilmenite, and secondary quartz, calcite and Fe-oxide are typical of weakly altered rhyolite (Fig. 3.7F). In one area (CBI-6-6-122), primary feldspar and groundmass are overprinted by secondary quartz, sericite and calcite (Fig. 3.8)

Aphanitic groundmass forms 60-75% of the andesite to rhyolite units, and consists of fine-grained quartz, and plagioclase microlites, with minor to moderate amounts of sericite and epidote. Feldspar phenocrysts form 15-30% of these rocks and are represented by fine- or medium-grained, subhedral to euhedral grains. The composition of one feldspar phenocryst was determined to be Or_{98} (compositions determined by electron probe micro-analysis), although the majority of the feldspar phenocrysts in these rocks are interpreted to be plagioclase. Generally, the feldspars

show weak to moderate alteration to sericite, epidote and ilmenite, and to a lesser extent, quartz, sericite and calcite alteration, with very minor Fe-oxide alteration.

Secondary mafic minerals comprise 5-25% of the andesitic to rhyolitic rocks and are dominated by fine- or medium-grained epidote, with lesser amounts of fine-grained chlorite and ilmenite. Epidote generally forms within the groundmass or as an alteration product of feldspar. Spherical aggregates of medium-grained epidote are commonly observed, and are interpreted to represent relict vesicles. Ilmenite is typically rimmed by fine-grained secondary titanite and leucoxene.

3.3 Petrographic Description of Veins

Veins and veinlets within the Huntington Mountain pluton and the East Bay Hills volcanic suite are generally composed of quartz, plus varying amounts of calcite, epidote and sericite (Fig. 3.9A). The margins of most veins and veinlets consist of fine-grained quartz, sericite and Fe-oxides. Two styles of veins are recognized within these two rock suites: (1) discontinuous veinlets that are 1 mm in width and trend along grain boundaries (Fig. 3.9B), and (2) well-defined veins that are 1 mm to 2 cm in width and cross-cut host rocks (Figs. 3.9C, D). The abundance of these two types varies; type 1 occurs in both volcanic and plutonic rocks, whereas type 2 is generally restricted to the volcanic rocks. The overall abundance of veins within these two rock suites is low, generally <1% by surface expression.

Figure 3.2. Photographs of rocks from the Huntington Mountain pluton and East Bay Hills volcanic suite. Rock surfaces have been wetted down to highlight features. A - CBI-6-6-56, medium-grained subophitic diorite. B - CBI-6-6-102, fine-grained diorite, strong replacement by chlorite-epidote-sericite-quartz-ilmenite, and cut by a discontinuous quartz vein. C - CBI-6-6-105, coarse-grained leucogranite with red-brick perthitic feldspar, subhedral milky white quartz and abundant ilmenite-chlorite. D - CBI-6-6-55, syenogranite, weak porphyritic texture formed by fine-grained granophyric K-feldspar-quartz surrounding euhedral laths of K-feldspar and plagioclase. E - CBI-6-6-40, weakly porphyritic basalt with moderate replacement by quartz-sericite-calcite and minor epidote-chlorite. F - CBI-6-6-17, rhyolite tuff with lapilli-sized clasts of microlitic quartz and minor feldspar, moderately replaced by quartz-sericite-calcite, with a well defined quartz-calcite vein.

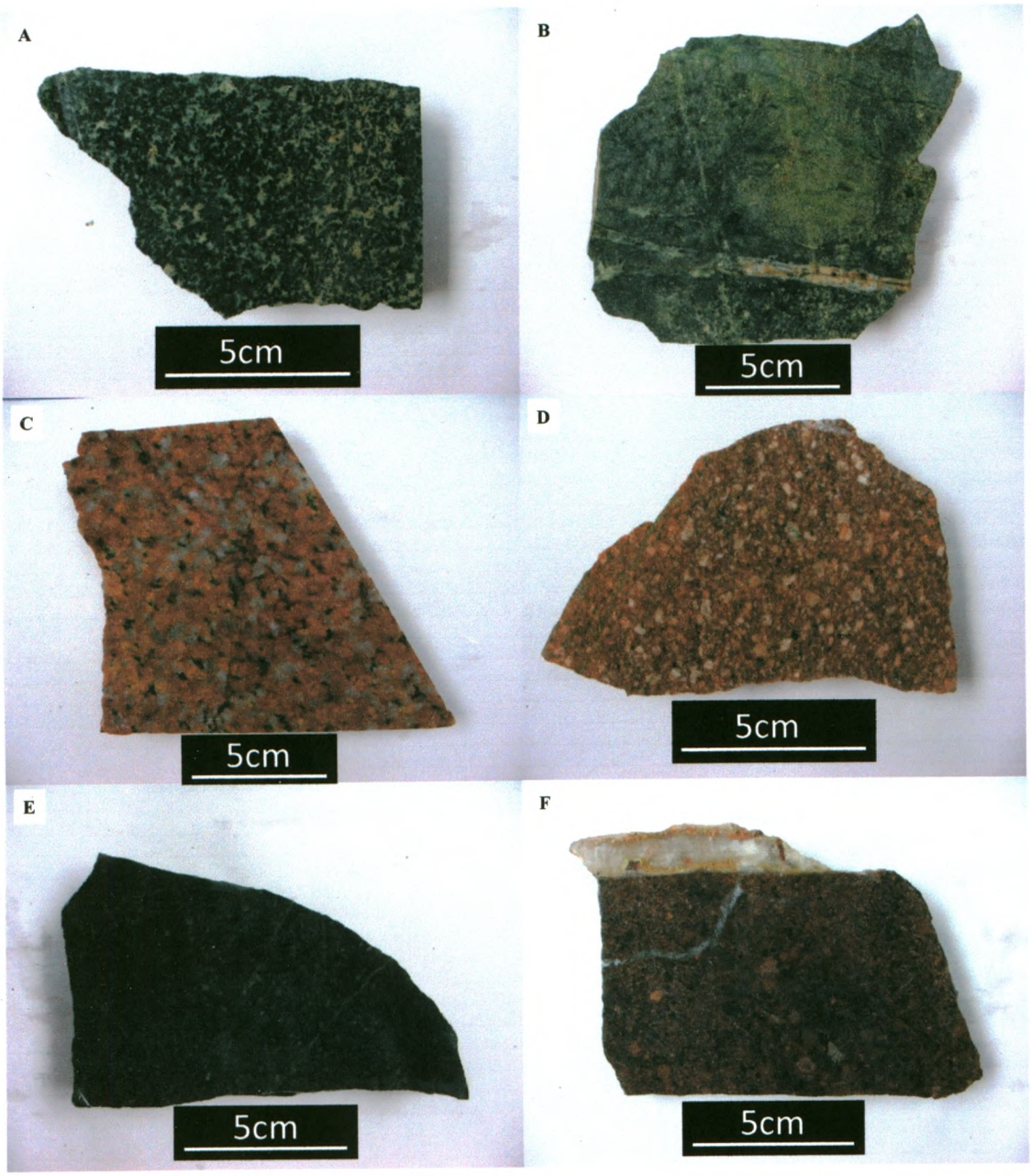
A
5cm
B
5cm
C
5cm
D
5cm
E
5cm
F
5cm

Figure 3.3. Photomicrographs of the Huntington Mountain pluton, diorite-granodiorite rocks. A - CBI-8-05-25, diorite with plagioclase partially replaced by sericite-epidote, and subophitic hornblende partially replaced by chlorite-epidote-ilmenite. B - CBI-6-6-103, diorite completely replaced by quartz-sericite-pyrite. C - CBI-6-6-82, diorite with plagioclase replaced by K-feldspar and overprinted by sericite, epidote and iron-oxide. D - CBI-6-6-83, diorite with plagioclase partially replaced by sericite-epidote, subophitic hornblende with partial replacement by epidote, and clinopyroxene replaced by sericite-epidote-ilmenite. E - CBI-6-6-87, diorite with replacement of biotite by chlorite-ilmenite, associated with secondary quartz. F - CBI-8-05-21, granodiorite with plagioclase partially replaced by sericite-epidote within the core and Fe-oxide along the rim, plagioclase partially embayed by bleb-like quartz. Mineral abbreviations, bio - biotite, cal - calcite, chl - chlorite, ep - epidote, hbl - hornblende, ilm - ilmenite, kfs - K-feldspar, plg - plagioclase, py - pyrite, qtz - quartz, ser - sericite.

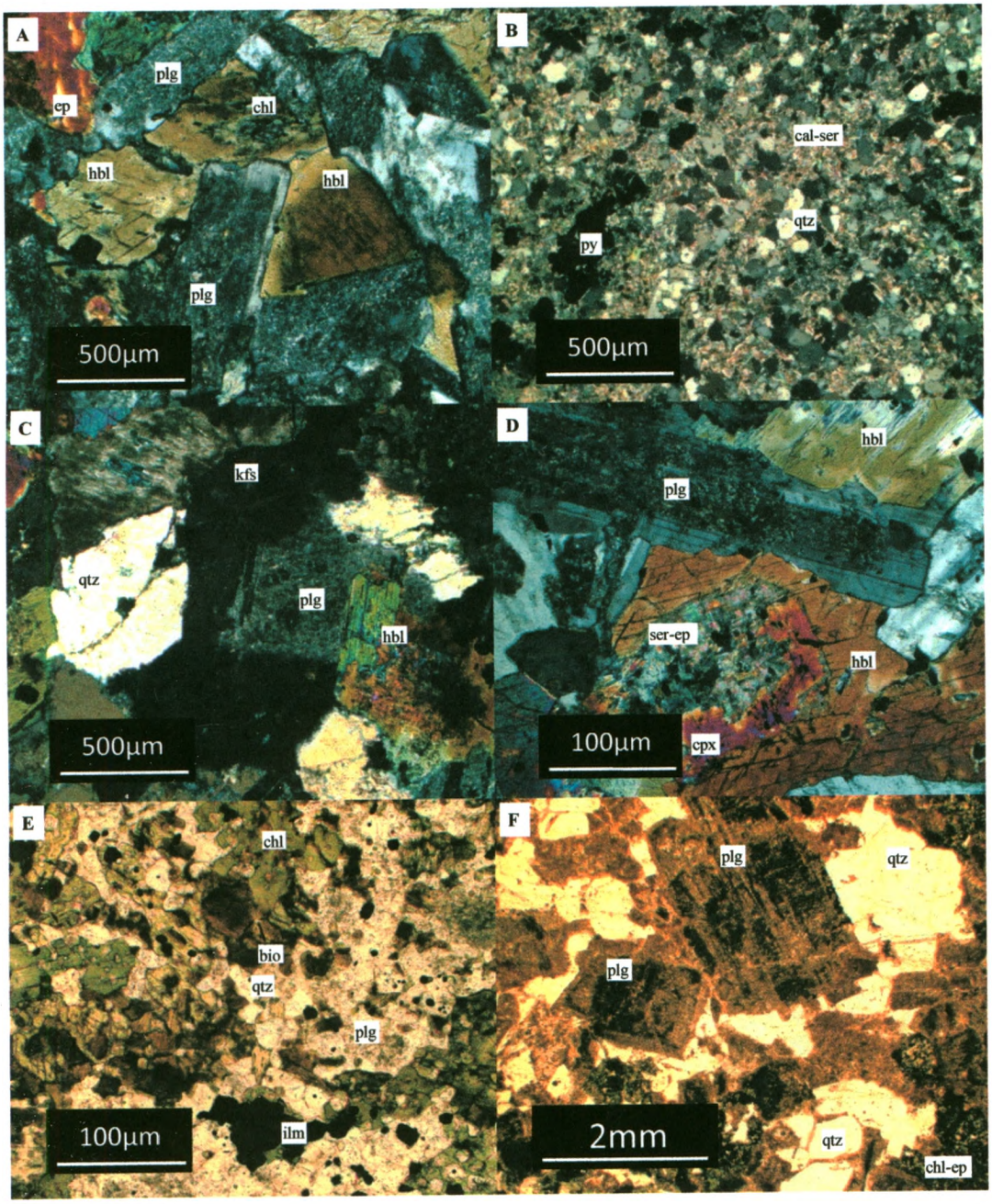
A
plg
ep
chl
hbl
hbl
plg
500µm
B
cal-ser
qtz
py
500µm
C
kfs
qtz
plg
hbl
500µm
D
hbl
plg
ser-ep
hbl
100µm
cpx
E
chl
bio
qtz
plg
100µm
ilm
F
plg
qtz
plg
2mm
qtz
chl-ep

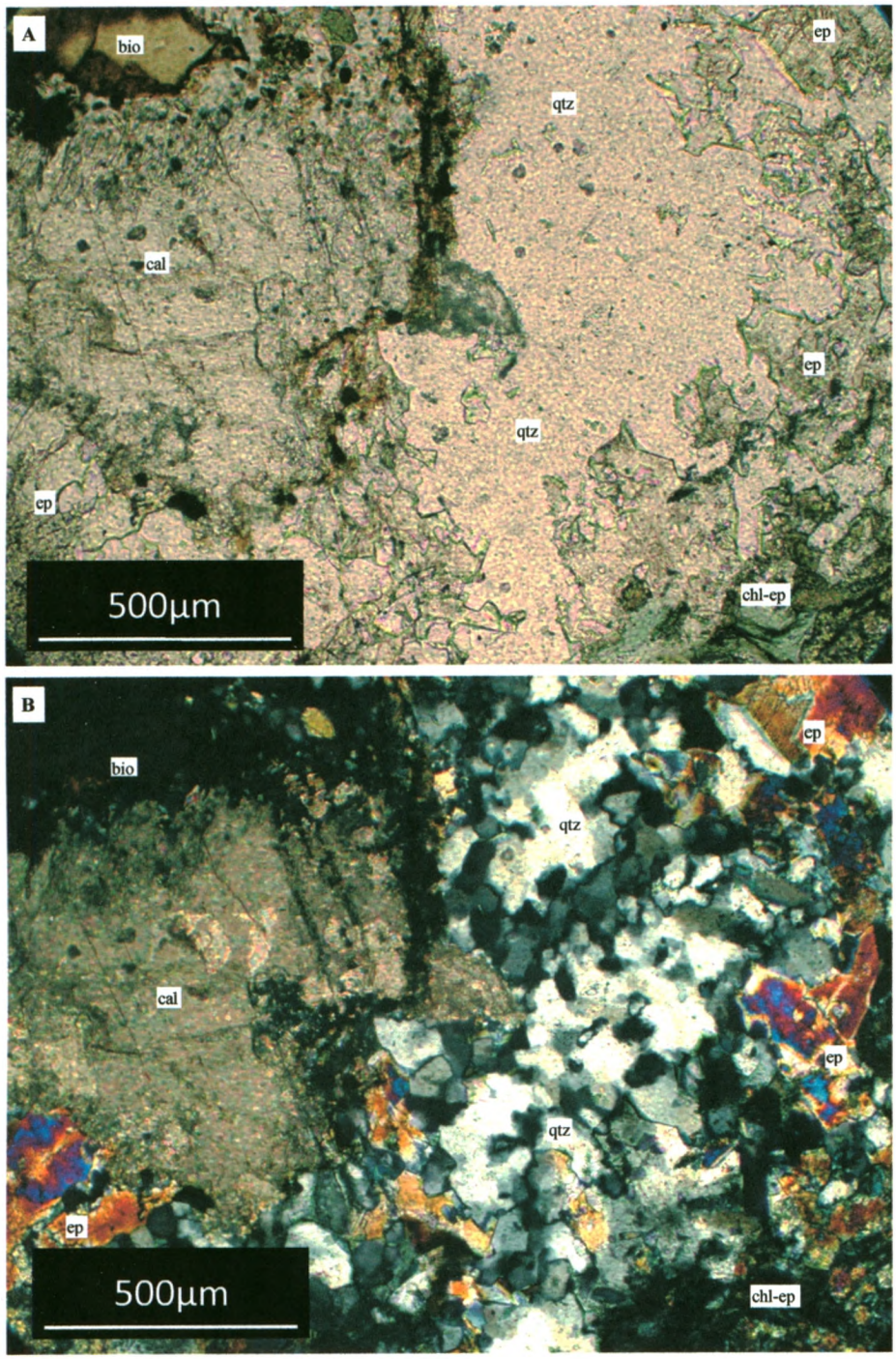

Figure 3.4. Photomicrographs of the paragenetic alteration sequence of diorite (sample CBI-8-05-25/26) from the Huntington Mountain pluton: (A) plane polarized light and (B) cross polarized light. These images show secondary chlorite-epidote overprinted by fine-grained quartz, which is then overprinted by calcite. Mineral abbreviations, bio - biotite, cal - calcite, chl - chlorite, ep - epidote, qtz - quartz.

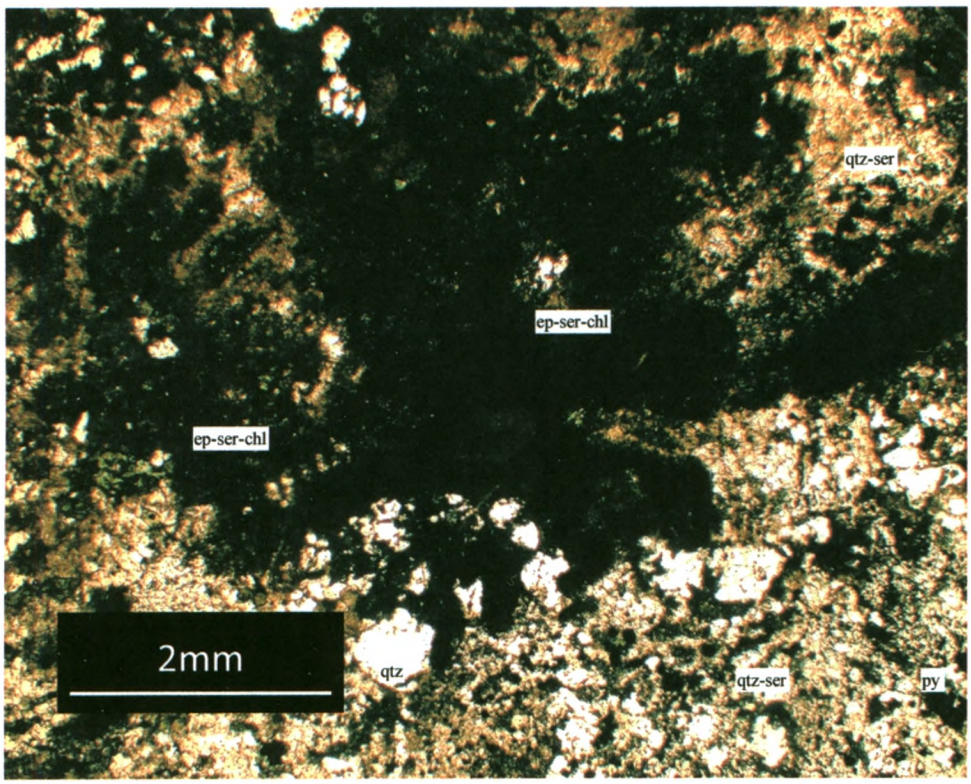

Figure 3.5. Photomicrograph of the paragenetic alteration sequence of diorite (sample CBI-6-6-104) from the Huntington Mountain pluton. The image shows phyllic alteration, consisting of fine-grained quartz-sericite-pyrite, overprinted by fine-grained epidote-sericite-chlorite, comprising the propylitic alteration assemblage alteration. Mineral abbreviations, chl - chlorite, ep - epidote, py - pyrite, qtz - quartz, ser - sericite.

Figure 3.6. Photomicrographs of the Huntington Mountain pluton, leucogranite and syenogranite. A - CBI-8-05-23, leucogranite with perthitic feldspar replaced by sericite-epidote-ilmenite and Fe-oxide. B - CBI-6-6-105, hypidiomorphic-granular leucogranite with quartz and perthitic feldspar, replaced by sericite-epidote-ilmenite. C - CBI-6-6-81, leucogranite with subhedral quartz and euhedral feldspar, replaced by sericite-epidote, surrounded by fine-grained granophyric feldspar and quartz. D - CBI-6-6-105, hypidiomorphic-granular leucogranite, rapakivi texture with perthitic feldspar mantled by plagioclase, weakly replaced by sericite-epidote. E - CBI-6-6-55, syenogranite with euhedral plagioclase and K-feldspar replaced by sericite-epidote and Fe-oxides, surrounded by fine-grained granophyric feldspar and quartz. F - CBI-6-6-55, syenogranite with subhedral quartz and K-feldspar, and euhedral plagioclase surrounded by fine-grained granophyric feldspar and quartz, weak sericite-epidote alteration. Mineral abbreviations, chl - chlorite, fs - perthitic feldspar, ep - epidote, ilm - ilmenite, kfs - K-feldspar, plg - plagioclase, qtz - quartz.

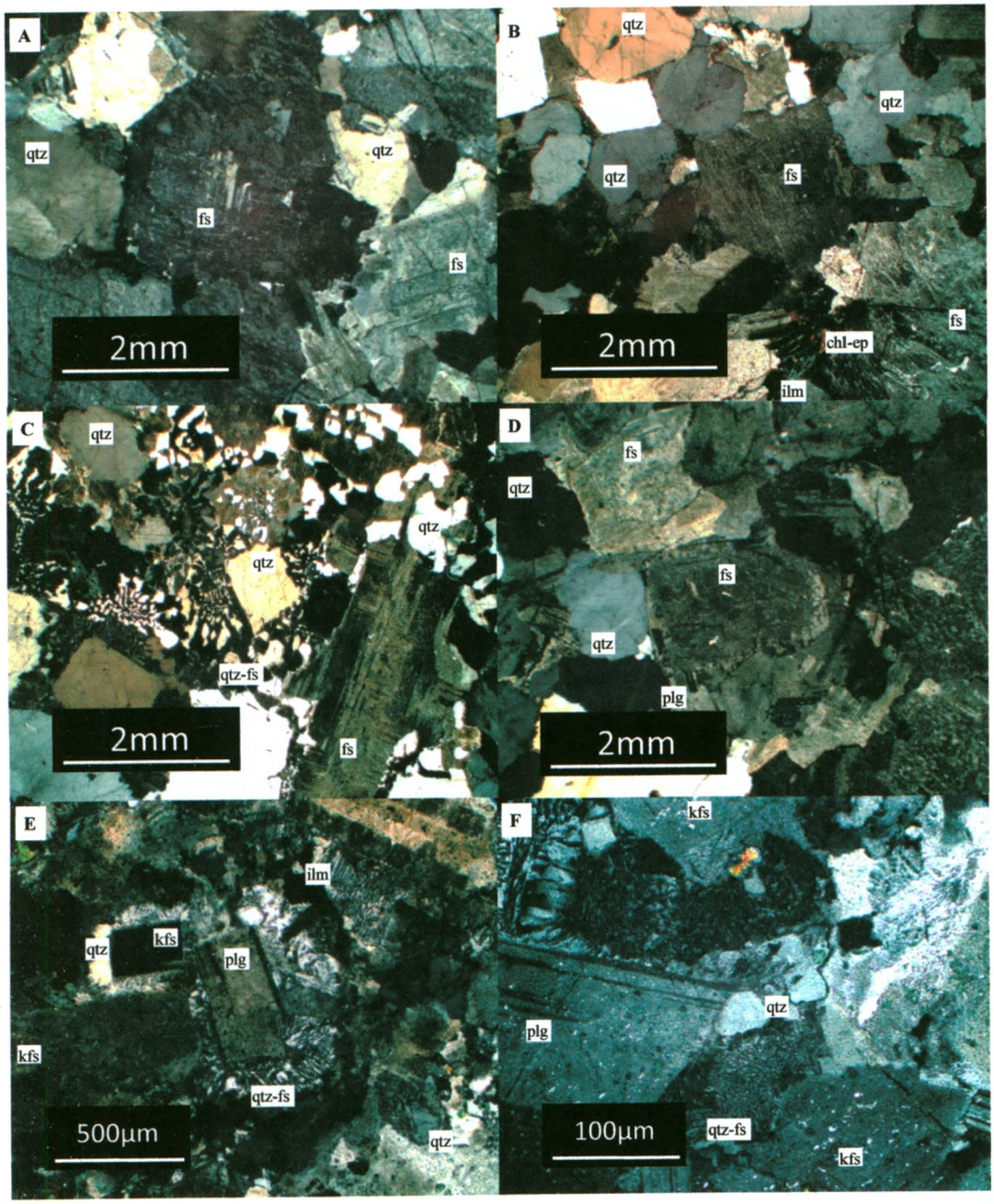
A
qtz
qtz
fs
fs
2mm
B
qtz
qtz
qtz
fs
fs
chl-ep
ilm
2mm
C
qtz
qtz
qtz
qtz-fs
fs
2mm
D
fs
qtz
fs
qtz
plg
2mm
E
ilm
qtz
kfs
plg
kfs
qtz-fs
500µm
qtz
F
kfs
qtz
plg
100µm
qtz-fs
kfs

Figure 3.7. Photomicrographs of the East Bay Hills volcanic rocks. A - CBI-6-6-39, porphyritic basalt with sericitized plagioclase and rare clinopyroxene phenocrysts, exhibiting weak to moderate epidote-chlorite-sericite alteration. B - CBI-6-6-112, aphanitic basalt with abundant epidote "clumps", exhibiting moderate to strong epidote-chlorite-sericite alteration. C - CBI-6-6-11, basalt completely overprinted by quartz-calcite-sericite alteration, with embayed granular quartz. D - CBI-8-05-28, porphyritic dacite with plagioclase replaced by sericite-epidote-pyrite alteration, and exhibiting weak quartz-calcite alteration within the groundmass. E - CBI-6-6-89, porphyritic andesite with weak to moderate flow banding and moderate replacement of plagioclase by epidote, chlorite and ilmenite. F - CBI-8-05-30, porphyritic K-feldspar rhyolite partially replaced by sericite and Fe-oxide. Mineral abbreviations, cal - calcite, chl - chlorite, ep - epidote, ilm - ilmenite, kfs - K-feldspar, plg - plagioclase, py - pyrite, qtz - quartz, ser - sericite.

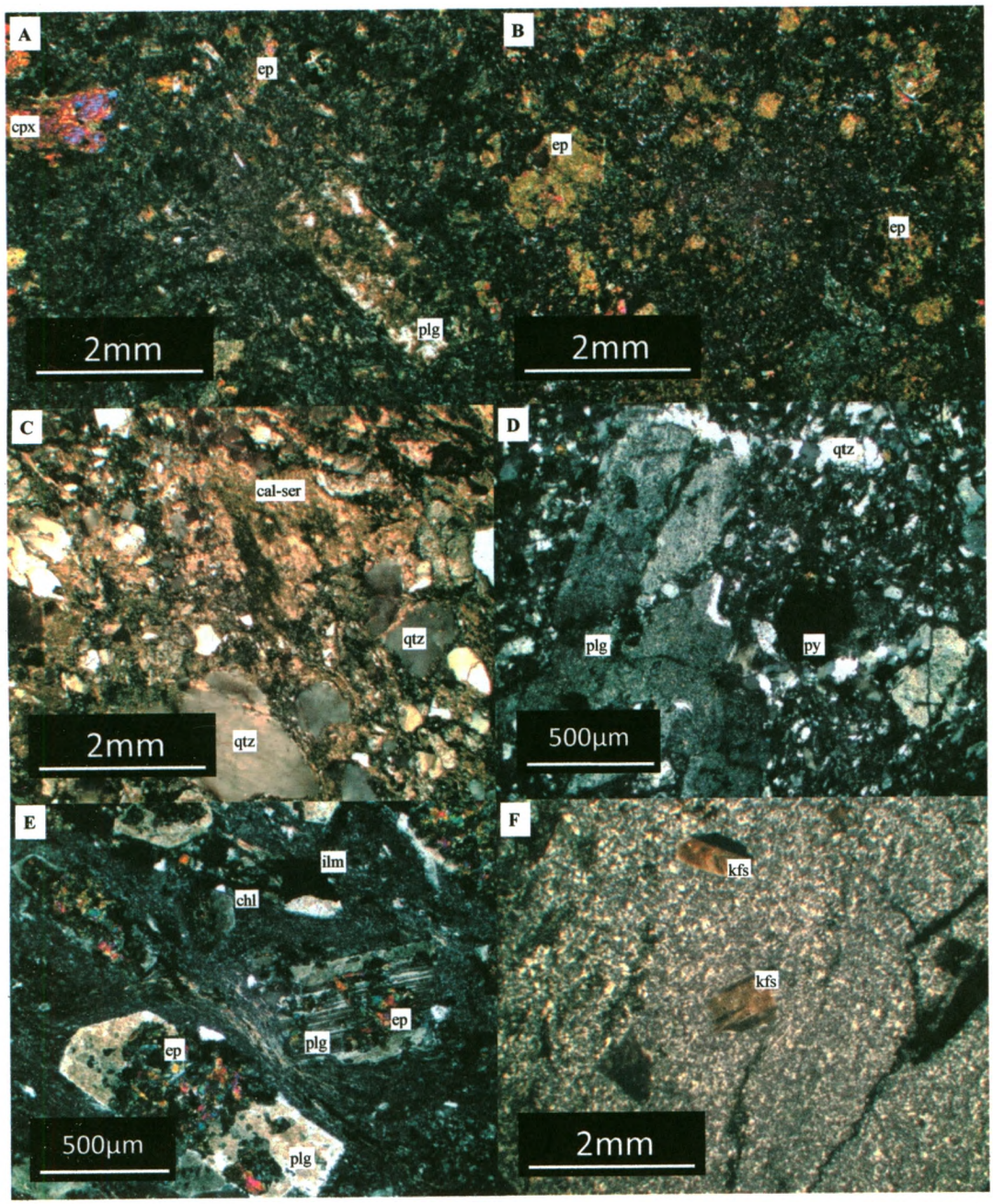
A
ep
cpx
plg
2mm
B
ep
ep
2mm
C
cal-ser
qtz
qtz
2mm
D
qtz
plg
py
500µm
E
ilm
chl
ep
plg
ep
500µm
plg
F
kfs
kfs
2mm

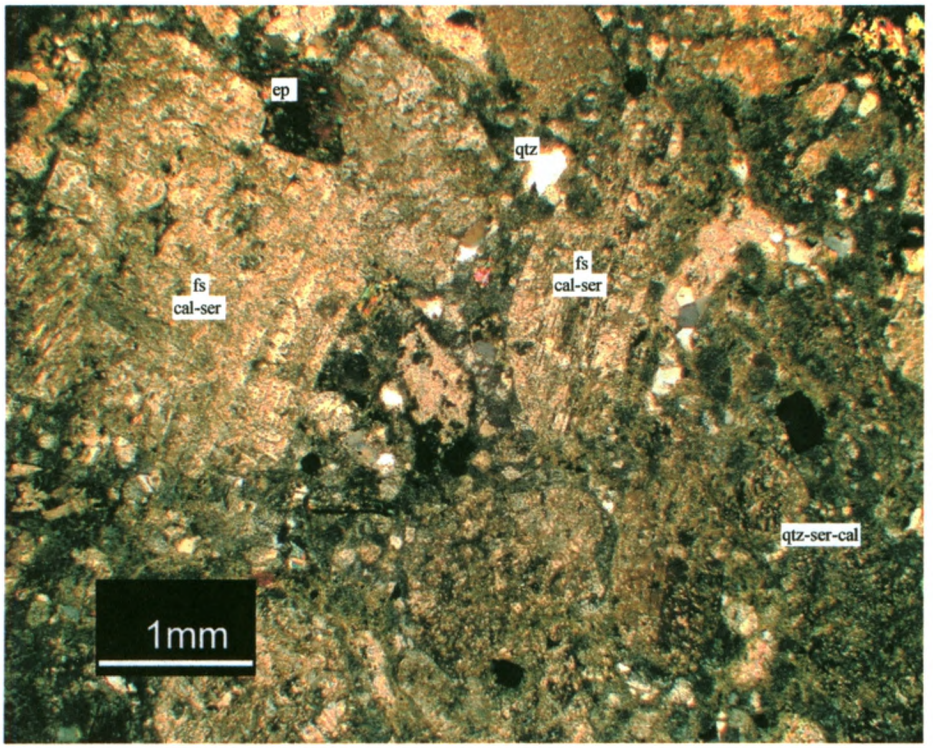

Figure 3.8. Photomicrograph of an andesite crystal tuff (CBI-6-6-122) from the East Bay Hills volcanic suite. The image shows strong quartz-sericite-calcite alteration with primary feldspar overprinted by secondary calcite-sericite, and the groundmass altered to secondary quartz, sericite, calcite. Mineral abbreviations, cal - calcite, ep - epidote, fs - feldspar, qtz - quartz, ser - sericite.

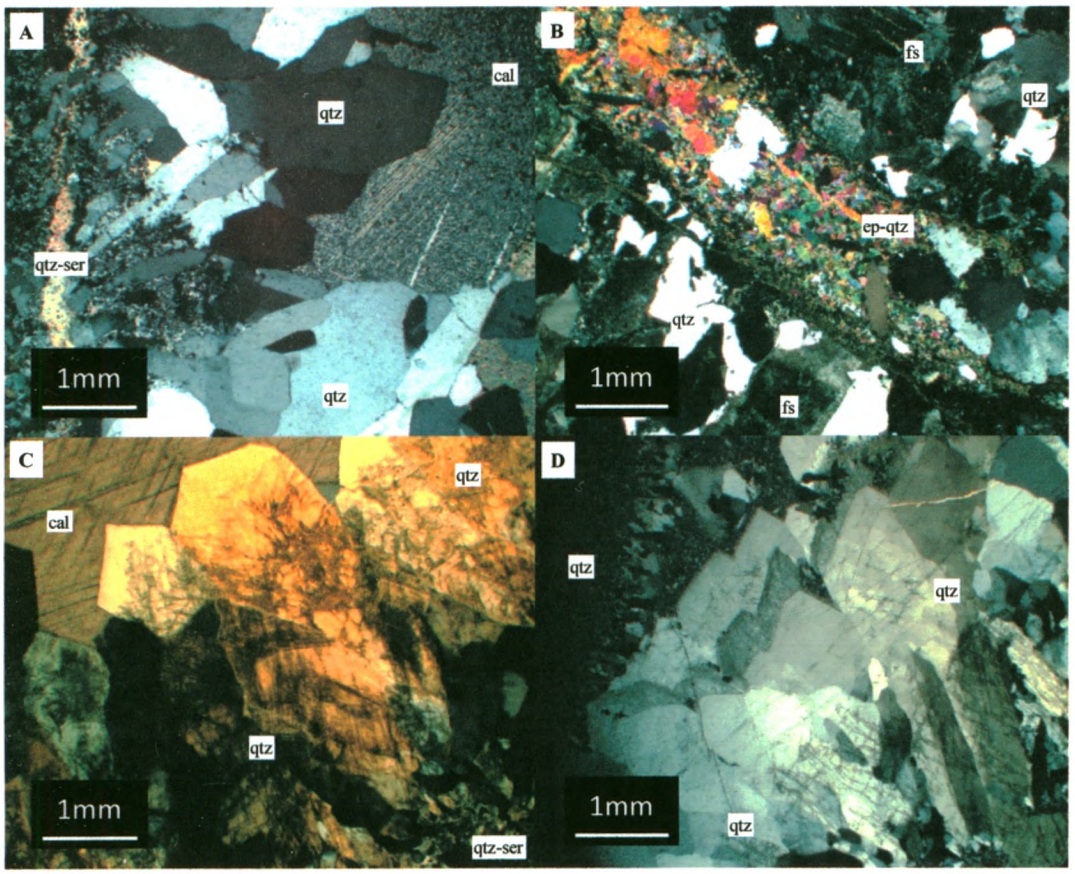

Figure 3.9. Photomicrographs of veins and veinlets from the Huntington Mountain pluton and East Bay Hills volcanic suite. A - CBI-6-6-17, well-defined quartz-calcite vein with medium-grained euhedral quartz and coarse-grained calcite, with a fine-grained quartz-sericite margin, hosted by rhyolite tuff. B - CBI-8-05-22, discontinuous quartz-epidote vein consisting of fine-grained subhedral quartz and epidote, hosted by granodiorite. C - CBI-6-6-112, well-defined quartz-calcite vein with medium-grained euhedral quartz and calcite, with fine-grained quartz-sericite along the margin of the vein, hosted by basalt. D - CBI-6-6-114, well-defined quartz vein with medium-grained quartz exhibiting multiple stages of growth, infilled by very fine-grained, amorphous silica within the interior of the vein, hosted by porphyritic quartz-feldspar rhyolite. Mineral abbreviations, cal - calcite, ep - epidote, fs - feldspar, qtz - quartz, ser - sericite.

3.4 Summary and Alteration Characteristics

The Huntington Mountain pluton and East Bay Hills volcanic suite represent cogenetic calc-alkaline magmatism, which is indicated by compositionally expanded granitoid rocks and volcanic rocks that are dominated by andesite to rhyolite. Given the close association with volcanic rocks of the same age, the abundance of granophyric textures and the development of weak porphyritic textures in some syenogranite and leucogranite rocks, it seems likely that magma emplacement occurred at high levels within the crust (e.g., Barr et al., 1996).

Three main types of alteration are observed in the rocks from Huntington Mountain pluton and the East Bay Hills volcanic suite (Table 3.1; Fig. 3.10). Type 1 consists of fine-grained chlorite, epidote, sericite and Fe-Ti oxides, and is considered a typical propylitic alteration assemblage (Meyer and Hemley, 1967), which likely formed within the temperature range of 300-450°C (Beane and Titley, 1981; Ferry, 1985; Criss and Taylor, 1986). This alteration is widespread throughout the study area, with its intensity varying from weak to strong, as defined by the abundance of alteration minerals. Generally, the rocks that experienced the greatest degree of propylitic alteration include areas within the syenogranite (Fig 3.10 - HHs), the granodiorite (Fig 3.10 - HHg), areas along the margin of the diorite (Fig 3.10 - HHd), the andesite (Fig 3.10 - HEac) and the dacite (Fig 3.10 - HHdt).

Type 2, quartz-sericite-calcite alteration consists of fine- to coarse-grained, anhedral quartz, sericite and calcite, with minor amounts of Fe-oxides, which likely formed within the temperature range of 200-300°C (Sheppard and Taylor, 1974; Beane and Titley, 1981). This type of alteration is more localized, including only a portion of

the basaltic unit along the shore of Bras d'Or Lake (Fig 3.10 - HEbs), the basaltic unit in the southwestern margin of the study area (Fig 3.10 - HEab), the andesite to rhyolite (Fig 3.10 - HEad) and the rhyolite in the northeastern margin of the study area (Fig. 3.10 - HEr). The alteration varies in intensity from moderate to strong, with primary minerals and textures generally having been partially to completely overprinted (e.g., Fig. 3.8). This alteration also appears to overprint, and hence, postdate the propylitic alteration (e.g., Fig. 3.4).

Type 3 consists of quartz, sericite and pyrite, and is considered a typical phyllic alteration assemblage (Meyer and Hemley, 1967), which likely formed at a temperature of ~600°C (Sheppard and Taylor, 1974; Beane and Titley, 1981). This alteration affects only a small number of samples (CBI-8-05-28; CBI-6-6-102 to CBI-6-6-104) and varies in intensity from moderate to strong, with most primary minerals having been partially overprinted by fine-grained, euhedral quartz, sericite and to a lesser extent pyrite. In one dioritic sample, CBI-6-6-103, all primary minerals and textures have been completely overprinted by this alteration (e.g., Fig. 3.3B). Phyllic alteration occurs mainly as localized zones in the diorite (Fig. 3.10 - HHd) and dacite (Fig. 3.10 - HEdt), which suggests that it may have developed during post-crystallization contact metamorphism between the two rock units (e.g., Meyer and Hemley, 1967). This interpretation is consistent with Barr et al. (1996), who observed features typical of contact metamorphism within the dacite, including the development of a hornfelic texture and pyrite mineralization. In one area (CBI-6-6-104), the phyllic alteration appears to be overprinted by the propylitic alteration (e.g., Fig. 3.5).

Table 3.1. Alteration types affecting the Huntington Mountain pluton and East Bay Hills volcanic suite.

Alteration Type	Localities	Mineralogy	Temperature*
(1) propylitic	All units	chlorite, epidote, sericite, Fe-Ti-oxides	[a]300-450°C
(2) quartz-sericite-calcite	localized areas of HEbs, HEab, HEad, HEr	quartz, sericite, calcite, Fe-oxides	[b]200-300°C
(3) phyllic	localized areas of HHd, HEdt	quartz, sericite, pyrite	[c]~600°C

*Temperature estimates based on: a - Beane and Titley, 1981; Ferry, 1985; Criss and Taylor, 1986, and, b and c - Sheppard and Taylor, 1974; Beane and Titley, 1981.

Figure 3.10. Alteration map of the Huntington Mountain pluton and East Bay Hills volcanic suite, including sample localities and geology.

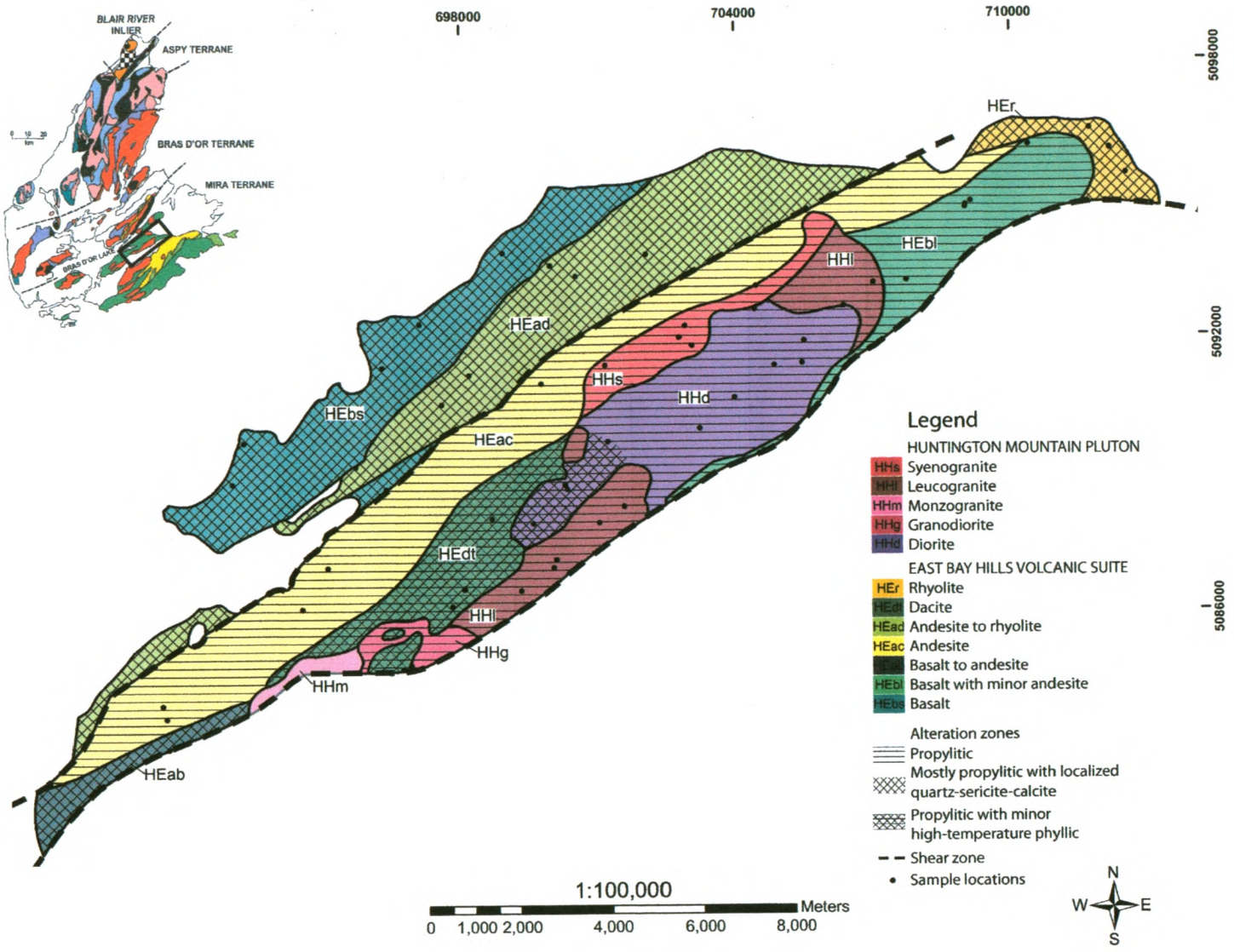
BLAIR RIVER INLIER
ASPY TERRANE
BRAS D'OR TERRANE
MIRA TERRANE
BRAS D'OR LAKE
0 10 20 km
698000
704000
710000
5098000
5092000
5086000
HEr
HEbl
HHl
HEad
HHs
HHd
HEbs
HEac
HEdt
HHl
HHg
HHm
HEab
Legend
HUNTINGTON MOUNTAIN PLUTON
HHs Syenogranite
HHl Leucogranite
HHm Monzogranite
HHg Granodiorite
HHd Diorite
EAST BAY HILLS VOLCANIC SUITE
HEr Rhyolite
HEdt Dacite
HEad Andesite to rhyolite
HEac Andesite
Basalt to andesite
HEbl Basalt with minor andesite
HEbs Basalt
Alteration zones
Propylitic
Mostly propylitic with localized quartz-sericite-calcite
Propylitic with minor high-temperature phyllic
Shear zone
Sample locations
1:100,000
Meters
0 1,000 2,000 4,000 6,000 8,000
N
W
E
S

Chapter 4. Stable Isotope Geochemistry of the Huntington Mountain Pluton and the East Bay Hills Volcanic Suite

4.1 Introduction

Oxygen- and hydrogen-isotope ratios have been used successfully in a variety of geologic settings to understand better the alteration of volcanic and plutonic rocks. Such data have been particularly important in understanding the evolution of hydrothermal fluids and the relative role of magmatic versus meteoric water (or seawater) in the formation of epithermal gold deposits (e.g., Field and Fifarek, 1985), base- and precious-metal porphyry deposits (e.g., Sheppard et al., 1971) and submarine volcanic-hosted massive sulphide deposits (e.g., Beaty and Taylor, 1982), as well as numerous non-mineralized systems (e.g., Taylor, 1971).

It is well established that the oxygen- and hydrogen-isotope ratios of silicate minerals and rocks can be used to suggest likely fluid source reservoirs (e.g., Sheppard, 1986). Typically, $\delta^{18}O$ values of magmatic water can range from +5 to +10‰, whereas surface water generally has $\delta^{18}O$ values that range from –20 to 0‰ (Sheppard, 1986). The δD values of both fluids are widely variable; however, magmatic water generally has a range of –85 to –50‰, while surficial water ranges from –120 to 0‰ (Sheppard, 1986). Silicate minerals in normal, unaltered igneous rocks have $\delta^{18}O$ values similar to those of magmatic water (Taylor, 1968). By comparing the oxygen- and hydrogen-isotope ratios obtained for a silicate rock or mineral with the typical $\delta^{18}O$ and δD values of normal igneous rocks and surface water, it may then be possible to determine whether the silicate rock or mineral has experienced post-crystallization interaction with surface water (i.e., seawater and/or meteoric water) over a range of temperatures. In particular,

^{18}O-depletion in rocks and minerals from normal igneous values is generally associated with interaction with hydrothermal fluids derived from seawater or meteoric water (e.g., Taylor, 1974).

The oxygen- and carbon-isotope ratios of hydrothermal calcite can also be used to suggest likely fluid reservoirs (e.g., Ohmoto and Rye, 1979). Typically, calcite formed from hydrothermal fluids that have interacted with igneous rocks would likely have $\delta^{18}O$ values of ~+8 to +15‰ and $\delta^{13}C$ values of ~ –15 to –5‰, while calcite formed from a meteoric-dominated hydrothermal fluid would have lower $\delta^{18}O$ and $\delta^{13}C$ values, <+8‰ for oxygen and ~ –35 to –10‰ for carbon (Ohmoto and Rye, 1979). Calcite derived from marine carbonate rocks would likely have $\delta^{18}O$ and $\delta^{13}C$ values of >+30‰ and ~0‰, respectively (Ohmoto and Rye, 1979).

The purpose of this chapter is to present and discuss the oxygen-, hydrogen- and carbon-isotope results for the Huntington Mountain pluton and East Bay Hills volcanic suite, with the purpose of determining the fluid source(s) and conditions responsible for post-crystallization hydrothermal alteration.

4.2 Oxygen-, Hydrogen- and Carbon-isotope Results

4.2.1 Whole-Rock Results

The whole-rock oxygen-isotope ($\delta^{18}O_{WR}$) results for the Huntington Mountain pluton and the East Bay Hills Volcanic suite are listed in Table 4.1. A total of 17 plutonic and 28 volcanic whole-rock samples were analyzed. The $\delta^{18}O_{WR}$ values of

plutonic rock samples range from –1.5 to +6.2‰. Volcanic rock samples have a wider range of values, from –3.8 to +9.5‰, but only three samples have values >+6.5‰.

The $\delta^{18}O_{WR}$ values of the diorite and granodiorite samples of the Huntington Mountain pluton range from –1.5 to +4.5‰, while syenogranite samples have slightly higher values, from –1.2 to +6.2‰. Leucogranite samples range in $\delta^{18}O_{WR}$ values from +0.2 to +7.1‰. Dacite samples are the most ^{18}O-depleted rocks of the East Bay Hills volcanic suite, with $\delta^{18}O_{WR}$ values of –3.8 to +0.6‰. Basaltic and andesitic samples present the widest range of $\delta^{18}O_{WR}$ values, from –1.9 to +9.5‰. Andesite-rhyolite and rhyolite samples also have a wide range of $\delta^{18}O_{WR}$ values, from +1.8 to +6.9‰, although rhyolite samples generally have higher values (>+4.6‰).

The whole-rock hydrogen-isotope (δD_{WR}) results for the Huntington Mountain pluton and East Bay Hills volcanic suite are also listed in Table 4.1. A total of 9 plutonic and 5 volcanic whole-rock samples were analyzed. The δD_{WR} values of samples from Huntington Mountain pluton range from –78 to –56‰, while samples from East Bay Hills volcanic suite have a slightly lower range of δD_{WR} values, from –93 to –70‰.

The plutonic rock samples tend to have higher δD_{WR} values than the volcanic rocks, ranging from –78 to –62‰ for diorite-granodiorite, –71 to –61‰ for syenogranite and –60 to –56‰ for leucogranite. The basaltic to andesitic samples have the lowest δD_{WR} values, with a range of –93 to –70‰. The other volcanic samples analyzed have δD_{WR} values of –70‰ for dacite and –77‰ for andesite-rhyolite.

4.2.2 Mineral Results

A total of 74 mineral samples from Huntington Mountain pluton and East Bay Hills volcanic suite were isolated for oxygen-isotope analysis, of which 6 samples of chlorite and one sample of sericite were further used for hydrogen-isotope analysis, and 10 calcite samples were analyzed for their oxygen- and carbon-isotope compositions. Mineral oxygen-isotope ($\delta^{18}O$), hydrogen-isotope (δD) and carbon-isotope ($\delta^{13}C$) results are listed in Table 4.1. The $\delta^{18}O$ values of mineral samples from the plutonic rocks range from –6.3 to +8.4‰, excepting one anomalous value of +15.1‰ for quartz reported earlier by Potter et al. (2008), while mineral separates from the volcanic rocks have a range of –5.3 to 14.3‰. The δD values of plutonic mineral samples range from –77 to –62‰, and one volcanic mineral sample yielded a δD value of –69‰. The $\delta^{13}C$ value of calcite from two plutonic rocks ranged from –3.8 to +0.1‰, while calcite from volcanic rock samples had $\delta^{13}C$ values of –7.4 to –3.2‰.

Minerals from the Plutonic Rock Suite

Quartz exhibited the greatest variability in $\delta^{18}O$ values with a range of –2.1 to +15.1‰. Quartz grains obtained from leucogranite yielded the highest $\delta^{18}O$ values for plutonic mineral samples, with a range of +4.8 to +15.1‰. A much lower range of $\delta^{18}O$ values observed in the quartz grains from the other felsic intrusions, with quartz from syenogranite having a range of +0.5 to +4.3‰, and quartz from granodiorite having a range of +1.3 to +1.5‰. Quartz from one diorite sample (CBI-6-6-103) had a $\delta^{18}O$ value of +3.3‰, which based on petrographic textures, represents secondary quartz, while quartz related to a small granite dyke within the diorite (CBI-8-05-27A) had a $\delta^{18}O$ value

of +4.8‰. Additionally, one quartz vein sample, which was obtained from a discontinuous quartz vein hosted by diorite (CBI-6-6-104), represented the most ^{18}O-depleted quartz sample, with a $\delta^{18}O$ value of –2.1‰. Disseminated calcite from the diorite (CBI-6-6-102) had a $\delta^{18}O$ value of +5.4‰ and a $\delta^{13}C$ value +0.1‰.

Feldspar samples from the plutonic rock suite ranged in $\delta^{18}O$ values from +1.4 to +5.2‰. Feldspar from leucogranite had the highest $\delta^{18}O$ values, with a range of +4.4 to +6.0‰, while $\delta^{18}O$ values of feldspar from syenogranite and granodiorite ranged from +1.8 to +3.5‰ and +2.9 to +3.1‰, respectively. A restricted range of $\delta^{18}O$ values was also obtained for feldspar from the diorite, +1.4 to +4.6‰, with only one sample (CBI-6-6-102) having a value <+2.4‰. Sericite from the plutonic rocks generally had similar values to feldspar, with $\delta^{18}O$ values of +1.4‰ (CBI-6-6-102) and +2.0‰ (CBI-6-6-103).

Mafic minerals obtained from the plutonic rocks had $\delta^{18}O$ values of –6.3 to +5.5‰. Hornblende samples, which were obtained only from diorite, had $\delta^{18}O$ values of +1.4 to +5.5‰. Chlorite generally had the lowest $\delta^{18}O$ values obtained for either the plutonic or volcanic rock suites, ranging from –6.3 to +3.3‰, with only one sample having a $\delta^{18}O$ value >+1.0‰. The δD values of chlorite from the plutonic rock suite ranged from –77 to –69‰, which is consistent with other plutonic and volcanic whole-rock δD values obtained during this study (Table 4.1).

Minerals from the Volcanic Rock Suite

Similar to the plutonic rock suite, quartz obtained from the volcanic rocks had a wide range of $\delta^{18}O$ values, –1.5 to +11.7‰. The majority of quartz from the volcanic

rocks comprises medium- or coarse-grained, phenocryst-like crystals or veins, with only one sample of fine-grained groundmass quartz. The latter quartz samples obtained from the groundmass of rhyolite has a $\delta^{18}O$ value of +8.2‰ (CBI-8-05-30). A wide range of $\delta^{18}O$ values was obtained for the medium- or coarse-grained quartz, from –1.5 to +11.7‰. However, based on petrographic textures (e.g., euhedral grain shapes and association with primary minerals), only one sample appears to represent primary quartz phenocrysts: a porphyritic rhyolite dyke with a $\delta^{18}O$ value of +6.4‰ (CBI-6-6-111). The other three quartz samples, which represent secondary quartz, had $\delta^{18}O$ values of –1.5‰ (dacite, CBI-8-05-28), +11.1‰ (andesite, CBI-6-6-52), and +11.7‰ (basalt to andesite, CBI-6-6-11). Quartz veins hosted by the volcanic rock samples generally had high $\delta^{18}O$ values, ranging from +6.1 to +10.5‰. Calcite obtained from these quartz veins had $\delta^{18}O$ values ranging from +6.0 to +14.3‰, and $\delta^{13}C$ values ranging from –7.4 to –3.2‰. Disseminated calcite had similar $\delta^{18}O$ and $\delta^{13}C$ values, ranging from +5.9 to +11.7‰ and –7.2 to –4.5‰, respectively.

Feldspar phenocrysts obtained from the volcanic rock suite had a wide range of $\delta^{18}O$ values, from –0.3 to +6.5‰. One feldspar sample from an andesitic crystal tuff (CBI-6-6-52) had a $\delta^{18}O$ value of –0.3‰, which represents the most ^{18}O-depleted feldspar sample obtained in this study. The felsic volcanic rocks had higher $\delta^{18}O$ values for feldspar, +3.3‰ for a rhyolite dyke (CBI-6-6-111) and +6.5‰ for a flow-banded rhyolite (CBI-8-05-30). Chlorite, from an andesitic crystal tuff (CBI-6-6-52) had a $\delta^{18}O$ value of –5.3‰ and a δD value of –69‰, which is similar to the results obtained for the plutonic rocks.

Table 4.1. Oxygen-, Hydrogen- and Carbon-isotope Results for the Huntington Mountain Pluton and East Bay Hills Volcanic Suite

Sample	Rock Unit	$\delta^{18}O_{wr}$	δD_{wr}	$\delta^{18}O_{qtz}$	$\delta^{18}O_{fs}$	$\delta^{18}O_{hbl}$	$\delta^{18}O_{chl}$	δD_{chl}	$\delta^{18}O_{ser}$	δD_{ser}	$\delta^{18}O_{cal}$	$\delta^{13}C_{cal}$
Huntington Mountain Pluton												
CBI-8-05-23	Leucogranite	5.9	-	6.4	5.2	-	[a]1.0	-	-	-	-	-
CBI-6-6-81	Leucogranite	5.8	-	6.2	5.0	-	[a]-1.2	-	-	-	-	-
CBI-6-6-105	Leucogranite	3.8	-56	4.8	4.4	-	[a]-3.3	-	-	-	-	-
CBI-6-6-106	Leucogranite	5.4	-	7.0	5.2	-	[a]-0.2	-	-	-	-	-
[c]EB91-014	Leucogranite	7.1	-60	[a]15.1	6.0	-	-	-	-	-	[a]8.4	[a]-3.8
[c]F16C-1582	Leucogranite	0.2	-	-	-	-	-	-	-	-	-	-
CBI-6-6-54	Syenogranite	6.2	-71	4.3	3.5	-	[a]-4.8	-	-	-	-	-
CBI-6-6-55	Syenogranite	1.4	-61	0.5	1.8	-	[a]-6.3	-	-	-	-	-
[c]F16C-1631	Syenogranite	4.3	-	-	-	-		-	-	-	-	-
[c]F16C-1635	Syenogranite	-1.2	-70	-	-	-	-	-	-	-	-	-
[c]F16C-1782	Syenogranite	5.5	-	-	-	-	-	-	-	-	-	-
CBI-8-05-21	Granodiorite	-	-	1.3	2.9	-	[a]-4.0	-	-	-	-	-
CBI-8-05-22	Granodiorite	1.2	-62	1.5	3.1	-	[a]-5.3	-	-	-	-	-
CBI-8-05-25	Diorite	2.7	-69	-	2.5	3.9	[a]-0.8	[a]-73	-	-	-	-
CBI-8-05-26	Diorite	-	-	-	3.6	-	[a]-0.7	-	-	-	-	-
CBI-8-05-27A	Diorite	-	-	4.8	3.8	-	[a]-1.7	-	-	-	-	-
CBI-8-05-27B	Diorite	-	-	-	-	-	[a]-1.0	-	-	-	-	-
CBI-6-6-56	Diorite	1.7	-72	-	2.5	1.7	[a]-5.2	[a]-73	-	-	-	-
CBI-6-6-82	Diorite	3.8	-	-	3.9	4.6	[a]0.1	-	-	-	-	-
CBI-6-6-83	Diorite	4.5	-78	-	4.3	5.5	[a]3.3	[a]-69	-	-	-	-
CBI-6-6-84	Diorite	2.2	-	-	2.4	3.5	-	-	-	-	-	-
CBI-6-6-86	Diorite	3.6	-69	-	4.6	3.3	[a]0.6	[a]-77	-	-	-	-
CBI-6-6-87	Diorite	3.6	-	-	3.8	4.5	-	-	-	-	-	-

Table 4.1. O-, H- and C-isotope Results (continued)

Sample	Rock Unit	$\delta^{18}O_{wr}$	δD_{wr}	$\delta^{18}O_{qtz}$	$\delta^{18}O_{fs}$	$\delta^{18}O_{hbl}$	$\delta^{18}O_{chl}$	δD_{chl}	$\delta^{18}O_{ser}$	δD_{ser}	$\delta^{18}O_{cal}$	$\delta^{13}C_{cal}$
Huntington Mountain Pluton												
CBI-6-6-102	Diorite	1.0	-	-	1.4	1.4	-	-	-	[a]-74	[a]5.4	[a]0.1
CBI-6-6-103	Diorite	1.9	-	[a]3.3	-	-	-	-	[a]2.0	[a]-62	-	-
CBI-6-6-104	Diorite	-1.5	-68	[b]-2.1	-	-	-	-	-	-	-	-
[c]F16C-1751	Diorite	3.1	-	-	-	-	-	-	-	-	-	-
East Bay Hills Volcanic Suite												
CBI-8-05-30	Rhyolite	6.6	-	8.2	6.5	-	-	-	-	-	-	-
		-	-	[b]10.1	-	-	-	-	-	-	[b]12.1	[b]-7.3
CBI-6-6-17	Rhyolite	5.5	-	-	-	-	-	-	-	-	[a]9.4	[a]-5.0
		-	-	[b]9.1	-	-	-	-	-	-	[b]7.3	[b]-5.2
CBI-6-6-80	Rhyolite	6.9	-	-	-	-	-	-	-	-	-	-
[c]FS91-53	Rhyolite	4.6	-	-	-	-	-	-	-	-	-	-
CBI-8-05-28	Dacite	-2.6	-70	-1.5	-	-	-	-	-	-	-	-
CBI-6-6-98	Dacite	-0.1	-	-	-	-	-	-	-	-	-	-
CBI-6-6-99	Dacite	0.6	-	-	-	-	-	-	-	-	-	-
CBI-6-6-101	Dacite	-3.8	-	-	-	-	-	-	-	-	-	-
CBI-6-6-93	Andesite to Rhyolite	1.8	-	-	-	-	-	-	-	-	-	-
CBI-6-6-94	Andesite to Rhyolite	4.1	-	-	-	-	-	-	-	-	-	-
CBI-6-6-95	Andesite to Rhyolite	-	-	[b]7.7	-	-	-	-	-	-	-	-
CBI-6-6-96	Andesite to Rhyolite	4.0	-	-	-	-	-	-	-	-	-	-
CBI-6-6-118	Andesite to Rhyolite	3.6	-	-	-	-	-	-	-	-	-	-
CBI-6-6-119	Andesite to Rhyolite	3.9	-77	-	-	-	-	-	-	-	[b]6.0	[b]-3.2
CBI-6-6-121	Andesite to Rhyolite	6.5	-	-	-	-	-	-	-	-	-	-

Table 4.1. O-, H- and C-isotope Results (continued)

Sample	Rock Unit	$\delta^{18}O_{wr}$	δD_{wr}	$\delta^{18}O_{qtz}$	$\delta^{18}O_{fs}$	$\delta^{18}O_{hbl}$	$\delta^{18}O_{chl}$	δD_{chl}	$\delta^{18}O_{ser}$	δD_{ser}	$\delta^{18}O_{cal}$	$\delta^{13}C_{cal}$
East Bay Hills Volcanic Suite												
CBI-6-6-50	Andesite	-0.5	-	-	-	-	-	-	-	-	-	-
CBI-6-6-51	Andesite	-0.7	-	-	-	-	-	-	-	-	-	-
CBI-6-6-52	Andesite	-0.6	-	[a]11.1	-0.3	-	[a]-5.3	[a]-69	-	-	-	-
CBI-6-6-89	Andesite	-1.1	-	-	-	-	-	-	-	-	-	-
CBI-6-6-90	Andesite	-1.9	-	-	-	-	-	-	-	-	-	-
[c]EB87-037	Andesite	0.5	-82	-	-	-	-	-	-	-	-	-
CBI-6-6-11	Basalt to Andesite	9.5	-93	[a]11.7	-	-	-	-	-	-	[a]9.8	[a]-4.5
CBI-6-6-88	Basalt to Andesite	-1.9	-79	-	-	-	-	-	-	-	-	-
CBI-6-6-110	Basalt to Andesite	0.0	-	-	-	-	-	-	-	-	-	-
CBI-6-6-111	Basalt to Andesite	3.3	-	6.4	3.3	-	-	-	-	-	-	-
CBI-6-6-112	Basalt to Andesite	-1.7	-	-	-	-	-	-	-	-	-	-
CBI-6-6-112A	Basalt to Andesite	-	-	[b]8.6	-	-	-	-	-	-	-	-
CBI-6-6-112B	Basalt to Andesite	-	-	[b]10.5	-	-	-	-	-	-	[b]14.3	[b]-7.4
CBI-6-6-112C	Basalt to Andesite	-	-	[b]7.9	-	-	-	-	-	-	-	-
CBI-6-6-114	Basalt to Andesite	5.4	-	-	-	-	-	-	-	-	-	-
CBI-6-6-38	Basalt	-	-	[b]6.1	-	-	-	-	-	-	-	-
CBI-6-6-39	Basalt	3.0	-	-	-	-	-	-	-	-	-	-
CBI-6-6-40	Basalt	1.9	-70	-	-	-	-	-	-	-	-	-
CBI-6-6-107	Basalt	3.1	-	-	-	-	-	-	-	-	[a]11.7	[a]-7.2
CBI-6-6-122	Basalt	5.7	-	-	-	-	-	-	-	-	[a]5.8	[a]-4.5
[c]MT6-397	Basalt	6.2	-	-	-	-	-	-	-	-	-	-

Note: a = disseminated secondary mineral; b = vein mineral; c = previously reported by Potter et al. (2008).
Mineral abbreviations, cal - calcite, chl - chlorite, fs - feldspar, hbl - hornblende, qtz - quartz, ser - sericite.

Chapter 5. Discussion

5.1 Significance of the Oxygen-isotope Results

Samples from the Huntington Mountain pluton have low $\delta^{18}O$ values, ranging from –1.5 to +6.2‰, while the samples from the East Bay Hills volcanic suite exhibit a wider range, from –3.8 to +9.2‰. The $\delta^{18}O$ values of normal unaltered plutonic and volcanic rocks, by comparison, typically range from ~ +6‰ for mafic rocks to ~ +10‰ for felsic rocks. Taylor (1968, 1974) has shown that fresh unaltered andesitic and basaltic rocks generally have uniform $\delta^{18}O$ values that range from +5.5 to +6.5‰, while fresh unaltered granites generally have $\delta^{18}O$ values ranging from +7.5 to +9.5‰. The results of the present study show that the majority of oxygen-isotope results from the Huntington Mountain pluton and East Bay Hills volcanic suite have $\delta^{18}O$ values lower than normal, unaltered igneous rocks (Fig. 5.1). For the Huntington Mountain plutonic suite, only two samples have $\delta^{18}O_{WR}$ values >+6‰ (Fig. 5.1A), while the East Bay Hills volcanic suite contains only five samples with $\delta^{18}O_{WR}$ values >+6‰ (Fig. 5.1B), out of a total of 54 whole-rock samples analyzed. A large majority of the samples from the Huntington Mountain pluton have $\delta^{18}O_{WR}$ values that range from +2 to +4‰, and in the East Bay Hills volcanic suite, a large number of samples have still lower values, ranging from –2 to 0‰.

Typically, igneous rocks with high $\delta^{18}O$ values (>+10‰) have either formed by the interaction with, or anatexis of high-^{18}O sedimentary rocks, or by low-temperature alteration (<200°C) (Longstaffe, 1982; Criss et al., 1984). In the latter setting, ^{18}O-enrichment of igneous rocks is a product of the larger isotopic fractionation between mineral(s) and water at lower temperatures (<200°C). This produces secondary minerals

with high $\delta^{18}O$ values, and/or, more rarely, partial to complete oxygen-isotope exchange of primary minerals (to generally higher values) with high-^{18}O hydrothermal fluids (Criss et al., 1984).

Igneous rocks with low $\delta^{18}O$ values (<+6‰) generally form either by the formation of a low-^{18}O magma though assimilation of low-^{18}O rocks that have previously interacted with low-^{18}O hydrothermal fluids (Taylor and Sheppard, 1986), or by post-magmatic water-rock interaction with meteoric-dominated hydrothermal fluids (or seawater) at high-temperature (~300-500°C) (e.g., Taylor, 1968, 1974; Criss and Taylor, 1986). In the latter example, common characteristics of hydrothermal fluids interacting with igneous rocks typically includes the development of secondary alteration minerals, such as alkali-feldspar, quartz, carbonate, sericite and epidote, saussuritization of feldspar, with its partial to complete replacement by sericite and epidote, and replacement of biotite by chlorite, and ilmenite by titanite-leucoxene (Taylor, 1974). In contrast, low-^{18}O igneous rocks that are formed by the assimilation of a low-^{18}O protolith are composed mostly of primary minerals, and lack secondary alteration minerals (Taylor and Sheppard, 1986).

Samples obtained from the Huntington Mountain pluton and East Bay Hills volcanic suite exhibit strong textural evidence for post-crystallization hydrothermal alteration. These features include partial to complete replacement of primary igneous minerals and textures by secondary alteration minerals, a range of alteration assemblages suggesting varying hydrothermal fluid temperatures, and the formation of secondary minerals along primary mineral grain boundaries and as fracture-filling veins. In addition, the vast majority of whole-rock and mineral samples have low $\delta^{18}O$ values

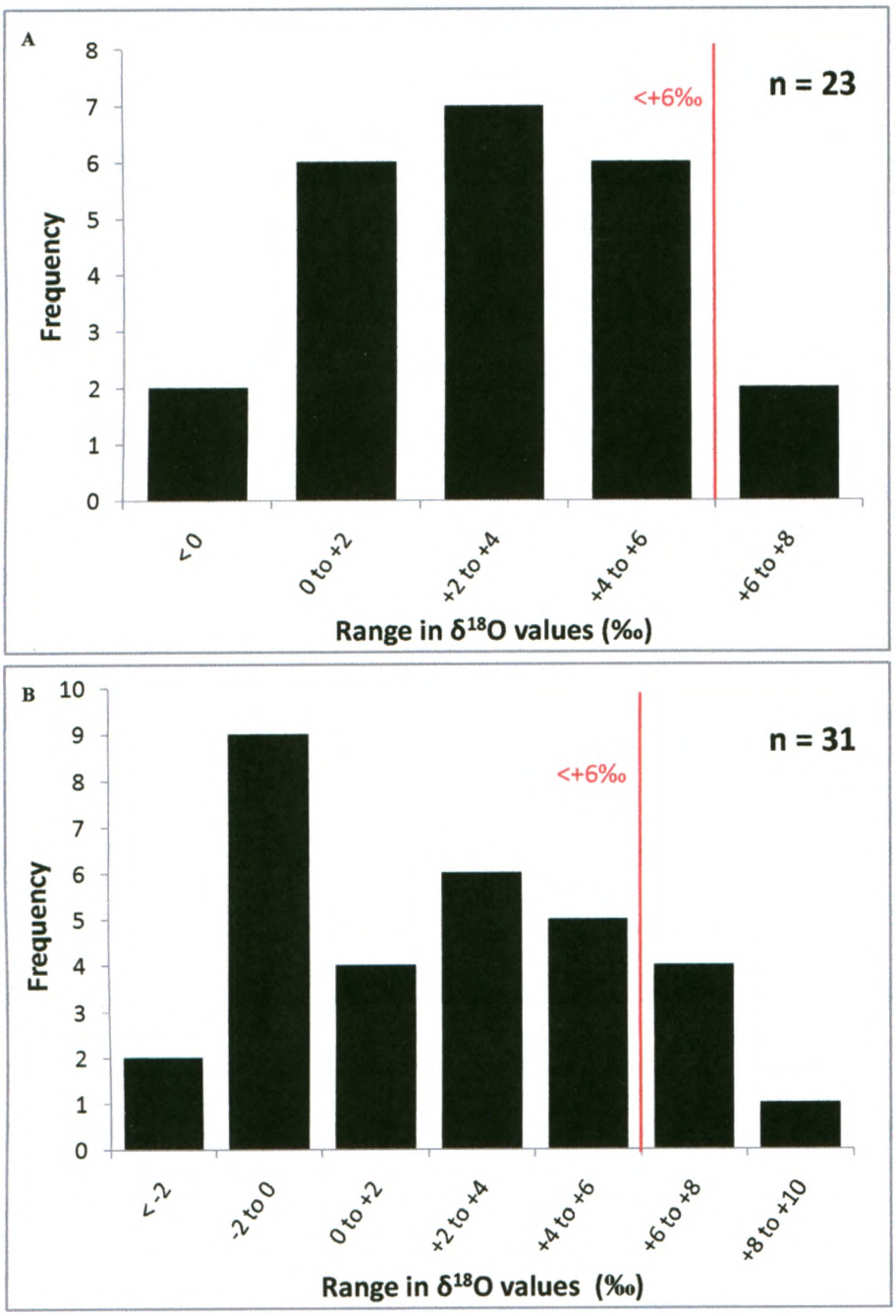

Figure 5.1. Histograms of $\delta^{18}O_{WR}$ values obtained for the Huntington Mountain pluton (A) and East Bay Hills volcanic suite (B). The lower limit of $\delta^{18}O$ values for normal igneous rocks is also shown (+6‰) (e.g., Taylor, 1974).

(<+6‰), which suggests water-rock interaction with low $\delta^{18}O$ hydrothermal fluids. On this basis, it is unlikely that the low $\delta^{18}O$ values obtained for the Huntington Mountain pluton and East Bay Hills volcanic suite were acquired by assimilation of a low-^{18}O protolith. A general inverse correlation exists between the degree of sample alteration and their $\delta^{18}O$ values. Samples that exhibit high-temperature propylitic alteration generally have the lowest $\delta^{18}O$ values, whereas other samples characterized by lower temperature quartz-calcite-sericite alteration have somewhat higher $\delta^{18}O$ values (Fig. 5.2, Appendix B). Chlorite, a dominant mineral in the propylitic alteration assemblage, is the most abundant secondary mineral in the Huntington Mountain pluton and East Bay Hills volcanic suite, and commonly occurs together with epidote, sericite, quartz, ilmenite and Fe-oxides. Texturally, the propylitic assemblage is characterized by fine-grained, pervasive alteration. Chlorite from the two suites has $\delta^{18}O$ values ranging from –6.3 to +3.3‰, with the majority <0‰. A few chlorite samples have $\delta^{18}O$ values >0‰, and are likely the product of reaction at lower water/rock ratios. In this latter scenario, chlorite likely formed as a partial replacement of primary hornblende and biotite, inheriting a portion of its oxygen-isotope ratio from its precursors.

The low $\delta^{18}O$ values obtained for most chlorite samples, and their general association with other secondary minerals, suggest that chlorite likely crystallized from high-temperature, low-^{18}O hydrothermal fluids. The hydrothermal fluid responsible for the widespread propylitic alteration was likely a meteoric-dominated hydrothermal fluid. Potter et al. (2008) also recognized the widespread occurrence of propylitic alteration in the igneous rocks across the Mira terrane, and its general correlation with low $\delta^{18}O$ values.

Figure 5.2. Map of the Huntington Mountain pluton and East Bay Hills volcanic suite illustrating the alteration characteristics and $\delta^{18}O$ values (‰) of samples from this study and Potter et al. (2008).

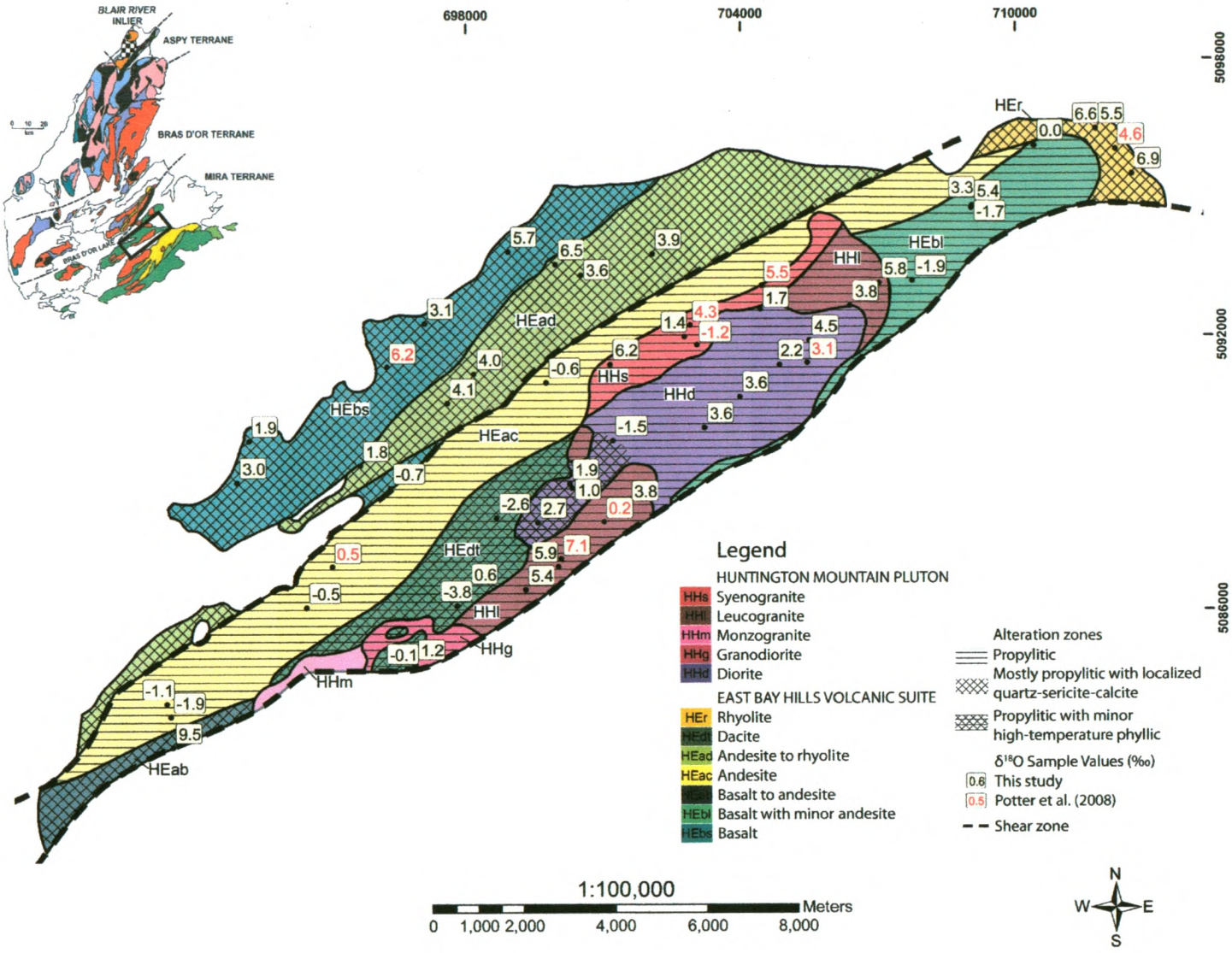
BLAIR RIVER INLIER
ASPY TERRANE
BRAS D'OR TERRANE
MIRA TERRANE
BRAS D'OR LAKE
698000
704000
710000
5098000
5092000
5086000
HEr
HEdt
HEad
HEac
HEab
HEbl
HEbs
HHl
HHs
HHd
HHm
HHg
Legend
HUNTINGTON MOUNTAIN PLUTON
HHs Syenogranite
HHl Leucogranite
HHm Monzogranite
HHg Granodiorite
HHd Diorite
EAST BAY HILLS VOLCANIC SUITE
HEr Rhyolite
HEdt Dacite
HEad Andesite to rhyolite
HEac Andesite
HEab Basalt to andesite
HEbl Basalt with minor andesite
HEbs Basalt
Alteration zones
Propylitic
Mostly propylitic with localized quartz-sericite-calcite
Propylitic with minor high-temperature phyllic
δ18O Sample Values (‰)
0.6 This study
0.5 Potter et al. (2008)
Shear zone
1:100,000
0 1,000 2,000 4,000 6,000 8,000 Meters
N
W
E
S

Secondary quartz and calcite from the Huntington Mountain pluton and East Bay Hills volcanic suite have a large range of $\delta^{18}O$ values, from +3.3 to +15.1‰, although the majority are >+5.4‰. Calcite samples have $\delta^{18}O$ values that range from +5.4 to +9.8‰, while three secondary quartz samples have slightly higher values, ranging from +11.1 to +15.1‰. The large number of high $\delta^{18}O$ values obtained for secondary quartz and calcite, and their common association with each other, and with secondary sericite, suggest their crystallization from lower temperature, low-^{18}O hydrothermal fluids. Secondary quartz, sericite and calcite, which comprise the lower temperature alteration assemblage, form localized alteration zones that commonly overprint primary igneous minerals (e.g., Fig 3.8), and in some areas (e.g., sample CBI-6-6-11), have completely replaced all primary igneous minerals and textures (e.g., Fig. 3.7C). In another area (CBI-8-05-26), secondary quartz and calcite overprint secondary chlorite and epidote, which implies that the high-temperature propylitic alteration predated the quartz-sericite-calcite alteration (e.g., Fig. 3.4). On this basis, it is suggested that all secondary quartz and calcite with $\delta^{18}O$ values >+5.4‰, and likely all occurrences of the lower temperature quartz-sericite-calcite alteration assemblage, formed from low-^{18}O meteoric-dominated hydrothermal fluids at ~200 to 300°C (Section 3.4), which postdated formation of the widespread higher temperature (~300 to 450°C) propylitic alteration assemblage (Section 3.4).

It is also apparent that, although a general correlation between alteration and ^{18}O-depletion exists for most plutonic and volcanic rock samples, the trend is not sustained for a small number of plutonic and volcanic rock samples, which include CBI-6-6-54 (syenogranite) with a $\delta^{18}O_{WR}$ value of +6.2‰, EB91-014 (leucogranite) with a $\delta^{18}O_{WR}$

value of +7.1‰, and CBI-6-6-40 (basalt) with a $\delta^{18}O_{WR}$ value of +1.9‰ (Appendix B). For these (and other) anomalous samples, the $\delta^{18}O$ values seem to be influenced by additional parameters that determine local water/rock ratios and the degree of alteration. These parameters typically include rock type, previous alteration and regional-scale structures in the study area.

Rock type appears to be a major control on the ^{18}O-depletion (or ^{18}O-enrichment) of most samples. Diorite samples mainly have low $\delta^{18}O$ values, with only one sample >+3.8‰ (Fig. 5.2 - HHd), while leucogranite samples typically have higher $\delta^{18}O$ values, with only one sample <+3.8‰ (Fig. 5.2 - HHl). Similarly, basaltic samples generally have low $\delta^{18}O$ values with the majority <+5.4‰ (Fig. 5.2 - HEab, HEbl, HEbs), while rhyolite samples have higher $\delta^{18}O$ values, with only one sample <+5.5‰ (Fig. 5.2 - HEr). The correlation between rock type and $\delta^{18}O$ values is mainly dependent on the percentage of primary mafic versus felsic minerals.

The mineralogy of a rock, in particular its percentage of mafic versus felsic minerals, and Ca-rich plagioclase versus Na-rich plagioclase, is an important control on oxygen-isotope compositions, given that mafic minerals and Ca-rich plagioclase are generally the least resistant to interaction with hydrothermal fluids and are partially to completely replaced by secondary alteration minerals (Taylor, 1971; Criss and Taylor, 1986). Olivine, pyroxene, hornblende and biotite are typically replaced by chlorite-epidote-Fe-oxides, and Ca-rich plagioclase, which is also a common constituent of mafic rocks, is normally replaced by epidote-sericite, with minor calcite. The secondary minerals produced during this process generally acquire their oxygen-isotope ratios through exchange with the hydrothermal fluids. Therefore, a mafic rock initially

containing a large percentage of primary mafic minerals and Ca-rich plagioclase altered to secondary phases would more likely acquire $\delta^{18}O$ values that reflect the oxygen-isotope composition of the hydrothermal fluid than a felsic rock containing Na-rich plagioclase and fewer mafic minerals. This is the case for the Huntington Mountain pluton and East Bay Hills volcanic suite, with diorite and basaltic samples generally having the lowest $\delta^{18}O_{WR}$ values, and leucogranite and rhyolite samples typically having the highest $\delta^{18}O_{WR}$ values.

Felsic rocks tend to be more resistant to alteration by hydrothermal fluids because they contain fewer primary mafic minerals and are dominated by primary Na-rich feldspar and quartz. Generally, quartz is resistant to post-crystallization oxygen-isotope exchange with hydrothermal fluids, especially at lower temperatures (<300°C) (e.g., Taylor, 1971, 1974; Longstaffe, 1982). Felsic rocks also contain Na-rich plagioclase and K-feldspar, which are susceptible to replacement by mainly sericite, calcite and clay minerals. Ca-rich plagioclase is generally even more susceptible to such alteration than Na-rich plagioclase and K-feldspar, and indeed, the Ca-rich plagioclase from diorite samples exhibits a stronger degree of alteration than Na-rich plagioclase and K-feldspar from leucogranite samples (see Section 3). Epidote is a major alteration product of the Ca-rich plagioclase. Replacement of Ca-rich plagioclase by epidote-sericite typically occurs at higher temperatures than the replacement of Na-rich plagioclase by sericite-calcite-clay minerals (e.g., Taylor, 1974; Criss and Taylor, 1986).

Another likely contributor to the variations in $\delta^{18}O$ values of altered plutonic and volcanic rock samples is permeability. Typically, volcanic rocks are more highly jointed than plutonic rocks, which gives the former a higher permeability (Criss and Taylor,

1986). In the present study, andesite from the East Bay Hills volcanic suite tends to be heavily jointed (Barr et al., 1996) and exhibits a high degree of alteration (e.g., Fig. 3.7E). Its plutonic equivalent, diorite, is massive and unjointed, and generally exhibits a lower degree of alteration (e.g., Fig. 3.2A/B, Fig. 3.3A). The $\delta^{18}O$ values of the andesite samples are generally lower than those of diorite, with the andesite having only one sample >–0.5‰ and diorite having only one sample <+1.0‰.

Dacite from the East Bay Hills volcanic suite generally has the lowest $\delta^{18}O_{WR}$ values obtained in this study. A thermal overprint of the dacite has been recognized in previous mapping and petrologic studies of this rock unit (e.g., Barr et al., 1996). This overprint was likely a product of post-crystallization contact metamorphism as the cooling diorite interacted with the adjacent dacite. Evidence for this overprint includes the development of fine-grained hornfelic textures and fine-grained assemblages of quartz and pyrite (Barr et al., 1996, 1998). In addition, localized occurrences of quartz-sericite-pyrite were observed in diorite samples (CBI-6-6-102 to CBI-6-6-104), which are typical of a high-temperature phyllic alteration assemblage (e.g., Fig. 3.3B).

Interaction with autometasomatic fluids of dominantly magmatic origin emanating from the diorite could provide an explanation for the formation of this high-temperature alteration assemblage. However, this interpretation is inconsistent with the very low $\delta^{18}O$ values obtained for the dacite and diorite samples from this area (–3.8 to +2.7‰). These data instead suggest that this alteration assemblage formed during interaction with meteoric-dominated hydrothermal fluids. These apparently conflicting observations could be explained if the areas characterized by high-temperature phyllic alteration had been overprinted by interaction with lower temperature hydrothermal

fluids. Figure 3.5 provides one illustration of the high-temperature, quartz-sericite-pyrite phyllic alteration assemblage overprinted by fine-grained epidote-sericite-chlorite (i.e., the lower temperature propylitic alteration assemblage).

A small number of mainly volcanic samples from the East Bay Hills volcanic suite appear to have been affected by processes associated with regional-scale tectonism. Two major shear zones, trending southwest-northeast, are present in the study area, one located along the southeastern margin of the plutonic and volcanic rocks, and the other separating the andesite (Fig. 5.2 - HEac) from the andesite to rhyolite suite (Fig. 5.2 - HEad). The age of these structures is not well constrained; however, movement along these structures during the Carboniferous was crucial for opening large strike-slip basins (Bradley and Bradley, 1986). On a regional scale, the $\delta^{18}O_{WR}$ values of the andesite and andesite to rhyolite suites suggest that post-hydrothermal alteration movement occurred along the shear zone that separates these two suites. Andesite samples from the southeastern side of the shear zone have $\delta^{18}O_{WR}$ values ranging from –1.9 to +0.5‰, with only one sample >–0.5‰ (Fig. 5.2 - HEac), while andesite to rhyolite samples obtained from the northwestern side of the shear zone have $\delta^{18}O_{WR}$ values ranging from +1.8 to +6.5‰, with only one sample <+3.6‰ (Fig. 5.2 - HEad). Also, there is a greater abundance of localized low-temperature quartz-sericite-calcite alteration associated with samples collected on the northwestern side of the shear zone, while on the southeastern side, the higher temperature propylitic assemblage dominates. These observations suggest that the water-rock interaction with hydrothermal fluids likely occurred prior to movement along the shear zone.

Primary minerals from the Huntington Mountain pluton and East Bay Hills volcanic suite also appear to have lower $\delta^{18}O$ values than those of normal, unaltered primary igneous minerals (e.g., Taylor and Epstein, 1962; Taylor, 1968). Commonly, the primary phases are partially to completely replaced by secondary minerals, which likely formed during interaction with the hydrothermal fluids. The low $\delta^{18}O$ values obtained for the remaining primary mineral samples from the Huntington Mountain pluton and East Bay Hills volcanic suite were likely acquired by post-crystallization oxygen-isotope exchange with the meteoric-dominated hydrothermal fluids. The majority of the variations in the $\delta^{18}O$ values between samples of the same mineral phase likely reflect differing water/rock ratios and alteration characteristics, which are controlled by temperature, permeability, previous alteration and differences in rock type.

A particularly important diagnostic feature of low-^{18}O igneous rocks that have interacted with post-magmatic, hydrothermal fluids is the occurrence of oxygen-isotope disequilibrium between co-existing mineral phases (Taylor, 1971, 1974) (Fig. 5.3). In normal unaltered igneous rocks, and rocks formed from a low-^{18}O magma, coexisting quartz-feldspar pairs have $\Delta^{18}O_{qtz\text{-}fs}$ values of ~0 to +2‰ (Taylor and Epstein, 1962; Taylor, 1968). However, igneous rocks that have interacted with low-^{18}O hydrothermal fluids commonly have anomalously high-$\Delta^{18}O_{qtz\text{-}fs}$ values (>+2‰). During this process, the $\delta^{18}O$ values of feldspar and sometimes quartz are lowered through exchange with high-temperature low-^{18}O hydrothermal fluids (~300-450°C). Quartz is more resistant than feldspar to interaction with hydrothermal fluids. Hence, feldspar continues to undergo oxygen-isotope exchange at lower temperatures, thus leading to higher $\Delta^{18}O_{qtz\text{-}fs}$ values (Sheppard et al., 1971; Longstaffe, 1982). At still lower temperatures (~200-

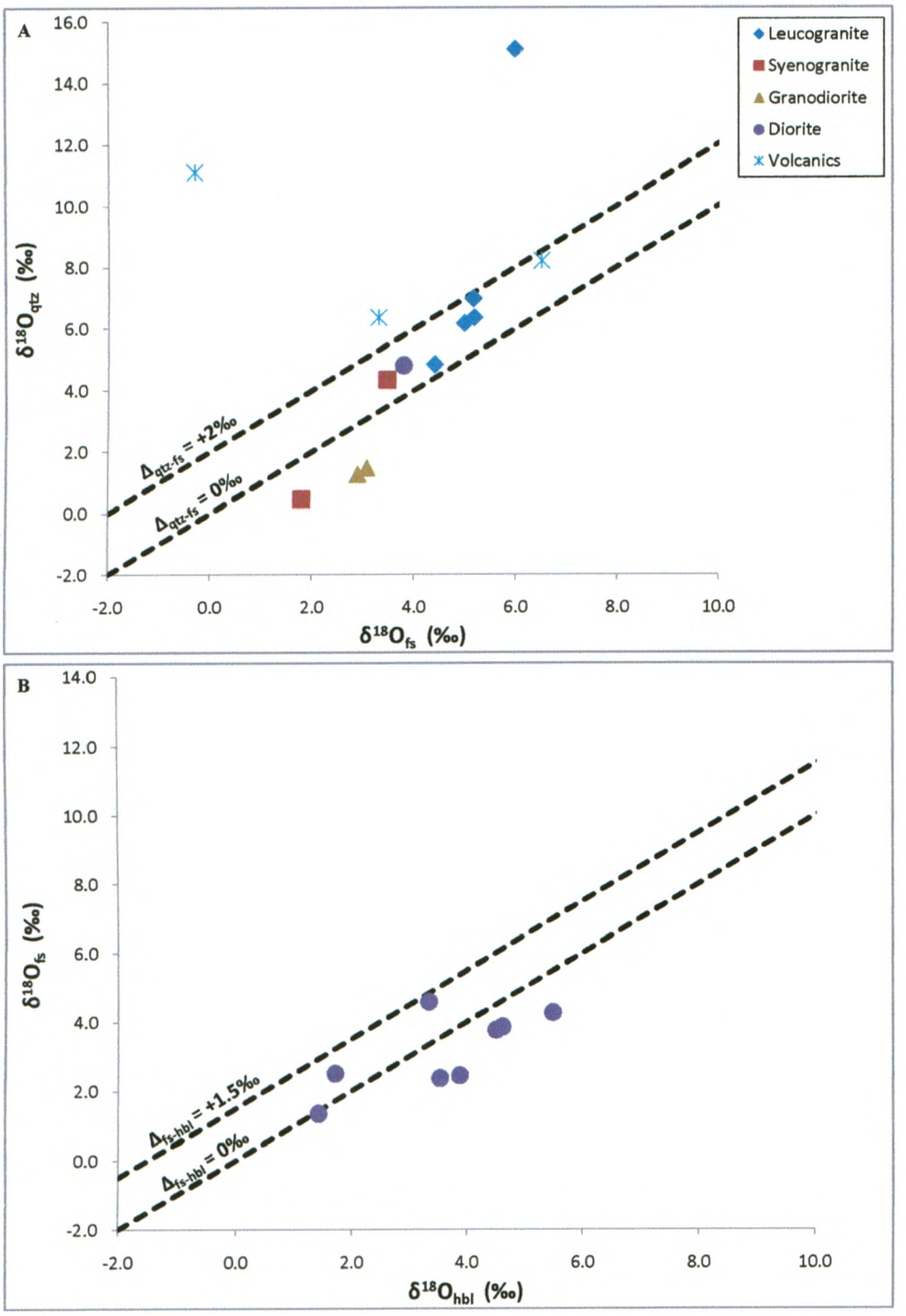

Figure 5.3. $\Delta^{18}O_{mineral\text{-}mineral}$ plots for coexisting mineral pairs from the Huntington Mountain pluton and East Bay Hills volcanic suite, (A) quartz-feldspar, (B) feldspar-hornblende (diorite). The $\Delta^{18}O_{qtz\text{-}fs}$ and $\Delta^{18}O_{fs\text{-}hbl}$ values of unaltered igneous coexisting mineral pairs normally range from ~0 to +2‰ for quartz-feldspar, and ~0 to +1.5‰ for feldspar-hornblende (Taylor and Epstein, 1962; Taylor, 1968).

300°C) only feldspar continues to undergo oxygen-exchange (Longstaffe, 1982). Because of increased oxygen-isotope fractionation between feldspar and the hydrothermal fluids at these temperatures, the feldspar may become enriched in ^{18}O, resulting in the $\Delta^{18}O_{qtz\text{-}fs}$ values to become lower than expected for unaltered igneous quartz-feldspar pairs; in some cases the $\Delta^{18}O_{qtz\text{-}fs}$ values may become negative.

Coexisting feldspar-hornblende pairs may also indicate whether samples have undergone water-rock interaction with low-^{18}O hydrothermal fluids. Typically, unaltered igneous feldspar-hornblende pairs have $\Delta^{18}O_{fs\text{-}hbl}$ values of ~0 to +1.5‰ (Taylor and Epstein, 1962; Taylor, 1968). In contrast, coexisting feldspar-hornblende pairs that have undergone water-rock interaction with low-^{18}O hydrothermal fluids commonly have $\Delta^{18}O_{fs\text{-}hbl}$ values <0‰ (Longstaffe, 1982). Feldspar is commonly less resistant than hornblende to oxygen-isotope exchange with hydrothermal fluids, typically resulting in lower $\delta^{18}O$ values of feldspar compared with hornblende (Longstaffe, 1982).

The $\Delta^{18}O_{qtz\text{-}fs}$ and $\Delta^{18}O_{fs\text{-}hbl}$ values of coexisting mineral pairs from the Huntington Mountain pluton and East Bay Hills volcanic suite range from –1.6 to +11.4‰ for quartz-feldspar, and –1.4 to 1.3‰ for feldspar-hornblende (Figs. 5.3A,B; Appendix C). Many $\Delta^{18}O_{qtz\text{-}fs}$values lie outside of the field for magmatic quartz-feldspar pairs; the $\Delta^{18}O_{fs\text{-}hbl}$ values are also sometimes smaller or reversed (i.e., negative) relative to typical values for igneous feldspar-hornblende pairs. It is likely that these samples were affected by interaction with low-^{18}O hydrothermal fluids.

Some coexisting mineral pairs have $\Delta^{18}O_{qtz\text{-}fs}$ and $\Delta^{18}O_{fs\text{-}hbl}$ values within the normal igneous field (Fig. 5.3; all but one leucogranite quartz-feldspar pairs and two diorite feldspar-hornblende pairs). Typically, coexisting mineral pairs that crystallized

from a low-^{18}O magma have such $\Delta^{18}O_{mineral\text{-}mineral}$ values, notwithstanding their anomalously low $\delta^{18}O$ values. However, the petrographic evidence suggests that these particular samples have been altered (e.g., Fig. 3.6A - CBI-8-05-23). The $\Delta^{18}O_{qtz\text{-}fs}$ and $\Delta^{18}O_{fs\text{-}hbl}$ values instead indicate oxygen-isotope exchange with low-^{18}O hydrothermal fluids over higher (~300-450°C), and then lower (~200-300°C) temperatures. There is no evidence to support the occurrence of low-^{18}O magmas in any of the plutonic and volcanic rocks studied here. This interpretation is consistent with Potter et al. (2008), who also reported oxygen-isotope evidence for post-magmatic hydrothermal alteration of the Huntington Mountain pluton and East Bay Hills volcanic suite, as well as for other igneous rocks of the Mira terrane.

5.1.1 Possible Source(s) for the Hydrothermal Fluids

Previous studies have shown that the hydrothermal fluids associated with plutonic and volcanic rocks formed within a volcanic-arc setting are commonly characterized by three main sources, which include: (i) magmatic water ($\delta^{18}O_{H2O}$ = +6 to +10‰), (ii) meteoric water ($\delta^{18}O_{H2O}$ < 0‰), and (iii) seawater ($\delta^{18}O_{H2O} \approx$ 0‰) (e.g., Taylor, 1974; Criss and Taylor, 1986; Sheppard, 1986). Hydrothermal systems associated with deep, cooling intrusive bodies (e.g., porphyry and mesothermal systems) are typically dominated by magmatic water, and have $\delta^{18}O$ values within the range of normal igneous rocks (+6 to +10‰) (e.g., Taylor and Sheppard, 1986). Shallow hydrothermal systems associated with a cooling pluton and related volcanic rocks are commonly dominated by meteoric water, or in some instances a mixture of early magmatic-dominated and late meteoric-dominated hydrothermal fluids (e.g., Sheppard et al., 1971). Interaction

between cooling plutonic-volcanic rocks and circulating meteoric-dominated hydrothermal fluids typically results in localized zones of ^{18}O-depletion (e.g., Taylor, 1971, 1974). Such interaction is also possible, albeit more rarely, between seawater and a cooling pluton and related volcanic rocks (e.g., White Island, New Zealand). Giggenbach et al. (2003) demonstrated that the geothermal activity on White Island is caused by mixing of magmatic-dominated fluids with seawater, which infiltrates into the permeable volcanic rocks.

On a larger scale, interaction between heated meteoric water and cooling plutonic-volcanic rocks is also common in modern geothermal systems (e.g., Baja California peninsula, Mexico and the Taupo Volcanic Zone, New Zealand), where extensional volcanism, initiated by rifting and regional transtensional faulting, causes infiltration and circulation of meteoric-dominated hydrothermal fluids, and subsequently large scale ^{18}O-depletion (e.g., Cole, 1994). However, ^{18}O-enrichment also tends to occur in this setting, with the meteoric-dominated hydrothermal fluids demonstrating positive ^{18}O-shifts as they exchange with plutonic and volcanic rocks at increasingly lower temperatures (Craig, 1963; Cole, 1994).

5.1.2 Characterization of the Hydrothermal Fluid(s)

Two dominant alteration assemblages are observed throughout the Huntington Mountain pluton and East Bay Hills volcanic suite: (i) a typical propylitic assemblage, consisting of chlorite-epidote-sericite-ilmenite, and (ii) a quartz-sericite-calcite assemblage. Given the mineral associations of these two assemblages, temperatures of ~300-450°C are suggested for the propylitic alteration assemblage, and ~200-300°C for

the quartz-sericite-calcite alteration assemblage (Sheppard and Taylor, 1974; Beane and Titley, 1981; Ferry, 1985; Criss and Taylor, 1986). Given the widespread oxygen-isotope disequilibrium between coexisting primary and secondary minerals, it is difficult to determine the temperature and isotopic composition of the hydrothermal fluids. That said, an attempt has been made to estimate these parameters using mineral-water oxygen-isotope fractionation factors (Appendix D). These calculations yielded temperature estimates ranging from 165 to 550°C and corresponding fluid compositions ($\delta^{18}O_{H2O}$) of ~ –8.6 to +5.5‰. A large majority of these calculated temperatures range from ~250 to 400°C, with fluid compositions of ~ –4.5 to +0.5‰.

Additionally, two coexisting quartz-calcite pairs, which formed within a fracture-fill vein (sample CBI-6-6-17) and as secondary alteration products (sample CBI-6-6-11), appear to be texturally associated with each other (Figs. 3.9A & 3.7C, respectively); hence, their $\delta^{18}O$ values likely reflect those of an equilibrium assemblage. Using the oxygen-isotope fractionation factors for quartz-water (Matsuhisa et al., 1979) and calcite-water (Freidman and O'Neil, 1977), it was possible to obtain quartz-calcite crystallization temperatures of 229°C for the vein assemblage and 218°C for the secondary alteration assemblage, and fluid compositions ($\delta^{18}O_{H2O}$) of –0.8‰ and +1.2‰, respectively (Appendix D).

A second approach was also used to estimate the hydrothermal fluid conditions during alteration of the Huntington Mountain pluton and East Bay Hills volcanic suite. Oxygen-isotope mineral-water fractionation curves were calculated using the $\delta^{18}O$ values of mineral samples from the plutonic and volcanic rocks (Figs. 5.4 & 5.5). Points of intersection among these curves represent possible equilibrium conditions for the phases

involved. Given the temperature estimates for the two alteration assemblages (Section 3.4), only intersections between 150 and 500°C are considered below.

Two samples from the Huntington Mountain pluton were examined in detail, a diorite (sample CBI-6-6-82) with a $\delta^{18}O_{WR}$ value of +3.8‰ and a leucogranite (sample CBI-6-6-81) with a $\delta^{18}O_{WR}$ value of +5.8‰. For sample CBI-6-6-82 (Fig. 5.4A), the curves for plagioclase and secondary chlorite intersect at ~475°C and a $\delta^{18}O_{H2O}$ value of ~+2.0‰, while the curves for secondary chlorite and diorite (whole-rock) intersect at ~225°C and a $\delta^{18}O_{H2O}$ value of ~ –1.5‰. For sample CBI-6-6-81, four intersecting mineral-water fractionation curves are noteworthy (Fig. 5.4B). The curves for quartz and feldspar intersect at ~350°C and a $\delta^{18}O_{H2O}$ value of ~+1.0‰, while the curve for secondary chlorite intersects the quartz and feldspar curves at ~275°C and a $\delta^{18}O_{H2O}$ value of ~ –1.5‰ (quartz), and ~250°C, with a $\delta^{18}O_{H2O}$ value of ~ –2.5‰ (feldspar). The chlorite curve also intersects the granite curve at ~175°C and a $\delta^{18}O_{H2O}$ value of ~ –4.5‰.

Two samples from the East Bay Hills volcanic suite were examined in detail, a rhyolite (sample CBI-8-05-30) with a $\delta^{18}O_{WR}$ value of +6.6‰, and an andesite (sample CBI-6-6-52) with a $\delta^{18}O_{WR}$ value of –0.5‰. For sample CBI-8-05-30 (Fig. 5.5A), the curves for "primary" quartz and feldspar intersect at ~400°C and a $\delta^{18}O_{H2O}$ value of ~ +3.5‰. These curves also intersect the rhyolite curve at temperatures of 400-500°C, with corresponding $\delta^{18}O_{H2O}$ values of +3.5 to +5.0‰. The similarity between the vein and "primary" quartz curves suggests that both acquired their $\delta^{18}O$ values from the same fluid, albeit at different temperatures. For sample CBI-6-6-52 (Fig. 5.5B), the feldspar and secondary chlorite curves intersect at ~325°C and a $\delta^{18}O_{H2O}$ value of ~ –5.0‰. The curve for secondary quartz has higher $\delta^{18}O$ values at any given

temperature than the other coexisting mineral phases, which suggests that secondary quartz formed at lower temperatures , unless an extremely ^{18}O-rich fluid was involved. At ~200-300°C the fluid responsible for the secondary quartz would have a $\delta^{18}O_{H2O}$ value of ~0 to +4‰.

The petrographic data suggest that the widespread, high-temperature propylitic alteration formed earlier than the low-temperature quartz-calcite-sericite alteration (Section 3.4). Given the large number of low $\delta^{18}O$ values obtained for samples affected by propylitic alteration, and the smaller number of high $\delta^{18}O$ values obtained for samples affected by quartz-calcite-sericite alteration, it is most likely that the propylitic alteration assemblage was associated with higher temperature, meteoric-dominated hydrothermal fluids, while the quartz-sericite-calcite alteration assemblage was associated with lower temperature, more ^{18}O-rich hydrothermal fluids. To confirm this, $\delta^{18}O_{H2O}$ values were calculated for mineral samples affected by and/or formed by the propylitic alteration using temperatures typical of propylitic alteration (300-450°C) (Fig. 5.6A). These $\delta^{18}O_{H2O}$ values range from –9.0 to –0.4‰, with many <–3‰, consistent with dominance of the high-temperature, hydrothermal fluids by meteoric water.

Possible sources for the more ^{18}O-rich fluid involved in the lower temperature alteration include seawater (~0‰) and magmatic water (+6 to +10‰). The $\delta^{18}O_{H2O}$ values for quartz-calcite pairs from a fracture-fill vein (Appendix D - sample CBI-6-6-17) and from secondary alteration of primary phases (Appendix D - sample CBI-6-6-11) suggest that seawater-dominated hydrothermal fluids may have been involved in the lower temperature quartz-sericite-calcite alteration. However, seawater alone cannot

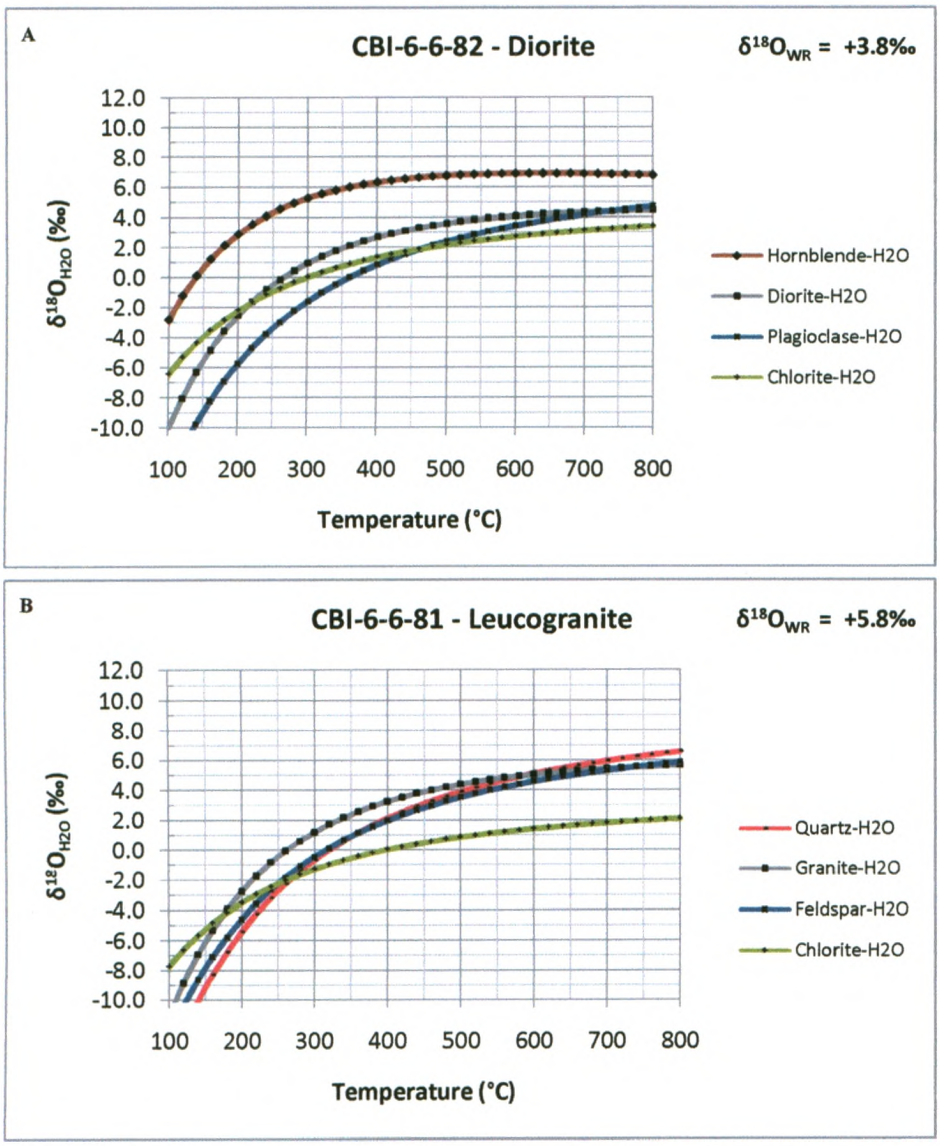

Figure 5.4. Mineral-water fractionation curves for diorite (A) and leucogranite (B) from the Huntington Mountain pluton. These curves were calculated using the $\delta^{18}O$ values listed in Table 4.1, and the following fractionation factors: chlorite-H_2O (Wenner and Taylor, 1971), diorite- H_2O (Zhao and Zheng, 2003), alkali feldspar (feldspar)-H_2O (O'Neil and Taylor, 1967), granite- H_2O (Zhao and Zheng, 2003), hornblende-H_2O (Zheng, 1993), plagioclase-H_2O (O'Neil and Taylor, 1967) and quartz-H_2O (Matsuhisa et al., 1979).

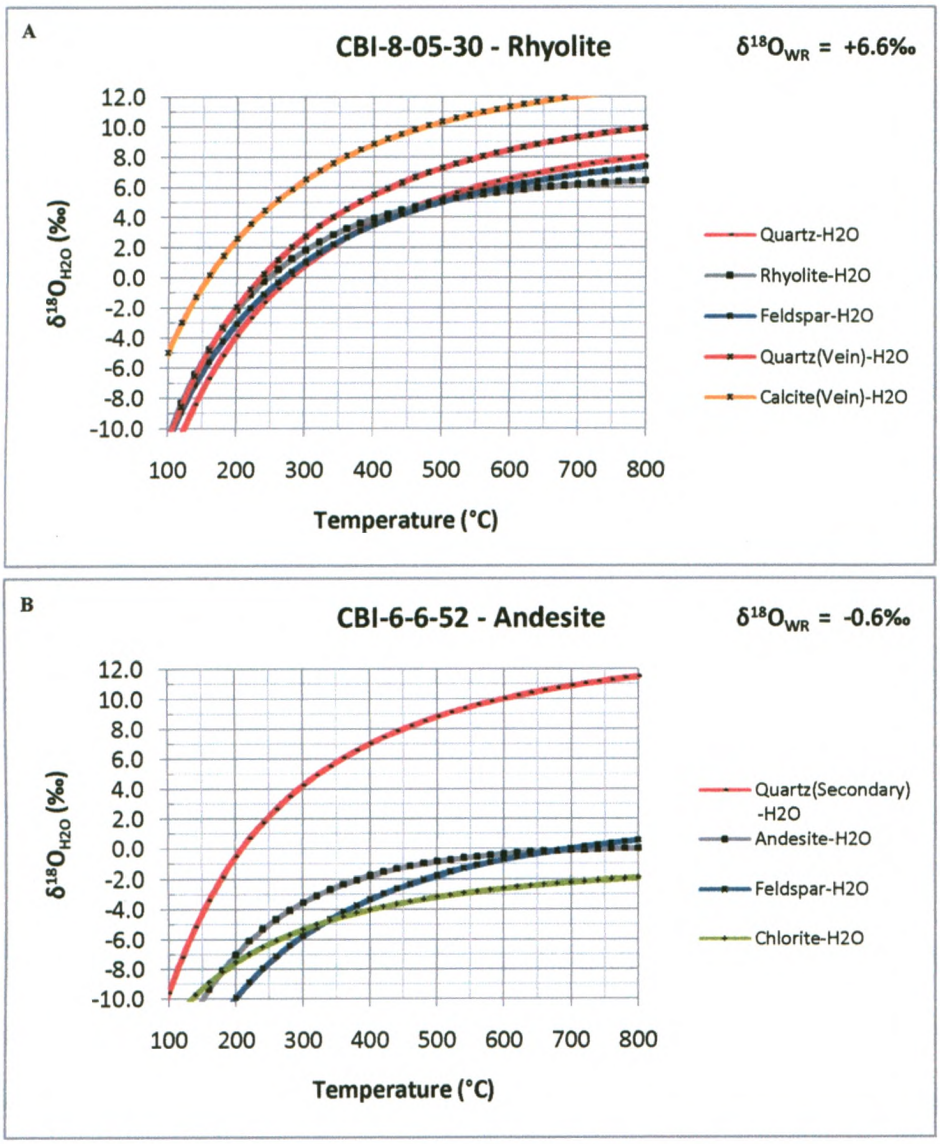

Figure 5.5. Mineral-water fractionation curves for rhyolite (A) and andesite (B) from the East Bay Hills volcanic suite. These curves were calculated using the $\delta^{18}O$ values listed in Table 4.1, and the following fractionation factors: andesite-H_2O (Zhao and Zheng, 2003), calcite-H_2O (Friedman and O'Neil, 1977), chlorite-H_2O (Wenner and Taylor, 1971), alkali feldspar (feldspar)-H_2O (O'Neil and Taylor, 1967), quartz-H_2O (Matsuhisa et al., 1979) and rhyolite-H_2O (Zhao and Zheng, 2003).

explain why secondary quartz from andesite (sample CBI-6-6-52, Fig. 5.5B) has such high estimated $\delta^{18}O_{H2O}$ values (~0 to +4‰). Seawater also cannot explain how secondary quartz from leucogranite (e.g., EB91-014), as well as fracture-fill quartz-calcite veins from basaltic rocks (e.g., CBI-6-6-112B & CBI-6-6-107), could have acquired such high $\delta^{18}O$ values (+8.4 to 15.1‰). To produce such values within the temperature range of the quartz-sericite-quartz alteration assemblage (200-300°C), $\delta^{18}O_{H2O}$ values for the hydrothermal fluid of –3.2 to +9.5‰ would have been required (Fig. 5.6B). Thus, while seawater-dominated hydrothermal fluids appear to have been largely responsible for the formation of secondary quartz and fracture-fill quartz-calcite veins, varying mixtures of heated meteoric water (<0‰) and magmatic water (~+6 to +10‰) could also have produced these high $\delta^{18}O$ values (e.g., Taylor, 1974).

Previous studies have shown that hydrothermal fluids typically evolve from magmatic-dominated to meteoric-dominated, with the magmatic-dominated hydrothermal fluids forming higher temperature alteration assemblages (potassic and phyllic), while the meteoric-dominated fluids form lower temperature alteration assemblages (propylitic and argillic) (e.g., Meyer and Hemley, 1967; Taylor, 1974; Ulrich et al., 2001; Harris and Golding, 2002). In this scenario, high lithostatic pressures, which are associated with high-temperature, magmatic-dominated hydrothermal fluids generated by a cooling pluton, restrict meteoric water from entering the magmatic hydrothermal system. Once temperatures decrease and the lithostatic pressures associated with the internal magmatic hydrothermal system become lower than the external hydrostatic pressures associated with the meteoric hydrothermal system, the meteoric-dominated hydrothermal fluids collapse onto the magmatic hydrothermal system and mixing can occur (Taylor, 1974).

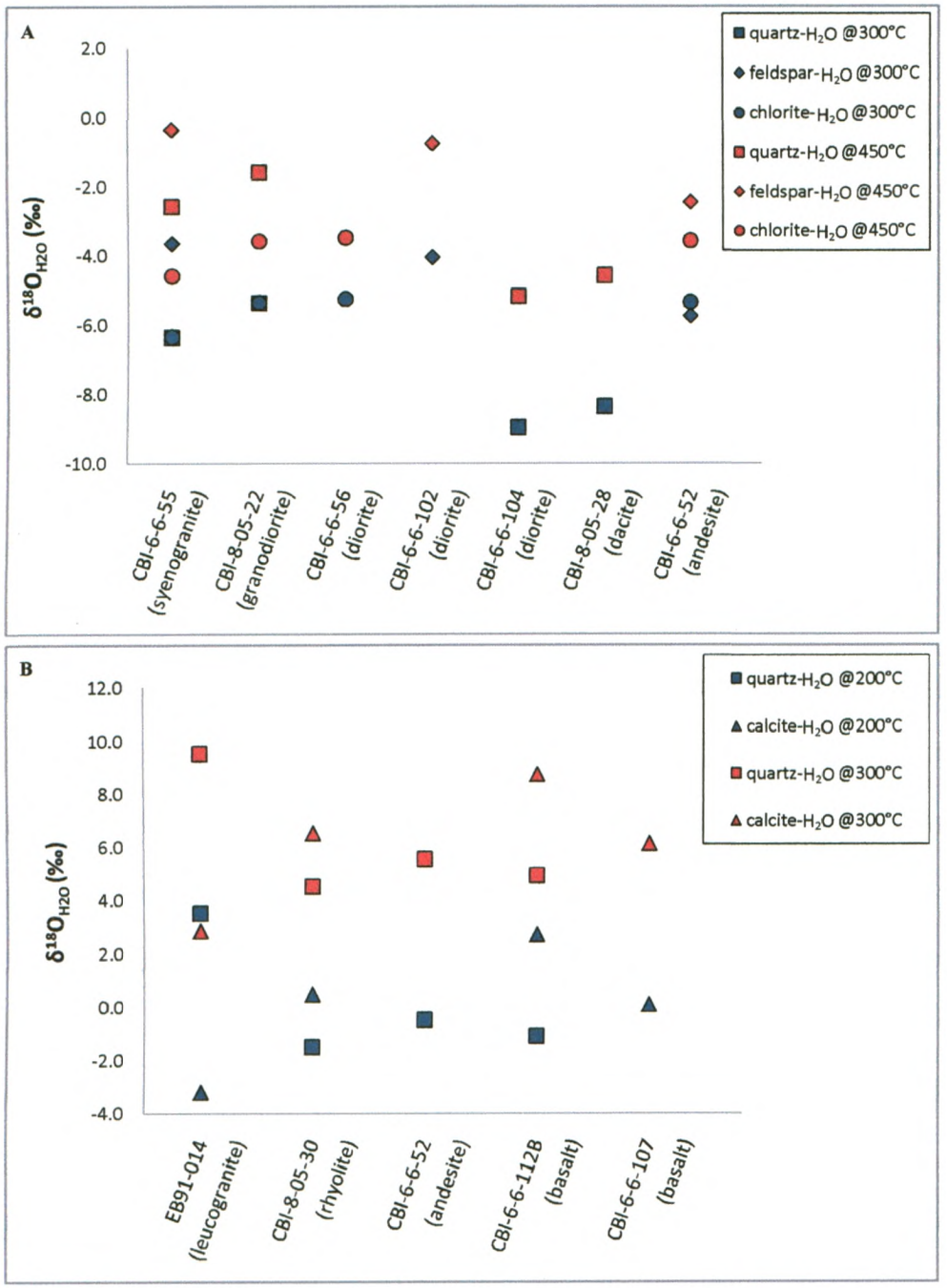

Figure 5.6. Calculated hydrothermal fluid compositions ($\delta^{18}O_{H2O}$) using a selection of minerals from Table 4.1. Samples with low $\delta^{18}O$ values were used for calculations at 300 and 450°C (A). Samples with high $\delta^{18}O$ values were used for calculations at 200 and 300°C (B). The following fractionation factors were employed: calcite-H_2O (Friedman and O'Neil, 1977), chlorite-H_2O (Wenner and Taylor, 1971), alkali feldspar(feldspar)-H_2O (O'Neil and Taylor, 1967) and quartz-H_2O (Matsuhisa et al., 1979).

The early high-temperature alteration assemblages are typically represented by $\delta^{18}O$ values within normal magmatic range (+6 to +10‰), while the late propylitic alteration assemblages generally have low $\delta^{18}O$ values (<+6‰) (Sheppard et al., 1971; Taylor, 1971, 1974; Ulrich et al., 2001, Harris and Golding, 2002). However, such a model is inconsistent with the petrographic and isotopic data for the Huntington Mountain pluton and East Bay Hills volcanic suite, which suggest that the more ^{18}O-rich hydrothermal fluids were present in the system later than the meteoric-dominated hydrothermal fluids.

Another possible explanation for the formation of more ^{18}O-rich hydrothermal fluids later in the evolution of the system is progressive ^{18}O-enrichment of the initial meteoric-dominated hydrothermal fluids through oxygen-isotope exchange with the rocks of the Huntington Mountain pluton and East Bay Hills volcanic suite. This type of interaction is common in active geothermal systems, and generally consists of meteoric-dominated hydrothermal fluids acquiring distinctive positive ^{18}O-shifts as they exchange with plutonic and volcanic rocks (e.g., Craig, 1963; Taylor, 1974; Criss and Taylor, 1986; Cole, 1994). These ^{18}O-shifts are controlled by temperature and water/rock ratios, which locally tend to be influenced by mineralogy and permeability (Taylor, 1974; Cole, 1994). In section 5.1 it was demonstrated that mineralogy and permeability were possible causes of the variations in the $\delta^{18}O$ values of samples (see Table 4.1). This scenario can also explain how such a wide range of $\delta^{18}O_{H2O}$ values could be obtained from: (1) coexisting primary and secondary mineral pairs (–8.6 to +5.5‰, Appendix D), (2) mineral-water fractionation curves (~ –5.0 to +5.0‰, Figs. 5.4 & 5.5), (3) primary mineral samples affected by early propylitic alteration (–9.0 to –0.4‰, Fig. 5.6A), and (4) vein and

secondary minerals representing the later quartz-sericite-calcite alteration (–3.2 to +9.5‰, Fig. 5.6B).

5.2 Significance of the Hydrogen-isotope Results

Samples from the Huntington Mountain pluton and East Bay Hills volcanic suite have a restricted range of δD_{WR} values, ranging from –93 to –56‰, with only one sample <–82‰. These generally fall within the accepted range of δD values for normal unaltered igneous rocks (–85 to –50‰) (e.g., Sheppard, 1986). However, igneous rocks that have undergone hydrogen-isotope exchange with mid- to low-latitude meteoric water or seawater can also acquire such compositions (e.g., Longstaffe, 1982). Given that the samples of this study contain abundant hydrous, secondary alteration minerals (i.e., chlorite, epidote and sericite), and are characterized by low $\delta^{18}O$ values that suggest interaction with low-^{18}O hydrothermal fluids, it is likely that the δD_{WR} values also reflect this process. Potter et al. (2008) reported similar δD_{WR} values for igneous rocks of the Mira terrane, which they attributed to such alteration.

The lowest δD_{WR} value was obtained for sample CBI-6-6-11, which is a basalt sample that has been completely overprinted by the low-temperature quartz-sericite-calcite alteration assemblage (Fig 3.7C). This sample was collected proximal to the regional-scale shear zone at the southeastern margin of the study area (e.g., Fig. 3.1), and may have undergone hydrogen-isotope exchange with post-hydrothermal alteration fluids, given that the shear zone likely represents a fluid conduit.

Secondary chlorite has δD values that range from –77 to –69‰, and two samples of sericite have δD values of –74‰ and –62‰. Chlorite provides the majority of the

hydrogen represented in the whole-rock samples, and mineral δD values lie within the range expected for minerals that precipitated from, or underwent hydrogen-isotope exchange with mid- to low-latitude meteoric-dominated hydrothermal fluids.

5.2.1 Characterization of the Hydrothermal Fluid(s)

Coexisting chlorite and sericite pairs could not be obtained from the plutonic and volcanic samples, which caused difficulty in evaluating whether differences in fluid-compositions or formation temperatures existed for chlorite versus sericite formation. The association of chlorite with the high-temperature propylitic alteration suggests its formation at higher temperatures than sericite in the quartz-sericite-calcite alteration assemblages. However, sericite is also associated with epidote as an alteration product of feldspar; hence not all sericite may have formed at lower temperatures than chlorite.

The δD values of whole-rock and hydrous mineral samples from the Huntington Mountain pluton and East Bay Hills volcanic suite were used to estimate hydrothermal fluid compositions within the temperature range of the propylitic alteration assemblage (300 to 450°C). Fluid compositions were calculated using the δD and $\delta^{18}O$ values of secondary chlorite and sericite, together with the chlorite-water isotope fractionation factors of Graham et al. (1984) for hydrogen and Wenner and Taylor (1971) for oxygen, and the muscovite-water isotope fractionation factors of Suzuoki and Epstein (1976) for hydrogen and Friedman and O'Neil (1977) for oxygen. Given the small number of δD values obtained for secondary chlorite, direct calculation of δD_{H2O} was not always possible. However, since the δD_{WR} values reflect hydroxyl groups released mostly from secondary chlorite, they were assumed to be equivalent to chlorite in the calculations.

Hence, fluid compositions were also calculated from the δD and $\delta^{18}O$ values of whole-rock samples using the chlorite-water hydrogen-isotope fractionation factor of Graham et al. (1984) for δD_{H2O} and the rock-water oxygen-isotope fractionation factor of Zhao and Zheng (2003).

For secondary chlorite and sericite, the calculated fluid compositions have δD_{H2O} values of –41 to –13‰ and $\delta^{18}O_{H2O}$ values of –6.3 to +3.3‰ at 300°C, and –51 to –25‰ (δD_{H2O}) and –4.5 to +5.0‰ ($\delta^{18}O_{H2O}$) at 450°C (Fig. 5.7). Several secondary chlorite samples have a restricted range δD_{H2O} and $\delta^{18}O_{H2O}$ values, which are grouped near the Global Meteoric Water Line (e.g., Craig, 1961). These likely represent chlorite that crystallized directly from meteoric-dominated hydrothermal fluids at 300-450°C. Three chlorite samples have higher $\delta^{18}O_{H2O}$ values, ranging from –0.9 to +5.0‰. Petrographic evidence for these three samples suggests that they are direct alteration products of primary hornblende and biotite (e.g., Fig. 3.3E). This chlorite likely inherited some oxygen directly from these precursors, therefore yielding higher $\delta^{18}O_{chl}$ values than other secondary chlorite samples (Section 5.1). A large range of fluid compositions was calculated for secondary sericite samples. The discrepancy between the δD_{H2O} values of chlorite and sericite within the temperature range of 300-450°C likely reflects that the fractionation of muscovite(sericite)-water is more sensitive to temperature changes than the fractionation between chlorite and water.

A similar range of fluid compositions was calculated for whole-rock samples, with δD_{H2O} values ranging from –47 to –20‰ and $\delta^{18}O_{H2O}$ values ranging from –7.1 to +2.5‰ for 300°C, and –51 to –25‰ (δD_{H2O}) and –3.8 to +5.9‰ ($\delta^{18}O_{H2O}$) for 450°C (Fig. 5.8). These form a linear array of δD_{H2O} and $\delta^{18}O_{H2O}$ values, with fluid

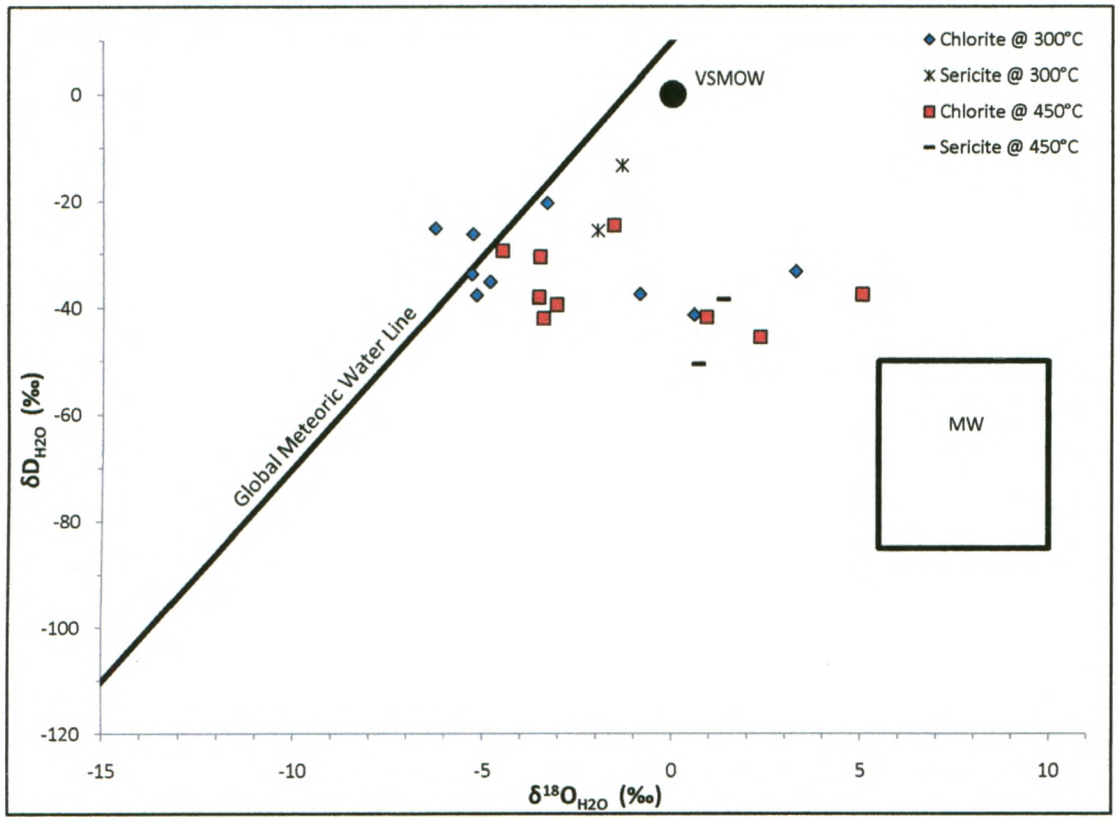

Figure 5.7. Fluid compositions (δD_{H2O} and $\delta^{18}O_{H2O}$) calculated for chlorite and sericite from the Huntington Mountain pluton and East Bay Hills volcanic suite (Table 4.1). These compositions were calculated at 300 and 450°C, using the hydrogen-isotope fractionation factors for chlorite-H_2O (Graham et al., 1984) and muscovite (sericite)-H_2O (Suzuoki and Epstein, 1976), and the oxygen-isotope fractionation factors for chlorite- H_2O (Wenner and Taylor, 1971) and muscovite (sericite)-H_2O (Friedman and O'Neil, 1977). The Global Meteoric Water Line, the present composition of ocean water (VSMOW) and field for magmatic water (MW) are also shown, modified from Sheppard (1986).

compositions trending towards higher $\delta^{18}O_{H2O}$ values away from the Global Meteoric Water Line, while showing only minor variations in δD_{H2O} values. This shift in $\delta^{18}O_{H2O}$ values is very similar to the distinctive ^{18}O-shifts characteristic of modern geothermal systems (e.g., Craig, 1963; Criss and Taylor, 1986), in which initial meteoric-dominated hydrothermal fluids become progressively enriched in ^{18}O during continued oxygen-isotope exchange with the igneous rocks through which they pass. Because of the low hydrogen content of the initially unaltered igneous rocks, the δD_{H2O} values of the early meteoric-dominated hydrothermal fluids commonly remain unchanged during this water-rock interaction (e.g., Craig, 1963; Taylor, 1974; Criss and Taylor, 1986; Cole, 1994). Accordingly, the original composition of the initial meteoric-dominated hydrothermal fluid can be estimated from the mean δD_{H2O} value of the whole-rock samples, which yielded a δD_{H2O} value of –36‰ for samples considered here, within the temperature range of 300-450°C. This result was then used to calculate an initial $\delta^{18}O_{H2O}$ value of –5.8‰, using the equation of for the Global Meteoric Water Line (Fig. 5.8).

Previous oxygen- and hydrogen-isotope studies of modern geothermal systems (e.g., Craig, 1963; Taylor, 1974; Cole, 1994) have demonstrated that, although temperature is a major cause of these ^{18}O-shifts, water/rock ratios dominantly control the extent of ^{18}O-depletion of the host rocks. To test this suggestion, fluid compositions were calculated for a range of water/rock ratios using the equations of Ohmoto and Rye (1974) (Fig. 5.8). In these calculations, it was assumed that the initial composition of the hydrothermal fluid had a δD_{H2O} value of –36‰ and a $\delta^{18}O_{H2O}$ value of –5.8‰, and that the composition of magmatic water associated with an intermediate to felsic magma had δD_{H2O} and $\delta^{18}O_{H2O}$ values of –60‰ and +7.0‰, respectively (e.g., Ohmoto and Rye,

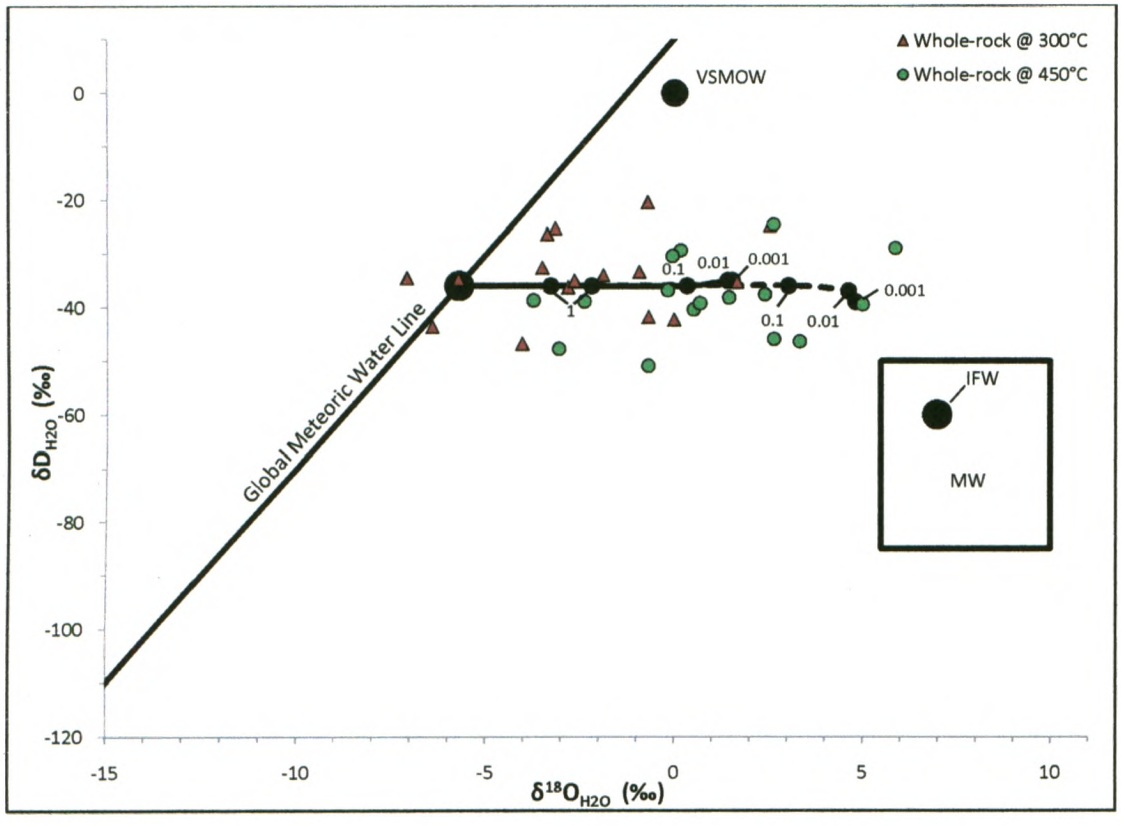

Figure 5.8. Fluid compositions (δD_{H2O} and $\delta^{18}O_{H2O}$) calculated for whole-rock samples from the Huntington Mountain pluton and East Bay Hills volcanic suite (Table 4.1). These were calculated at 300 and 450°C, using the hydrogen-isotope fractionation factor for chlorite-H_2O (Graham et al., 1984) and the oxygen-isotope fractionation factors for rock-H_2O (Zhao and Zheng, 2003). Additionally, water/rock ratios (1, 0.1, 0.01 and 0.001) were calculated for 300°C (solid line) and 450°C (dashed line) following the method of Ohmoto and Rye (1974). The modern Global Meteoric Water Line, the present composition of ocean water (VSMOW), the field for magmatic water (MW) and the composition of intermediate to felsic magmatic water (IFW) are shown here, modified from Sheppard (1986).

1974). Additionally, the isotopic fractionations between rock and water ($\Delta D_{r\text{-}w}$ & $\Delta^{18}O_{r\text{-}w}$) were calculated at 300°C and 450°C using the hydrogen-isotope chlorite-water fractionation factor of Graham et al. (1984) and the oxygen-isotope feldspar-water fractionation factor of O'Neil and Taylor (1967). These calculated fluid compositions form a linear trend of progressive ^{18}O-enrichment away from the Global Meteoric Water Line, which also coincides with a progressive lowering of water/rock ratios. This suggests that the samples likely acquired and retained their δD values from meteoric-dominated hydrothermal fluids, and that variations in temperature and water/rock ratios were not dominant factors in controlling the δD_{H2O} values of the hydrothermal fluid. In contrast, temperature and water/rock ratios were important controls of the $\delta^{18}O_{H2O}$ values of the hydrothermal fluids that interacted with the Huntington Mountain pluton and East Bay Hills volcanic suite, as shown in Section 5.1.

5.3 Significance of the Oxygen- and Carbon-isotope Results for Calcite

Vein and secondary calcite samples from the Huntington Mountain pluton and East Bay Hills volcanic suite have a wide range of $\delta^{13}C$ values, –7.4 to +0.1‰, and $\delta^{18}O$ values, +5.4 to +14.3‰, which are typical of calcite from hydrothermal ore deposits (Ohmoto and Rye, 1979). A negative correlation was observed between the carbon- and oxygen-isotopes of calcite (Fig. 5.9). The progressive increase in the $\delta^{18}O$ values of calcite suggests that it crystallized from a hydrothermal fluid that was either cooling, or underwent an ^{18}O-shift. Given that the secondary silicate minerals (i.e., quartz and chlorite) also demonstrate a positive ^{18}O-shift in hydrothermal fluid composition, the latter appears to be a more likely explanation. The wide range of $\delta^{13}C$ values suggests

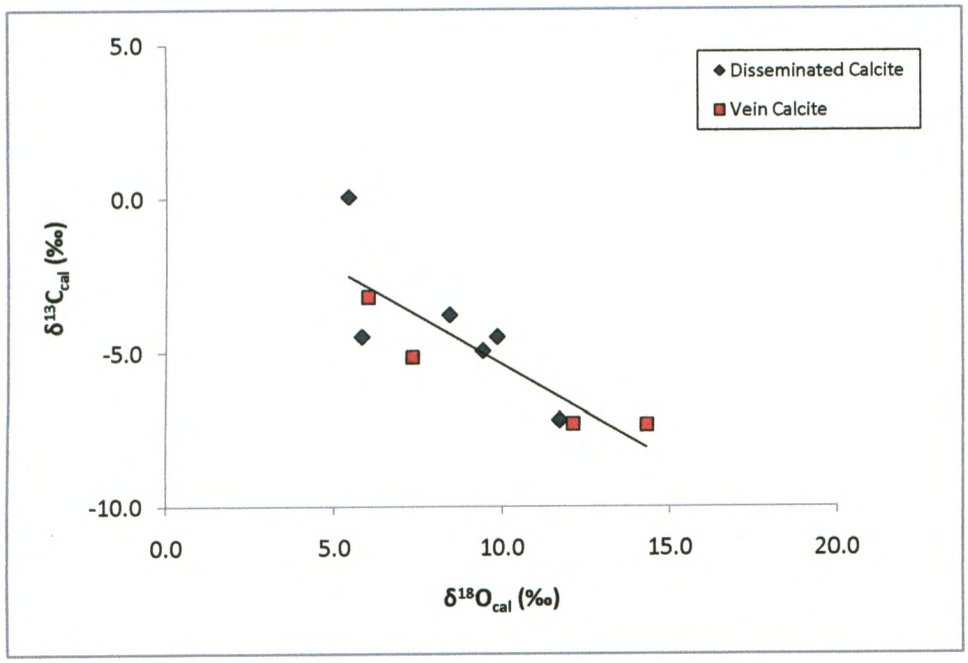

Figure 5.9. Vein and disseminated secondary calcite samples from the Huntington Mountain pluton and East Bay Hills volcanic suite.

that calcite precipitated from a mixed hydrothermal fluid (Ohmoto and Rye, 1979). Previous carbon-isotope studies have demonstrated that retrograde cooling of a hydrothermal fluid, from 300 to 200°C, which is within the range of the lower temperature quartz-sericite-calcite alteration assemblage, results in ^{13}C-enrichment of only ~2‰, and that variations in $\delta^{13}C$ values of secondary carbonates beyond this range result from mixing of multiple carbon sources in the hydrothermal fluid (e.g., Sheppard et al., 1971; Ohmoto and Rye, 1979; Chacko et al., 1991; Zheng and Hoefs, 1993). However, positive correlations between $\delta^{13}C$ and $\delta^{18}O$ values of the secondary carbonates are typical of this scenario, generally reflecting mixing between earlier high-temperature magmatic-dominated hydrothermal fluids ($\delta^{13}C \approx -10$ to -5‰) and later low-temperature seawater-dominated hydrothermal fluids ($\delta^{13}C \approx 0$‰) (Ohmoto and Rye, 1979).

5.3.1 Characterization of the Hydrothermal Fluid(s)

The carbon- and oxygen-isotope fluid compositions of the hydrothermal fluids responsible for forming the vein and disseminated secondary calcite were calculated by using two coexisting quartz-calcite pairs that yielded formation temperatures of 229°C (CBI-6-6-17) and 218°C (CBI-6-6-11), and oxygen-isotope fluid compositions ($\delta^{18}O_{H2O}$) of –0.8‰ and +1.2‰ (Section 5.1.2; Appendix D). Given that CO_2 appears to be the dominant carbon phase in the hydrothermal fluids (Potter et al., unpublished data), the carbon-isotope fluid compositions were then calculated using these formation temperatures and the CO_2-calcite fractionation factor of Chacko et al. (1991), which yielded $\delta^{13}C_{CO2}$ values of –2.9‰ for vein calcite (CBI-6-6-17) and –3.9‰ for disseminated secondary calcite (CBI-6-6-11) (Appendix D).

The fluid compositions were also estimated for all vein and disseminated secondary calcite samples using the fractionation factors of Chacko et al. (1991) for CO_2-calcite ($\delta^{13}C_{CO2}$) and Friedman and O'Neil (1977) for calcite-H_2O ($\delta^{18}O_{H2O}$), for the temperature range of 200-300°C (Fig. 5.10). This range was chosen because calcite is associated with the quartz-sericite-calcite alteration assemblage (Sections 3.4 & 5.1) and the two coexisting quartz-calcite samples (CBI-6-6-17 & CBI-6-6-11) yielded temperatures within this range. The $\delta^{13}C_{CO2}$ values obtained from these calculations range from –6.6 to +2.9‰ (Fig. 5.10A). A much wider range of $\delta^{18}O_{H2O}$ values was obtained, –4.1 to +8.7‰ (Fig. 5.10B), similar to that calculated using the oxygen-isotope compositions of the secondary silicate minerals (Section 5.1.2). The wide range of $\delta^{13}C_{CO2}$ and $\delta^{18}O_{H2O}$ values obtained for these vein and secondary calcite samples suggests a complex evolution for the hydrothermal fluids at this stage of alteration.

The petrographic data demonstrate that the calcite samples with the lowest $\delta^{18}O_{H2O}$ values interacted with the earlier hydrothermal fluids most closely associated with high-temperature propylitic alteration assemblage (e.g., sample CBI-6-6-102), while those with the highest $\delta^{18}O_{H2O}$ values were associated with the later hydrothermal fluids responsible for the lower temperature quartz-sericite-calcite alteration assemblage (e.g., vein sample CBI-6-6-17, Fig. 3.9A, and disseminated secondary calcite sample CBI-6-6-11, Fig. 3.7C).

The earlier hydrothermal fluids seem to have higher $\delta^{13}C_{CO2}$ (e.g., +2.9‰) and lower $\delta^{18}O_{H2O}$ (e.g., –4.1‰) values. These carbon-isotope fluid compositions suggest that seawater or carbonate derived from seawater may have been the carbon source for the early hydrothermal fluids (e.g., Ohmoto and Rye, 1979), while their $\delta^{18}O_{H2O}$ values

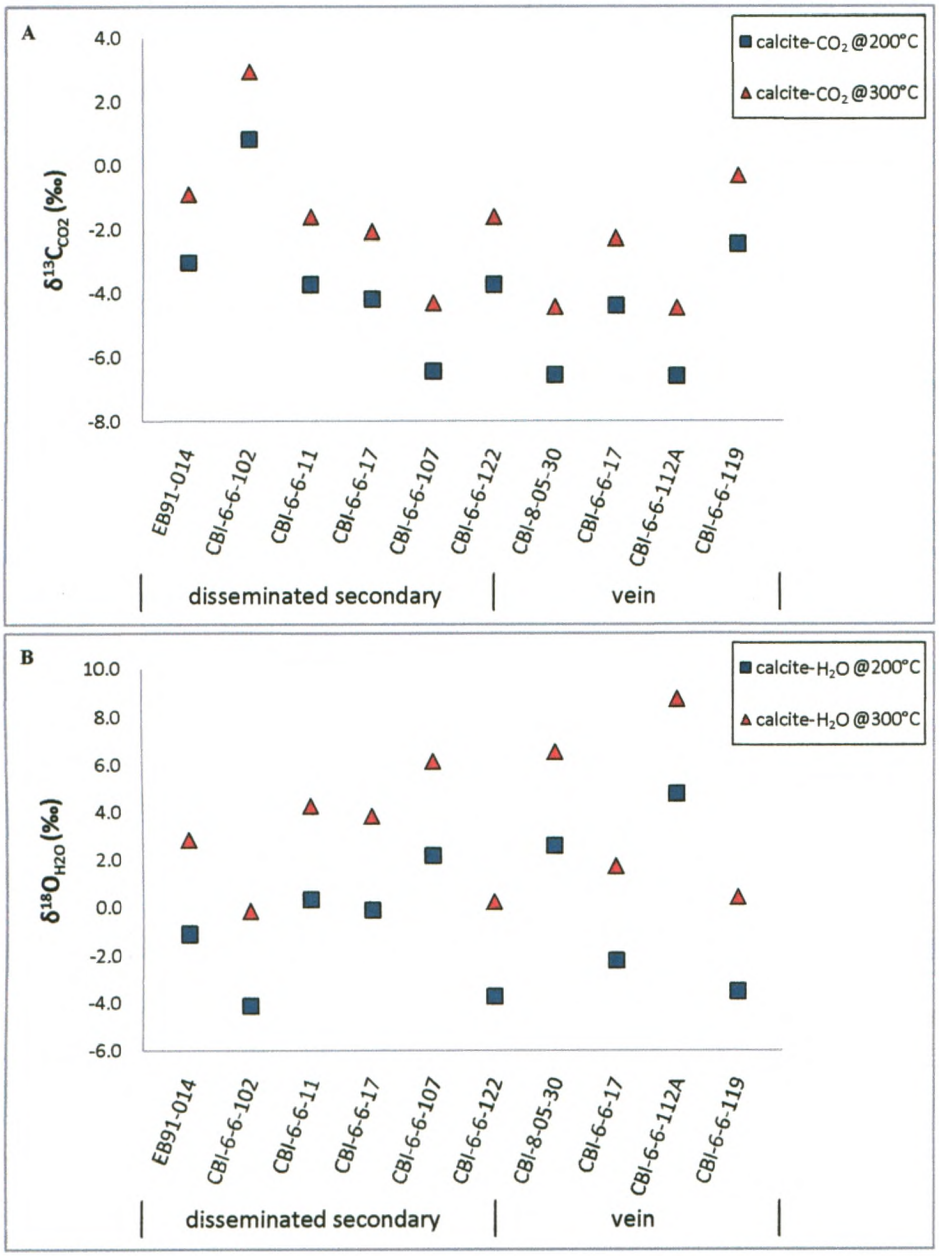

Figure 5.10. Fluid compositions for vein and disseminated secondary calcite samples from the Huntington Mountain pluton and East Bay Hills volcanic suite. These compositions were calculated at 200°C and 300°C using the carbon-isotope CO_2-calcite fractionation factor of Chacko et al. (1991) (A), and the oxygen-isotope calcite-H_2O fractionation factor of Friedman and O'Neil (1977) (B).

were most likely acquired from meteoric-dominated hydrothermal fluids (e.g., Taylor, 1974). Interaction of the meteoric-dominated hydrothermal fluids with marine carbonate prior to interaction with the Huntington Mountain pluton and East Bay Hills volcanic suite provides the simplest explanation for these results (e.g., Ohmoto and Rye, 1979).

The later hydrothermal fluids appear to have lower $\delta^{13}C_{CO2}$ (e.g., –6.6‰) and higher $\delta^{18}O_{H2O}$ (e.g., +8.7‰) values. These fluid compositions suggest that meteoric water was dominant in the later hydrothermal fluids (e.g., Ohmoto and Rye, 1979), and became progressively enriched in ^{18}O during oxygen-isotope exchange with the Huntington Mountain pluton and East Bay Hills volcanic suite.

5.4 Origin and Timing of the Hydrothermal Fluid Movement(s)

The timing of the ^{18}O-depletion of the Huntington Mountain pluton and East Bay Hills volcanic suite is critical for understanding the tectonic history of Cape Breton Island (e.g., Barr et al., 1998; Hibbard et al., 2007; Potter et al., 2008). Recent oxygen-isotope studies have shown that the Mira terrane is distinct from the Bras d'Or terrane, Aspy terrane and Blair River Inlier in its widespread content of low-^{18}O igneous rocks, which were likely formed by post-crystallization water-rock interaction with meteoric-dominated hydrothermal fluids (Potter et al., 2008). Hydrothermal fluid movements are commonly linked with the formation of ore deposits, and hence the timing of this ^{18}O-depletion is also likely important for understanding the occurrence of mineralization in the Mira terrane. Two possibilities are proposed here to establish the timing of ^{18}O-depletion of the Huntington Mountain pluton and East Bay Hills volcanic suite: (1) water-rock interaction involving meteoric-dominated hydrothermal fluids, which formed

large fluid convection cells as the pluton and surrounding host-rock cooled immediately after crystallization (620 Ma), and (2) regional infiltration of meteoric-dominated hydrothermal fluids into deep extensional basins formed during the final stages of 575-560 Ma Coastal Belt volcanism.

In the first scenario, hydrothermal fluids were mobilized by the onset of geothermal activity during the final stages of volcanism in the East Bay Hills volcanic suite (ca. 620 Ma). Emplacement of the Huntington Mountain pluton into these volcanic rocks prior to the final stage of volcanism provided sufficient heat to form hydrothermal convection cells (e.g., Taylor, 1974). Given the permeable nature of many volcanic rock sequences (i.e., the development of joints and cleavage along bedding surfaces), hydrothermal fluids could readily move through the volcanic rocks, and given the near-surface emplacement of the pluton (Barr et al., 1996), meteoric water would comprise a dominant fraction of these hydrothermal fluids (e.g., Taylor, 1971, 1974; Criss and Taylor, 1986). These convecting hydrothermal fluids ultimately collapsed onto and interacted with the cooling pluton by migrating along fractures and grain boundaries (Fig. 5.11) (e.g., Taylor, 1971, 1974). The formation of such hydrothermal fluid convection cells could have resulted in widespread ^{18}O-depletion of the Huntington Mountain pluton and East Bay Hills volcanic suite.

In the classical oxygen-isotope studies of hydrothermally altered epizonal plutonic rocks, Taylor (1968, 1971, 1974) recognized that many plutonic rocks and their host volcanic rocks have low $\delta^{18}O$ values (<+6 ‰), which were the product of oxygen-isotope exchange between primary igneous minerals and meteoric-dominated hydrothermal fluids. In many examples of this interaction, the whole-rock $\delta^{18}O$ values of

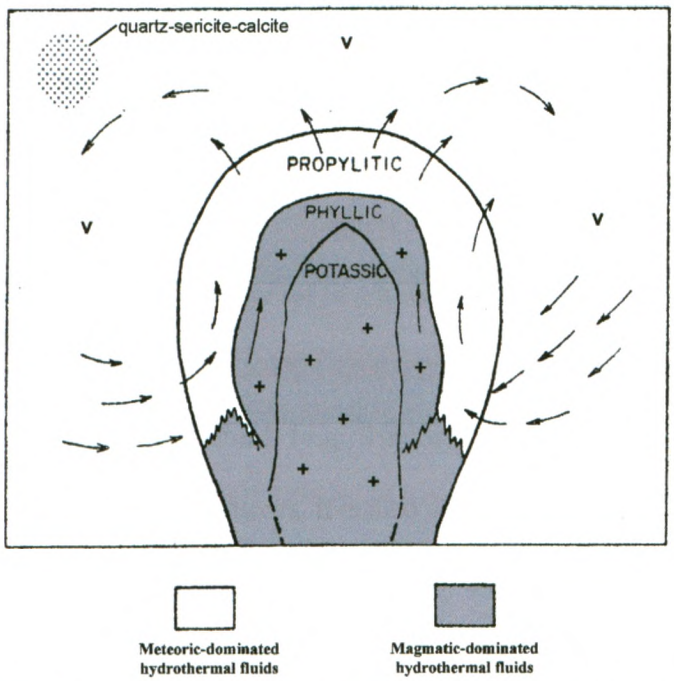

Figure 5.11. Classic model of convecting meteoric-dominated hydrothermal fluids as they interact with a cooling pluton (+) and its related volcanic rocks (v), and the alteration zones associated with magmatic- and meteoric-dominated hydrothermal fluids, after Taylor (1971, 1974).

these plutonic and volcanic rocks formed a 'bull's eye' pattern of ^{18}O-depletion in plan view, consisting of a systematic lowering of $\delta^{18}O$ values towards the center, or along the intrusive contacts of a pluton (Taylor, 1974). Commonly, the most ^{18}O-depleted rocks occur at the center of the 'bull's eye' pattern and represent the hottest and highest degree of oxygen-isotope exchange with meteoric-dominated hydrothermal fluids (e.g., Taylor 1971, 1974; Criss and Taylor, 1986). The highest $\delta^{18}O$ values occur along the margin of the 'bull's eye' pattern, and represent areas that have either retained their primary igneous $\delta^{18}O$ values, or experienced oxygen-isotope exchange with much lower temperature meteoric-dominated hydrothermal fluids (e.g., Taylor, 1971, 1974; Criss and Taylor, 1986). Given these temperature gradients, it is also common to find widespread oxygen-isotope disequilibrium between coexisting minerals (Taylor, 1971).

Detailed mapping and petrography of fossil hydrothermal systems has shown that varying alteration assemblages are also a common consequence of these temperature gradients (e.g., Meyer and Hemley, 1967; Taylor, 1974; Criss and Taylor, 1986). Typically, the hottest areas of a hydrothermal system (>500°C) are represented by potassic and/or phyllic alteration, with primary minerals replaced by potassium feldspar-biotite-quartz-sulphides (potassic alteration) and quartz-sericite-pyrite (phyllic alteration) (e.g., Meyer and Hemley, 1967; Sheppard et al., 1971). These styles of alteration are typically associated with magmatic-dominated hydrothermal fluids, which are generated immediately after crystallization of a magma body, with $\delta^{18}O$ values similar to normal igneous rocks (Fig. 5.11) (e.g., Ulrich et al., 2001, Harris and Golding, 2002). In cooler areas of the hydrothermal system (~200 to 450°C), the alteration is characterized by a propylitic alteration assemblage, which typically consists mainly of primary igneous

minerals replaced by chlorite-epidote-sericite-Fe-Ti oxides. Such propylitic alteration assemblages are commonly associated with meteoric-dominated hydrothermal fluids (Fig. 5.11) and large-scale ^{18}O-depletion (e.g., Taylor, 1971, 1974). The coolest areas of a hydrothermal system (~150 to 300°C) are commonly represented by the replacement of primary igneous minerals by quartz-sericite-calcite and clay minerals (argillic alteration assemblage) (Meyer and Hemely, 1967), which are also generally associated with meteoric-dominated hydrothermal fluids (Sheppard and Taylor, 1974). Given the large mineral-H_2O fractionation at these temperatures, the $\delta^{18}O$ values of this alteration tend to be much higher than counterparts formed earlier, at higher temperatures (Sheppard and Taylor, 1974).

Results for the Huntington Mountain pluton and East Bay Hills volcanic suite do not easily match this classical pattern of alteration and accompanying ^{18}O-depletion (or ^{18}O-enrichment) (Table 5.1). Instead, only minor variations are observed in their alteration assemblages, with a very large portion of the samples being affected by propylitic alteration. Only a small number of samples contain the phyllic alteration assemblage (e.g., CBI-6-6-102 to CBI-6-6-104), and their $\delta^{18}O$ values suggest oxygen-isotope exchange with meteoric dominated-hydrothermal fluids. A small number of samples also appear to have retained primary igneous $\delta^{18}O$ values (e.g., CBI-6-6-11 and CBI-6-6-122), but their primary minerals are typically partially replaced by quartz-sericite-calcite, which again suggests interaction with lower temperature meteoric-dominated hydrothermal fluids (Sheppard and Taylor, 1974). Additionally, the 'bull's eye' pattern of ^{18}O-depletion appears to be absent (Fig. 5.2). Instead, ^{18}O-depletion appears to be regionally pervasive and controlled mostly by temperature and water/rock

Table 5.1. Comparison of classic alteration types to those recognized in this study, including abundance and typical $\delta^{18}O$ values.

Alteration Type	Classical	This Study
potassic	[a] strong alteration, normal- to high-^{18}O rocks	absent
phyllic	[b] moderate alteration, normal- to high-^{18}O rocks	rare, very low-^{18}O rocks
propylitic	[c] strong alteration, low-^{18}O rocks	strong, low-^{18}O rocks
quartz-sericite-calcite	[d] moderate alteration, high-^{18}O rocks	rare to weak, high-^{18}O rocks

[a] - Meyer and Hemley (1967); Sheppard et al. (1971); [b] - Ulrich et al. (2001); Harris and Golding (2002); [c] -Taylor (1974); Criss and Taylor (1986); [d] - Sheppard and Taylor (1974).

ratios (Section 5.1.2), with some local control by physical characteristics of the Huntington Mountain pluton and East Bay Hills volcanic suite (e.g., mineralogy and permeability; Section 5.1). It seems unlikely, therefore, that the ^{18}O-depletion was caused by the generation of localized hydrothermal convection cells during cooling of the Huntington Mountain pluton and East Bay Hills volcanic suite at ca. 620 Ma.

A second scenario was proposed by Potter et al. (2008), who suggested that the ^{18}O-depletion of the Huntington Mountain pluton and East Bay Hills volcanic suite was part of widespread (regional) alteration related to the formation of extensional basins during the late stages of volcanism in the Coastal belt (ca. 575-560 Ma). During this time, cessation of subduction and transition to transtensional rifting resulted in the initial separation of the Mira terrane from Gondwana (Potter et al., 2008). This initial rifting of the Mira terrane is marked by bimodal, within-plate volcanism and the formation of clastic sedimentary extensional basins (Barr et al., 1998). Direct evidence for these processes is found in the Coastal belt, with the ca. 575-560 Ma Fourchu Group representing volcanic rocks, which formed in a subduction-related volcanic arc setting, while the ~560 Ma Main-à-Dieu Group, which is commonly interbedded with, or overlying the Fourchu Group, consists of volcanic-rich clastic sedimentary rocks and epiclastic rocks formed within intra-arc extensional basins (Barr et al., 1996, 1998). Although it is suggested that these represent facies equivalents of a similar tectonic environment (e.g., Barr et al., 1998), it is also likely that the transition from arc volcanism (Fourchu Group) to deposition of clastic sedimentary rocks and epiclastic rocks (Main-à-Dieu Group) marked the cessation of subduction and onset of transtensional rifting (Potter et al., 2008).

In this model, large-scale extensional faults served as fluid conduits for the infiltration of meteoric water deep into the crust, while continued volcanism during the initial stages of rifting would have heated these fluids (Fig. 5.12) (Potter et al., 2008). A modern analogue for such behavior exists in the Baja California peninsula, Mexico, where cessation of subduction and transition to transtensional faulting along the Baja California margin ca. 7-8 Ma, resulted in rifting of the Baja California peninsula away from northwestern Mexico (Michaud et al., 2006). Large-scale infiltration of meteoric water occurs along a series of NW-SE trending extensional faults, which were initiated during this initial rifting of Baja California, and is the source of extensive geothermal activity throughout the region (Portugal et al., 2000). Given the size of the Baja California peninsula (~145,000 km^2) and the longevity of extensional faulting related to this transtensional regime (up to 7-8 Ma), large-scale infiltration and circulation of meteoric-dominated hydrothermal fluids deep in the Baja California peninsula crust should produce widespread alteration (e.g., Portugal et al., 2000).

Another possible modern analogue for the Huntington Mountain pluton and East Bay Hills volcanic suite is provided by the Taupo Volcanic Zone, North Island, New Zealand, which spans an area of ~17,500 km^2. The Taupo Volcanic Zone is characterized by calc-alkaline volcanism within a subduction-related setting, focused within an extensional intra-arc rift (Cole, 1990). Rotational motion along the subduction zone beneath the North Island, and transtensional faulting along the North Island Shear belt over the last 5 Ma, are largely responsible for continued rifting within the central North Island. The associated transtensional faulting and continued volcanism has resulted in widespread geothermal activity throughout the Taupo Volcanic Zone (e.g., Hedenquist,

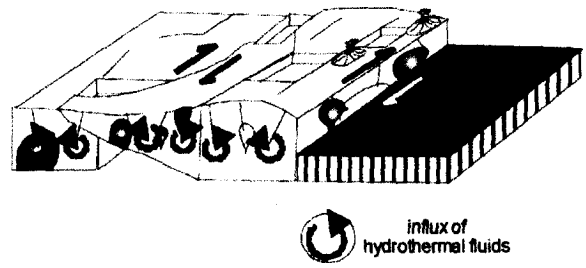

Figure 5.12. Model for large-scale transform faulting during the early stages of rifting, and infiltration and circulation of meteoric-dominated hydrothermal fluids, modified after Murphy and Nance (1996) by Potter et al. (in press).

1986). Extensive geothermal activity in the region has resulted from large-scale infiltration and circulation of meteoric-dominated hydrothermal fluids, which has been accompanied by widespread water-rock interaction and ^{18}O-depletion of the host crustal rocks (e.g., Cole, 1994; Simmons and Christenson, 1994).

To test this model for the ^{18}O-depletion of the Huntington Mountain pluton and East Bay Hills volcanic suite, meteoric water compositions were estimated for 620 Ma, 595 Ma and 560 Ma (Fig. 5.13), using the known paleolatitude estimates of Avalonia for the respective ages (Murphy et al., 2004) based on the present global δD and $\delta^{18}O$ values of meteoric water for these latitudes (Taylor, 1997). These results were then combined with the Global Meteoric Water Line, which yielded δD_{H2O} and $\delta^{18}O_{H2O}$ values of –86‰ and –12‰ (620 Ma), –22‰ and –4‰ (595 Ma) and –38‰ and –6‰ (560 Ma), respectively. These meteoric water compositions were then compared to the calculated hydrothermal fluid compositions for whole-rock samples at 300°C and 450°C (Section 5.2.1 and Fig. 5.8).

The meteoric water $\delta^{18}O$ and δD values estimated for Avalonia at 560 Ma provide the best match to the water compositions calculated using the whole-rock oxygen- and hydrogen-isotope compositions of the hydrothermal fluid (300-450°C) over a range of water/rock ratios. From this, it is concluded that the hydrothermal alteration of the Huntington Mountain pluton and East Bay Hills volcanic suite was part of the larger ^{18}O-depletion of the Mira terrane, ca. 575-560 Ma. This regional hydrothermal alteration arose from large-scale infiltration and movement of meteoric-dominated hydrothermal fluids along a network of transtensional faults – movement that was facilitated and

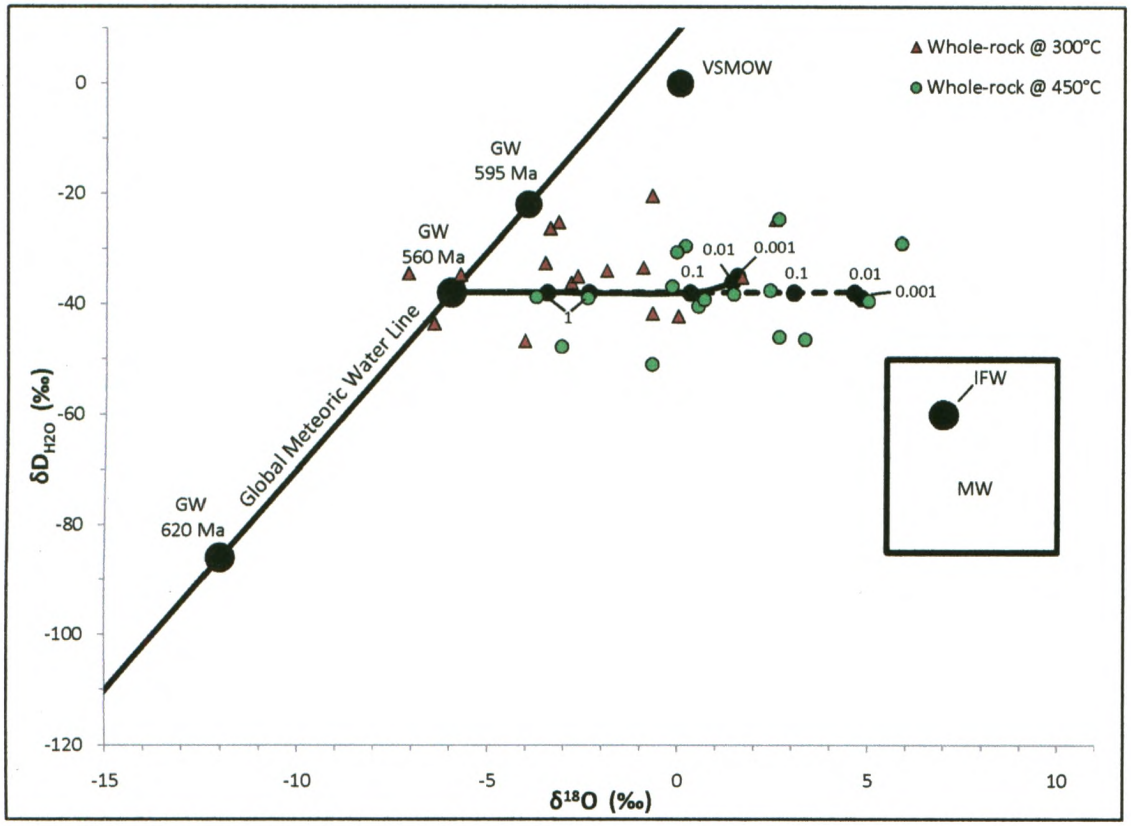

Figure 5.13. Fluid compositions (δD_{H2O} and $\delta^{18}O_{H2O}$) calculated for whole-rock samples from the Huntington Mountain pluton and East Bay Hills volcanic suite (Table 4.1). These were calculated at 300 and 450°C, using the hydrogen-isotope fractionation factor for chlorite-H_2O (Graham et al., 1984) and the oxygen-isotope fractionation factors for rock-H_2O (Zhao and Zheng, 2003). Additionally, water/rock ratios (1, 0.1, 0.01 and 0.001) were calculated for 300°C (solid line) and 450°C (dashed line) following the method of Ohmoto and Rye (1974). Meteoric water (GW) fluid compositions for 620 Ma, 595 Ma and 560 Ma were calculated based on paleolatitude estimates for Avalonia. The modern Global Meteoric Water Line, the present composition of ocean water (VSMOW), the field for magmatic water (MW) and the composition of intermediate to felsic magmatic water (IFW) are shown here, modified from Sheppard (1986).

initiated by rifting and extensional-related volcanism in the Mira terrane, ca. 575-560 Ma.

5.5 Regional Implications for ^{18}O-depletion

5.5.1 ^{18}O-depletion of Other Avalonian Terranes

The results reported in this study suggest that ^{18}O-depletion of the Huntington Mountain pluton and East Bay Hills volcanic suite was caused by large-scale infiltration of meteoric-dominated hydrothermal fluids related to regional transtensional faulting during the late phases of Coastal Belt volcanism, ca. 575-560 Ma. Given that initial rifting of the Mira terrane resulted in regional transtensional faulting, other areas of the Mira terrane were also likely affected. Potter et al. (2008) have reported low $\delta^{18}O$ values for other late Proterozoic igneous rocks of the Mira terrane. A large number of low $\delta^{18}O$ values have been recognized also in late Proterozoic igneous rocks of other Avalonian terranes, including $\geq$+2.8‰ for the Avalon terrane of Newfoundland (Fryer et al., 1992; Potter et al., in press), $\geq$+5.8‰ for the Antigonish Highlands of northern mainland Nova Scotia (Potter et al., in press), $\geq$–1.2‰ for the Caledonia terrane of New Brunswick (Whalen et al., 1994; Ayuso et al., 1996; Potter et al., 2008) and $\geq$–3.4‰ for the Boston terrane of Massachusetts (Potter et al., in press). The similarities in the magmatic and tectonic histories of each Avalonian terrane, and the recognition of widespread pervasive propylitic alteration throughout Avalonia, suggests that the characteristic regional ^{18}O-depletion was likely the result of transtensional faulting and extensional-related volcanism throughout all Avalonian terranes (Potter et al., 2008; in press).

5.5.2 Mineralization in the Huntington Mountain Pluton and East Bay Hills Volcanic Suite

Mineralization of large base- and precious-metals is commonly linked to movement of meteoric-dominated hydrothermal fluids. In the Mira terrane, known mineralization occurs in two main locations, the Mindamar Zn-Pb-Cu-Ag-Au deposit located in the 680 Ma Stirling Group (Barr et al., 1996), and the Coxheath Cu-Mo-Au deposit located in the 620 Ma Coxheath Hills Group (Barr et al., 1996; Kontak et al., 2003). The preservation of mineralization and primary textural features associated with syn-magmatic mineralization of these two deposits (e.g., Barr et al., 1996; Kontak et al., 2003), and the apparent absence of such features within the Huntington Mountain pluton and East Bay Hills volcanic suite, suggests that these two mineral deposits were not significantly affected by the later 575-560 Ma hydrothermal fluid movements. This interpretation is confirmed by Potter et al. (2008), who reported high $\delta^{18}O$ values (+9.0 to +10.9‰) for rhyolite from the 680 Ma Stirling Group. In the Coxheath Hills Group, $\delta^{18}O$ values of +3.3‰ and +3.6‰ for granodiorite were also reported (Potter et al., 2008). Although these imply interaction with meteoric-dominated hydrothermal fluids, in comparison to granodiorite from the Huntington Mountain pluton (e.g., +1.2‰), they suggest that the Coxheath Hills Group was not as significantly affected by the hydrothermal fluid movements.

The Huntington Mountain pluton and East Bay Hills volcanic suite is barren of base- and precious-metal mineralization (Barr et al., 1996) to the best of our knowledge. This might suggest that large-scale infiltration of meteoric-dominated hydrothermal fluids into the Mira terrane remobilized and removed any syn-magmatic base- and precious-metal mineralization in the Huntington Mountain pluton and East Bay Hills

volcanic suite, whereas areas less affected by interaction with these meteoric-dominated fluids have had their primary base- and precious-metal mineralization preserved.

Chapter 6. Conclusions

1. The Huntington Mountain pluton and East Bay Hills volcanic suite represent cogenetic calc-alkaline magmatism that occurred at ca. 620 Ma, and are dominated by rocks of intermediate composition, mostly diorite and andesite. Other rock types include granodiorite, syenogranite, leucogranite, basalt, dacite and rhyolite. The occurrence of multiple magmatic intrusive events of varying compositions suggests an evolving magmatic source. Development of micro-granophyric and weak porphyritic textures in the syenogranite and leucogranite imply high-level emplacement of the pluton within the crust.

2. Three main alteration types are observed in the plutonic and volcanic rocks:

   (a) widespread, pervasive propylitic alteration, characterized by primary igneous minerals (i.e., feldspar, biotite and hornblende) partially to completely replaced by fine-grained chlorite, epidote, sericite and Fe-Ti oxides.

   (b) localized quartz-sericite-calcite alteration, characterized by primary igneous minerals partially to completely replaced by quartz, sericite and calcite. This alteration mostly affects localized areas of basaltic rocks in the southwestern and northwestern margins of the East Bay Hills volcanic suite. In some areas, the quartz-sericite-calcite alteration can be demonstrated to have overprinted the propylitic alteration.

(c) very localized phyllic alteration is characterized by primary igneous minerals and textures partially to completely replaced by quartz, sericite and pyrite. This alteration was observed mainly in three diorite samples (CBI-6-6-102 to CBI-6-6-104). The petrographic data suggest that it is the earliest alteration, likely reflecting magmatic-dominated hydrothermal fluids during the early stages of hydrothermal activity.

3. Oxygen-isotope disequilibrium is prevalent between coexisting mineral pairs ($\Delta^{18}O_{mineral\text{-}mineral}$) throughout the plutonic and volcanic rock sample suites, with a large portion of these having low $\delta^{18}O$ values. This suggests that the Huntington Mountain pluton and East Bay Hills volcanic suite experienced post-crystallization oxygen-isotope exchange with meteoric-dominated hydrothermal fluids.

4. Low $\delta^{18}O$ values are characteristic of most plutonic and volcanic rock samples affected by the propylitic alteration, and were acquired by their interaction with meteoric-dominated hydrothermal fluids at ~300-450°C. Samples affected by quartz-sericite-calcite alteration generally have high $\delta^{18}O$ values, which reflect the lower temperatures (~200-300°C) associated with this style of alteration.

5. Hydrothermal fluid compositions ($\delta^{18}O_{H2O}$) ranged from –9.0 to 0‰ for samples affected by propylitic alteration to ~ –3.2 to +9.5‰ for samples affected by the lower temperature quartz-sericite-calcite alteration. Results for hydrous minerals confirm this range of $\delta^{18}O$ fluid values, but also demonstrate only minor variations in δD values. This has produced a characteristic ^{18}O-shift of the fluid to the right of the Global Meteoric Water Line, which suggests that the initial meteoric-dominated hydrothermal fluids became progressively enriched in ^{18}O during water-rock interaction, and that water/rock ratios were important in controlling the extent of ^{18}O-depletion of the host rocks.

6. The hydrothermal fluid generation and movement likely occurred during the final stages of volcanism in the Coastal Belt, ca. 575-560 Ma. The development of large-scale transtensional faulting and extensional-related volcanism within the Mira terrane produced fluid conduits, which facilitated the deep infiltration, heating and circulation of meteoric-dominated hydrothermal fluids.

7. Low $\delta^{18}O$ values have also been reported for other igneous units of the Mira terrane (Potter et al., 2008) and elsewhere in Avalonia (e.g., Potter et al., in press). This suggests that the regional ^{18}O-depletion resulted from the development of large-scale transtensional faults and associated infiltration of meteoric-dominated hydrothermal fluids during the initial rifting of Avalonia from Gondwana.

References

Ayuso, R.A., Barr, S.M., and Longstaffe, F.J. 1996. Pb and O isotopic constraints on the source of granitic rocks from Cape Breton Island, Nova Scotia, Canada. American Journal of Science, **296**: 789-817.

Barr, S.M. 1993. Geochemistry and tectonic setting of late Precambrian volcanic and plutonic rocks in southeastern Cape Breton Island, Nova Scotia. Canadian Journal of Earth Sciences, **30**: 1147-1154.

Barr, S.M., and Hegner, E. 1992. Nd isotopic compositions of felsic igneous rocks in Cape Breton Island, Nova Scotia. Canadian Journal of Earth Sciences, **29**: 650-657.

Barr, S.M., and Macdonald, A.S. 1992. Devonian plutons in southeastern Cape Breton Island, Nova Scotia. Atlantic Geology, **28**: 101-113.

Barr, S.M., and Raeside, R.P. 1986. Pre-Carboniferous tectonostratigraphic subdivisions of Cape Breton Island, Nova Scotia. Maritime Sediments and Atlantic Geology, **22**: 252-263.

Barr, S.M., and Raeside, R.P. 1989. Tectono-stratigraphic terranes in Cape Breton Island, Nova Scotia: Implications for the configuration of the northern Appalachian orogen. Geology, **17**: 822-825.

Barr, S.M., and White, C.E. 1988. Petrochemistry of contrasting Late Precambrian volcanic and plutonic associations, Caledonian Highlands, southern New Brunswick. Maritime Sediments and Atlantic Geology, **24**: 353-372.

Barr, S.M., and White, C.E. 1996. Contrasts in late Precambrian - early Paleozoic tectonothermal history between Avalon composite terrane sensu stricto and the other possible peri-Gondwanan terranes in southern New Brunswick and Cape Breton Island, Canada. *In* Avalonian and Related Peri-Gondwanan Terranes of the Circum-North Atlantic. *Edited by* R.D. Nance and M.D. Thompson. Geological Society of America, Special Paper 304, pp. 95-108.

Barr, S.M., Dunning, G.R., Raeside, R.P., and Jamieson, R.A. 1990. Contrasting U–Pb ages from plutons in the Bras d'Or and Mira terranes of Cape Breton Island, Nova Scotia. Canadian Journal of Earth Sciences, **27**: 1200-1208.

Barr, S.M., White, C.E., and Macdonald, A.S. 1996. Stratigraphy, tectonic setting, and geological history of Late Precambrian volcanic-sedimentary-plutonic belts in southeastern Cape Breton Island, Nova Scotia. Geological Survey of Canada, Bulliten 468, 84 p.

Barr, S.M., Raeside, R.P., and White, C.E. 1998. Geological correlations between Cape Breton Island and Newfoundland, northern Appalachian orogen. Canadian Journal of Earth Sciences, **35**: 1252-1270.

Beane, R.E., and Titley, S.R. 1981. Porphyry copper deposits. Part II. Hydrothermal alteration and mineralization. Economic Geology and the Bulletin of the Society of Economic Geologists, 75th Anniversary Volume, pp. 235-269.

Beaty, D.W., and Taylor, H.P. Jr. 1982. Some petrologic and oxygen isotope relationships in the Amulet mine, Noranda, Quebec, and their bearing on the origin of Archean massive sulfide deposits. Economic Geology and the Bulletin of the Society of Economic Geologists, **77**: 1-17.

Bevier, M.L., Barr, S.M., White, C.E., and Macdonald, A.S. 1993. U–Pb geochronologic constraints on the volcanic evolution of the Mira (Avalon) terrane, southeastern Cape Breton Island, Nova Scotia. Canadian Journal of Earth Sciences, **30**: 1-10.

Bigeleisen, J., Perlman, M.L., and Prosser, H.C. 1952. Conversion of hydrogenic materials to hydrogen for stable isotopic analysis. Analytical Chemistry, **24**: 1356-1357.

Borthwick, J., and Harmon, R.S. 1982. A note regarding ClF_3 as an alternative to BrF_5 for oxygen isotope analysis. Geochimica et Cosmochimica Acta, **46**: 1665-1668.

Bradley, D.C., and Bradley, L.M. 1986. Tectonic significance of the Carboniferous Big Pond basin, Cape Breton Island, Nova Scotia. Canadian Journal of Earth Sciences, **23**: 2000-2011.

Chacko, T., Mayeda, T.K., Clayton, R.N., and Goldsmith, J.R. 1991. Oxygen and carbon isotope fractionations between CO_2 and calcite. Geochimica et Cosmochimica Acta, **55**: 2867-2882.

Clayton, R.N., and Mayeda, T.K. 1963. The use of bromine pentafluoride in the extraction of oxygen from oxides and silicates for isotopic analysis. Geochimica et Cosmochimica Acta, **27**: 43-52.

Cole, D.R. 1994. Evidence for oxygen isotope disequilibrium in selected geothermal and hydrothermal ore deposit systems. Chemical Geology, **111**: 283-296.

Cole, J.W. 1990. Structural control and origin of volcanism in the Taupo volcanic zone, New Zealand. Bulletin of Volcanology, **52**: 445-459.

Coplen, T.B. 1996. New guidelines for the reporting of stable hydrogen, carbon, and oxygen isotope ratio data. Geochimica et Cosmochimica Acta, **60**: 3359-3360.

Cormier, R.F. 1972. Radiometric ages of granitic rocks, Cape Breton Island, Nova Scotia. Canadian Journal of Earth Sciences, **9**: 1074-1086.

Craig, H. 1961. Isotopic variations in meteoric waters. Science, **133**: 1702-1703.

Craig, H. 1963. The isotopic geochemistry of water and carbon in geothermal areas. *In* Nuclear Geology on Geothermal Areas. *Edited by* E. Tongiorgi. Pisa, Consiglio Nazionale della Richerche, Spoleto, Italy, pp. 17-53.

Criss, R.E., and Taylor, H.P. Jr. 1986. Meteoric-hydrothermal systems. *In* Stable Isotopes in High Temperature Geological Processes. *Edited by* J.W. Valley, H.P. Taylor, Jr. and J.R. O'Neil. Mineralogical Society of America, Reviews in Mineralogy, Volume 16, pp. 373-424.

Criss, R. E., Ekren, E. B., and Hardyman, R. F. 1984. Casto ring zone; a 4,500-km^2 fossil hydrothermal system in the Challis volcanic field, central Idaho. Geology, **12**: 331-334.

Ferry, J. 1985. Hydrothermal alteration of Tertiary igneous rocks from the Isle of Skye, northwest Scotland. Contributions to Mineralogy and Petrology, **91**: 283.304.

Field, C.W., and Fifarek, R.H. 1985. Light stable-isotope systematics in the epithermal environment. *In* Geology and Geochemistry of Epithermal Systems. *Edited by* B.R. Berger and P.M. Bethke. Society of Economic Geologists, Reviews in Economic Geology, Volume 2, pp. 99-128.

Friedman, I., and O'Neil, J.R. 1977. Compilation of stable isotope fractionation factors of geochemical interest. *In* Data of geochemistry. *Edited by* M. Fleischer. U.S. Geological Survey, Washington, U.S.A. pp. KK1-KK11.

Fryer, B.J., Kerr, A., Jenner, G.A., and Longstaffe, F.J. 1992. Probing the crust with plutons: regional isotopic geochemistry of granitoid intrusions across insular Newfoundland. Current Research, **92-1**: 119-139.

Giggenbach, W.F., Shinohara, H., Kusakabe, M., and Ohba, T. 2003. Formation of acid volcanic brines through interaction of magmatic gases, seawater and rock within the White Island volcanic-hydrothermal system, New Zealand. *In* Volcanic, Geothermal, and Ore-forming Fluids: Rulers and Witnesses of Processes within the Earth. *Edited by* S.F. Simmons and I. Graham. Society of Economic Geologists, Special Publication Number 10, pp. 19-40.

Graham, C.M., Atkinson, J., and Harmon, R.S. 1984. Hydrogen isotope fractionation in the system chlorite-water. Progress in Experimental Petrology, **6**: 139-140.

Harris, A.C., and Golding, S.D. 2002. New evidence of magmatic-fluid–related phyllic alteration: Implications for the genesis of porphyry Cu deposits. Geology, **30**: 335-338.

Hedenquist., J.W. 1986. Geothermal systems of the Taupo Volcanic Zone: Their characteristics and relation to volcanism and mineralisation. *In* Late Cenozoic Volcanism in New Zealand. *Edited by* I.E.M. Smith. Royal Society of New Zealand, Bulletin 23, pp. 134-168.

Hermes, O.D., and Zartman, R.E. 1992. Late Proterozoic and Silurian alkaline plutons within the southeastern New England Avalon zone. Journal of Geology, **100**: 477-486.

Hibbard, J.P., van Staal, C.R., and Miller, B.V. 2007. Links among Carolinia, Avalonia, and Ganderia in the Appalachian peri-Gondwanan realm. *In* Whence the Mountains? Inquiries into the Evolution of Orogenic Systems: A Volume in Honor of Raymond A. Price. *Edited by* J.W. Sears, T.A. Harms, and C.A. Evenchick. Geological Society of America, Special Paper 433, pp. 291-311.

Keppie, J.D., Dallmeyer, R.D., and Murphy, J.B. 1990. Tectonic implications of $^{40}Ar/^{39}Ar$ hornblende ages from late Proterozoic-Cambrian plutons in the Avalon Composite Terrane, Nova Scotia, Canada. Geological Society of America Bulletin, **102**: 516-528.

Kontak, D.J., DeWolfe, J., and Finck, P.W. 2003. The Coxheath plutonic-volcanic belt (NTS 11K/01): a linked porphyry-epithermal mineralized system of Precambrian age. Nova Scotia Department of Natural Resources, Mineral Resources Branch, Report 2003-1, pp. 69-87.

Landing, E. 1991. Upper Precambrian through Lower Cambrian of Cape Breton Island: faunas, paleoenvironments, and stratigraphic revision. Journal of Paleontology, **65**: 570-595.

Landing, E. 1996. Avalon: insular continent by the latest Precambrian. *In* Avalonian and Related Peri-Gondwanan Terranes of the Circum-North Atlantic. *Edited by* R.D. Nance and M.D. Thompson. Geological Society of America, Special Paper 304, pp. 29-63.

Longstaffe, F.J. 1982. Stable isotopes in the study of granitic pegmatites and related rocks. *In* Short Course in Granitic Pegmatites in Science and Industry. *Edited by* P. Černý. Mineralogical Association of Canada, Volume 8, 373-404.

Lynch, G., and Ortega, J. 1997. Hydrothermal alteration and tourmaline-albite equilibria at the Coxheath porphyry Cu-Mo-Au deposit, Nova Scotia. Canadian Mineralogist, **35**: 79-94.

Matsuhisa, Y., Goldsmith, J.R., and Clayton, R.N. 1979. Oxygen isotopic fractionation in the system quartz-albite-anothite-water. Geochimica et Cosmochimica Acta, **43**: 1131-1140.

McKinney, C.R., McCrea, J.M., Epstein, S., Allen, H.A., and Urey, H.C. 1950. Improvements in mass-spectrometers for the measurement of small differences in isotope abundance ratios. The Review of Scientific Instruments, **21**: 724-730.

Meyer, C., and Hemley, J.J. 1967. Wall rock alteration. *In* Geochemistry of Hydrothermal Ore Deposits. *Edited by* H.L. Barnes. Holt, Rinehart and Winston, New York. pp. 166-235.

Michaud, F., Royer, J.Y., Bourgois, J., Dyment, J., Calmus, T., Bandy, W., Sosson, M. Mortera-Gutiérrez, C., Sichler, B., Rebolledo-Viera, M., and Pontoise, B. 2006. Oceanic-ridge subduction vs. slab break off: Plate tectonic evolution along the Baja California Sur continental margin since 15 Ma. Geology, **34**: 13-16.

Murphy, J.B., Keppie, J.D., Nance, R.D., and Dostal, J. 1990. The Avalon composite terrane of Nova Scotia. *In* Avalonian and Cadomian Geology of the North Atlantic. *Edited by* R.A. Strachan and G.K. Taylor. Blackie, Glasgow, pp. 195-213.

Murphy, J.B., Pisarevsky, S.A., Nance, R.D., and Keppie, J.D. 2004. Neoproterozoic early Paleozoic evolution of Peri-Gondwanan terranes: Implications for Laurentia-Gondwana connections. International Journal of Earth Sciences, **93**: 659-682.

Murphy, J.B., and Nance, R.D. 1996. Basement isotopic signatures and Neoproterozoic paleogeography of Avalonian-Cadomian and related terranes in the circum-North Atlantic. *In* Avalonian and Related Peri-Gondwanan Terranes of the Circum-North Atlantic. *Edited by* R.D. Nance and M.D. Thompson. Geological Society of America, Special Paper 304, pp. 333-346.

O'Brien, S.J., O'Brien, B.H., Dunning, G.R., and Tucker, R.D. 1996. Late Neoproterozoic Avalonian and related peri-Gondwanan rocks of the Newfoundland Appalachians. *In* Avalonian and Related Peri-Gondwanan Terranes of the Circum-North Atlantic. *Edited by* R.D. Nance and M.D. Thompson. Geological Society of America, Special Paper 304, pp. 9-28.

O'Neil, J.R., and Taylor, H.P. Jr. 1967. The oxygen isotope and cation exchange chemistry of feldspars. American Mineralogist, **52**: 1414-1437.

Ohmoto, H., and Rye, R.O. 1974. Hydrogen and oxygen isotope compositions of fluid inclusions in the Kuroko deposits, Japan. Economic Geology and the Bulletin of the Society of Economic Geologists, **69**: 509-567.

Ohmoto, H., and Rye, R.O. 1979. Isotopes of sulfur and carbon. *In* Geochemistry of Hydrothermal Ore Deposits. *Edited by* H.L. Barnes. John Wiley and Sons, New York., pp. 509-567.

Pe-Piper, G., Piper, D.J.W., and Koukouvelas, I. 1996. Precambrian plutons of the Cobequid Highlands, Nova Scotia, Canada. *In* Avalonian and Related Peri-Gondwanan Terranes of the Circum-North Atlantic. *Edited by* R.D. Nance and M.D. Thompson. Geological Society of America, Special Paper 304, pp. 121-132.

Portugal, E., Birkle, P., Barragán R., R.M., Arellano G., V.M., Tello, E., and Tello, M. 2000. Hydrochemical–isotopic and hydrogeological conceptual model of the Las Tres Vírgenes geothermal field, Baja California Sur, México. Journal of Volcanology and Geothermal Research, **101**: 223-244.

Potter, J., Longstaffe, F.J., and Barr, S.M. 2008. Regional ^{18}O-depletion of Neoproterozoic igneous rocks of Avalonia, Cape Breton Island and southern New Brunswick, Canada. Geological Society of America Bulletin, **120**: 347-367.

Potter, J., Longstaffe, F.J., Barr, S.M., Thompson, M.D., and White, C.E. in press. Altering Avalonia: oxygen isotopes and terrane distinction in the Appalachian peri-Gondwanan realm. Canadian Journal of Earth Sciences.

Raeside, R.P., and Barr, S.M. 1990. Geology and tectonic development of the Bras d'Or suspect terrane, Cape Breton Island, Nova Scotia. Canadian Journal of Earth Sciences, **27**: 1371-1381.

Sheppard, S.M.F. 1986. Characterization and isotopic variations in natural waters. *In* Stable Isotopes in High Temperature Geological Processes. *Edited by* J.W. Valley, H.P. Taylor, Jr. and J.R. O'Neil. Mineralogical Society of America, Reviews in Mineralogy, Volume 16, pp. 165-183.

Sheppard, S.M.F., and Taylor, H.P. Jr. 1974. Hydrogen and oxygen isotope evidence for the origins of water in the Boulder Batholith and the Butte ore deposits, Montana. Economic Geology and the Bulletin of the Society of Economic Geologists, **69**: 926-946.

Sheppard, S.M.F., Nielsen, R.L., and Taylor, H.P. Jr. 1971. Hydrogen and oxygen isotope ratios in minerals from porphyry copper deposits. Economic Geology and the Bulletin of the Society of Economic Geologists, **66**: 515-542.

Simmons, S.F., and Christenson, B.W. 1994. Origins of calcite in a boiling geothermal system. American Journal of Science, **294**: 361-400.

Suzuoki, T., and Epstein, S. 1976. Hydrogen isotope fractionation between OH-bearing minerals and water. Geochimica et Cosmochimica Acta, **40**: 1229-1240.

Taylor, H.P. Jr. 1968. The oxygen isotope geochemistry of igneous rocks. Contributions to Mineralogy and Petrology, **19**: 1-71.

Taylor, H.P. Jr. 1971. Oxygen isotope evidence for large-scale interaction between meteoric-ground waters and Tertiary granodiorite intrusions, Western Cascade Range, Oregon. Journal of Geophysical Research, **76**: 7855-7874.

Taylor, H.P. Jr. 1974. The application of oxygen and hydrogen isotope studies to problems of hydrothermal alteration and ore deposition. Economic Geology and the Bulletin of the Society of Economic Geologists, **69**: 843-883.

Taylor, H.P. Jr. 1997. Oxygen and hydrogen isotope relationships in hydrothermal mineral deposits. *In* Geochemistry of Hydrothermal Ore Deposits. *Edited by* H.L. Barnes. John Wiley and Sons, New York. pp. 229-302.

Taylor, H.P. Jr., and Epstein, S. 1962. Relationship between O^{18}/O^{16} ratios in coexisting minerals of igneous and metamorphic rocks; Part 1, Principles and experimental results. Geological Society of America Bulletin, **73**: 461-480.

Taylor, H.P. Jr. and Sheppard, S.M.F. 1986. Igneous Rocks: I. Processes of isotopic fractionation and isotope systematics. *In* Stable Isotopes in High Temperature Geological Processes. *Edited by* J.W. Valley, H.P. Taylor, Jr. and J.R. O'Neil. Mineralogical Society of America, Reviews in Mineralogy, Volume 16, pp. 227-271.

Ulrich, T., Günther, D., and Heinrich, C.A. 2001. The evolution of a porphyry Cu-Au deposit, based on LA-ICP-MS analysis of fluid inclusions: Bajo de la Alumbrera, Argentina. Economic Geology and the Bulletin of the Society of Economic Geologists, **96**: 1743-1774.

Vennemann, T.W., and O'Neil, J.R. 1993. A simple and inexpensive method of hydrogen isotope and water analyses of minerals and rocks based on zinc reagent. Chemical Geology, **103**: 227-234.

Weeks, L.J. 1954. Southeast Cape Breton Island, Nova Scotia. Geological Survey of Canada, Memoir 277, 112 p.

Wenner, D.B., and Taylor, H.P. Jr. 1971. Temperatures of serpentinization of ultramafic rocks based on $^{18}O/^{16}O$ fractionation between coexisting serpentine and magnetite. Contributions to Mineralogy and Petrology, **32**: 165-185.

Whalen, J.B., Jenner, G.A., Currie, K.L., Barr, S.M., Longstaffe, F.J., and Hegner, E. 1994. Geochemical and isotopic characteristics of granitoids of the Avalon Zone, southern New Brunswick: possible evidence for repeated delamination events. Journal of Geology, **102**: 269-282.

Williams, H. 1979. Appalachian orogen in Canada. Canadian Journal of Earth Sciences, **16**: 792-807.

Zhao, Z.F., and Zheng, Y.F. 2003. Calculation of oxygen isotope fractionation in magmatic rocks. Chemical Geology, **193**: 59-80.

Zheng, Y.F. 1993. Calculation of oxygen isotope fractionation in hydroxyl-bearing silicates. Earth and Planetary Science Letters, **120**: 247-263.

Zheng, Y.F., and Hoefs, J. 1993. Carbon and oxygen isotopic covariations in hydrothermal calcites. Mineralium Deposita, **28**: 79-89.

Appendix A. Sample Descriptions for the Huntington Mountain Pluton and East Bay Hills Volcanic Suite

Sample	*Easting	*Northing	Rock Unit	Description	"Alteration
Huntington Mountain Pluton					
CBI-8-05-23	699970	5086962	Leucogranite	Pink, medium-grained	1 - weak
CBI-6-6-81	706997	5093152	Leucogranite	Pink, medium-grained	1 - weak
CBI-6-6-105	701523	5088298	Leucogranite	Red-pink, coarse-grained	1 - weak to moderate
CBI-6-6-106	699255	5086455	Leucogranite	Red, fine-grained, weakly porphyritic	1 - weak
[c]EB91-014	700035	5087134	Leucogranite	-	-
[c]F16C-1582	700980	5087948	Leucogranite	-	-
CBI-6-6-54	701128	5091386	Syenogranite	Pink, fine-grained, weakly porphyritic	1 - weak to moderate
CBI-6-6-55	702739	5091982	Syenogranite	Pink, fine-grained, weakly porphyritic	1- moderate to strong
[c]F16C-1631	702868	5092231	Syenogranite	-	-
[c]F16C-1635	703016	5091804	Syenogranite	-	-
[c]F16C-1782	704439	5093092	Syenogranite	-	-
CBI-8-05-21	696840	5084826	Granodiorite	Red, medium-grained	1 - moderate
CBI-8-05-22	696840	5084826	Granodiorite	Red, medium-grained	1 - moderate
CBI-8-05-25	699530	5087930	Diorite	Grey, medium-grained	1 - moderate
CBI-8-05-26	699530	5087930	Diorite	Grey, medium-grained	1 - moderate
CBI-8-05-27A	699530	5087930	Diorite	Minor felsic dyke within diorite	1 - weak to moderate
CBI-8-05-27B	699530	5087930	Diorite	Grey, medium-grained	1 - weak to moderate
CBI-6-6-56	704403	5092583	Diorite	Grey, medium-grained	1 - moderate to strong
CBI-6-6-82	706357	5092651	Diorite	Grey-green, medium-grained	1 - moderate
CBI-6-6-83	705479	5091896	Diorite	Grey, medium-grained	1 - moderate
CBI-6-6-84	704824	5091368	Diorite	Grey, fine-grained	1 - moderate to strong
CBI-6-6-86	703946	5090670	Diorite	Green-grey, medium-grained	1 - moderate
CBI-6-6-87	703172	5089998	Diorite	Green-grey, fine-grained, weakly foliated	1 - moderate

Appendix A. Sample Descriptions (continued)

Sample	[a]Easting	[a]Northing	Rock Unit	Description	[b]Alteration
Huntington Mountain Pluton					
CBI-6-6-102	700285	5088682	Diorite	Green, coarse-grained, strong epi alteration	1 - strong, 3 - moderate
CBI-6-6-103	700234	5088775	Diorite	Gaussenized diorite	3 - strong
CBI-6-6-104	701178	5089721	Diorite	Green, fine-grained, minor discontinuous qtz vein	1 - strong, 3 - moderate
[c]F16C-1751	705434	5091416	Diorite	-	-
East Bay Hills Volcanic Suite					
CBI-8-05-30	711730	5096499	Rhyolite	Red-purple, aphanitic, flow-banded	1 - weak, 2 - moderate
CBI-6-6-17	711730	5096499	Rhyolite	Red-purple rhyolite tuff with qtz-cal vein	1 - weak, 2 - moderate
CBI-6-6-80	712525	5095531	Rhyolite	Red-purple rhyolite tuff	1 - weak, 2 - moderate
[c]FS91-53	712166	5096074	Rhyolite	Rhyolite flow	-
CBI-8-05-28	698619	5088033	Dacite	Grey-black, porphyritic, strong epi-ser alteration	1 - strong, 3 - moderate
CBI-6-6-98	696665	5084729	Dacite	Grey-black, fine-grained, massive	1 - moderate
CBI-6-6-99	698008	5086487	Dacite	Grey-black, aphanitic, massive	1 - strong
CBI-6-6-101	697748	5086111	Dacite	Grey-black, aphanitic, weakly porphyritic	1 - strong
CBI-6-6-93	695653	5089179	Andesite to Rhyolite	Grey-green, andesite fs crystal tuff, flow banded	1 - moderate, 2 weak
CBI-6-6-94	697552	5090545	Andesite to Rhyolite	Grey-green, andesite fs crystal tuff, flow banded	1 - weak, 2 - weak to moderate
CBI-6-6-95	697552	5090545	Andesite to Rhyolite	Coarse-grained well-defined qtz vein	-
CBI-6-6-96	698139	5091186	Andesite to Rhyolite	Purple, andesite fs crystal tuff	1 - weak, 2 - weak to moderate
CBI-6-6-118	700499	5093328	Andesite to Rhyolite	Blue-green, andesite fs crystal tuff	1 - weak, 2 - weak to moderate
CBI-6-6-119	702051	5093785	Andesite to Rhyolite	Blue-green, andesite fs crystal tuff, minor cal veins	1 - weak, 2 - weak to moderate
CBI-6-6-121	699942	5093570	Andesite to Rhyolite	Brown, rhyolite, aphanitic, weakly porphyritic	1, 2 - weak

Appendix A. Sample Descriptions (continued)

Sample	[a]Easting	[a]Northing	Rock Unit	Description	[b]Alteration
East Bay Hills Volcanic Suite					
CBI-6-6-50	694457	5086067	Andesite	Green fs crystal tuff	1 - moderate to strong
CBI-6-6-51	696318	5088683	Andesite	Green fs crystal tuff, minor lithic fragments	1 - moderate to strong
CBI-6-6-52	699724	5090994	Andesite	Green fs crystal tuff	1 - moderate to strong
CBI-6-6-89	691404	5083964	Andesite	Grey-green fs crystal tuff	1 - moderate to strong
CBI-6-6-90	691491	5083678	Andesite	Grey-green fs crystal tuff, minor qtz-cal veinlets	1, 2 - moderate
[c]EB87-037	695025	5086964	Andesite	Andesite crystal tuff	-
CBI-6-6-11	691533	5083004	Basalt to Andesite	Green, foliated, strong qtz-ser alteration	2 - strong
CBI-6-6-88	707719	5093206	Basalt to Andesite	Black-green, aphanitic basalt, massive	1 - strong
CBI-6-6-110	710393	5096153	Basalt to Andesite	Black, aphanitic basalt, massive	1 - strong
CBI-6-6-111	709137	5094924	Basalt to Andesite	Red rhyolite dyke, porphyritic	1 - weak to moderate
CBI-6-6-112	709010	5094795	Basalt to Andesite	Black, aphanitic basalt, massive	1 - strong
CBI-6-6-112A	709010	5094795	Basalt to Andesite	Maroon, aphanitic qtz vein	-
CBI-6-6-112B	709010	5094795	Basalt to Andesite	Milky qtz on margin of maroon qtz vein	-
CBI-6-6-112C	709010	5094795	Basalt to Andesite	Milky qtz vein within basalt	-
CBI-6-6-114	709024	5094847	Basalt to Andesite	Pink-brown rhyolite dyke, strong qtz-cal veining	1 - weak, 2 - moderate
CBI-6-6-38	692954	5088811	Basalt	Qtz vein within purple basalt	-
CBI-6-6-39	692954	5088811	Basalt	Black-green, aphanitic, weakly porphyritic	1 - moderate , 2 - weak
CBI-6-6-40	693211	5089718	Basalt	Black-green, aphanitic, massive	1 - moderate, 2 - weak
CBI-6-6-107	697080	5092300	Basalt	Black-green, aphanitic	1 - weak , 2 - moderate
CBI-6-6-122	698905	5093854	Basalt	Andesitic (?) fs crystal tuff,	2 - moderate to strong
[c]MT6-397	696254	5091348	Basalt	Rhyolite tuff	-

Note: a = sample locations, UTM projection, NAD27 zone 20; b = alteration types, (1) chlorite, epidote, sericite and Fe-Ti-oxides, (2) quartz, sericite and calcite, and (3) quartz, sericite and pyrite; c = Previously reported by Potter et al. (2008).
Mineral abbreviations, cal - calcite, chl - chlorite, epi - epidote, fs - feldspar, qtz - quartz, ser - sericite.

Appendix B. Whole-rock Oxygen-isotope Results for the Huntington Mountain Pluton and East Bay Hills Volcanic Suite

Sample	Rock Unit	[a]Alteration	$\delta^{18}O_{wr}$
Huntington Mountain Pluton			
CBI-8-05-23	Leucogranite	1 - weak	5.9
CBI-6-6-81	Leucogranite	1 - weak	5.8
CBI-6-6-105	Leucogranite	1 - weak to moderate	3.8
CBI-6-6-106	Leucogranite	1 - weak	5.4
[b]EB91-014	Leucogranite	-	7.1
[b]F16C-1582	Leucogranite	-	0.2
CBI-6-6-54	Syenogranite	1 - weak to moderate	6.2
CBI-6-6-55	Syenogranite	1- moderate to strong	1.4
[b]F16C-1631	Syenogranite	-	4.3
[b]F16C-1635	Syenogranite	-	-1.2
[b]F16C-1782	Syenogranite	-	5.5
CBI-8-05-21	Granodiorite	1 - moderate	-
CBI-8-05-22	Granodiorite	1 - moderate	1.2
CBI-8-05-25	Diorite	1 - moderate	2.7
CBI-8-05-26	Diorite	1 - moderate	-
CBI-8-05-27A	Diorite	1 - weak to moderate	-
CBI-8-05-27B	Diorite	1 - weak to moderate	-
CBI-6-6-56	Diorite	1 - moderate to strong	1.7
CBI-6-6-82	Diorite	1 - moderate	3.8
CBI-6-6-83	Diorite	1 - moderate	4.5
CBI-6-6-84	Diorite	1 - moderate to strong	2.2
CBI-6-6-86	Diorite	1 - moderate	3.6
CBI-6-6-87	Diorite	1 - moderate	3.6

Appendix B. Whole-rock O-isotope Results (continued)

Sample	Rock Unit	[a]Alteration	$\delta^{18}O_{wr}$
Huntington Mountain Pluton			
CBI-6-6-102	Diorite	1 - strong, 3 - moderate	1.0
CBI-6-6-103	Diorite	3 - strong	1.9
CBI-6-6-104	Diorite	1 - strong, 3 - moderate	-1.5
[b]F16C-1751	Diorite	-	3.1
East Bay Hills Volcanic Suite			
CBI-8-05-30	Rhyolite	1 - weak, 2 - moderate	6.6
CBI-6-6-17	Rhyolite	1 - weak, 2 - moderate	5.5
CBI-6-6-80	Rhyolite	1 - weak, 2 - moderate	6.9
[b]FS91-53	Rhyolite	-	4.6
CBI-8-05-28	Dacite	1 - strong, 3 - moderate	-2.6
CBI-6-6-98	Dacite	1 - moderate	-0.1
CBI-6-6-99	Dacite	1 - strong	0.6
CBI-6-6-101	Dacite	1 - strong	-3.8
CBI-6-6-93	Andesite to Rhyolite	1 - moderate, 2 weak	1.8
CBI-6-6-94	Andesite to Rhyolite	1 - weak, 2 - weak to moderate	4.1
CBI-6-6-95	Andesite to Rhyolite	-	-
CBI-6-6-96	Andesite to Rhyolite	1 - weak, 2 - weak to moderate	4.0
CBI-6-6-118	Andesite to Rhyolite	1 - weak, 2 - weak to moderate	3.6
CBI-6-6-119	Andesite to Rhyolite	1 - weak, 2 - weak to moderate	3.9
CBI-6-6-121	Andesite to Rhyolite	1, 2 - weak	6.5

Appendix B. Whole-rock O-isotope Results (continued)

Sample	Rock Unit	[a]Alteration	$\delta^{18}O_{wr}$
East Bay Hills Volcanic Suite			
CBI-6-6-50	Andesite	1 - moderate to strong	-0.5
CBI-6-6-51	Andesite	1 - moderate to strong	-0.7
CBI-6-6-52	Andesite	1 - moderate to strong	-0.6
CBI-6-6-89	Andesite	1 - moderate to strong	-1.1
CBI-6-6-90	Andesite	1, 2 - moderate	-1.9
[b]EB87-037	Andesite	-	0.5
CBI-6-6-11	Basalt to Andesite	2 - strong	9.5
CBI-6-6-88	Basalt to Andesite	1 - strong	-1.9
CBI-6-6-110	Basalt to Andesite	1 - strong	0.0
CBI-6-6-111	Basalt to Andesite	1 - weak to moderate	3.3
CBI-6-6-112	Basalt to Andesite	1 - strong	-1.7
CBI-6-6-112A	Basalt to Andesite	-	-
CBI-6-6-112B	Basalt to Andesite	-	-
CBI-6-6-112C	Basalt to Andesite	-	-
CBI-6-6-114	Basalt to Andesite	1 - weak, 2 - moderate	5.4
CBI-6-6-38	Basalt	-	-
CBI-6-6-39	Basalt	1 - moderate , 2 - weak	3.0
CBI-6-6-40	Basalt	1 - moderate, 2 - weak	1.9
CBI-6-6-107	Basalt	1 - weak , 2 - moderate	3.1
CBI-6-6-122	Basalt	2 - moderate to strong	5.7
[b]MT6-397	Basalt	-	6.2

Note: a = alteration types, (1) chlorite, epidote, sericite and Fe-Ti-oxides, (2) quartz, sericite and calcite, and (3) quartz, sericite and pyrite;
b = previously reported by Potter et al. (2008).
Whole-rock $\delta^{18}O$ values are reported in the standard δ-notation relative to VSMOW.

Appendix C. Oxygen-isotope Mineral-Mineral Separation Values

Sample	Rock Unit	$\Delta^{18}O_{qtz\text{-}fs}$	$\Delta^{18}O_{qtz\text{-}chl}$	$\Delta^{18}O_{fs\text{-}chl}$	$\Delta^{18}O_{fs\text{-}hbl}$	$\Delta^{18}O_{hbl\text{-}chl}$	$\Delta^{18}O_{qtz\text{-}ser}$	$\Delta^{18}O_{qtz\text{-}cal}$
Huntington Mountain Pluton								
CBI-8-05-23	Leucogranite	1.2	5.3	4.2	-	-	-	-
CBI-6-6-81	Leucogranite	1.2	7.4	6.2	-	-	-	-
CBI-6-6-105	Leucogranite	0.4	8.1	7.7	-	-	-	-
CBI-6-6-106	Leucogranite	1.8	7.2	5.3	-	-	-	-
[c]EB91-014	Leucogranite	9.1	-	-	-	-	-	[a]6.7
CBI-6-6-54	Syenogranite	0.9	9.1	8.3	-	-	-	-
CBI-6-6-55	Syenogranite	-1.3	6.7	8.1	-	-	-	-
CBI-8-05-21	Granodiorite	-1.6	5.3	6.9	-	-	-	-
CBI-8-05-22	Granodiorite	-1.6	6.7	8.3	-	-	-	-
CBI-8-05-25	Diorite	-	-	3.3	-1.4	4.7	-	-
CBI-8-05-26	Diorite	-	-	4.3	-	-	-	-
CBI-8-05-27A	Diorite	1.0	6.5	5.5	-	-	-	-
CBI-6-6-56	Diorite	-	-	7.7	0.8	6.9	-	-
CBI-6-6-82	Diorite	-	-	3.8	-0.8	4.5	-	-
CBI-6-6-83	Diorite	-	-	0.9	-1.2	2.2	-	-
CBI-6-6-84	Diorite	-	-	-	-1.2	-	-	-
CBI-6-6-86	Diorite	-	-	4.0	1.3	2.7	-	-
CBI-6-6-87	Diorite	-	-	-	-0.7	-	-	-
CBI-6-6-102	Diorite	-	-	-	-0.1	-	-	-
CBI-6-6-103	Diorite	-	-	-	-	-	[a]1.3	-

Appendix C. Oxygen-isotope Separation Values (continued)

Sample	Rock Unit	$\Delta^{18}O_{qtz\text{-}fs}$	$\Delta^{18}O_{qtz\text{-}chl}$	$\Delta^{18}O_{fs\text{-}chl}$	$\Delta^{18}O_{fs\text{-}hbl}$	$\Delta^{18}O_{hbl\text{-}chl}$	$\Delta^{18}O_{qtz\text{-}ser}$	$\Delta^{18}O_{qtz\text{-}cal}$
East Bay Hills Volcanic Suite								
CBI-8-05-30	Rhyolite	1.7	-	-	-	-	-	[b]-2.0
CBI-6-6-17	Rhyolite	-	-	-	-	-	-	[b]1.8
CBI-6-6-52	Andesite	11.4	[a]16.4	5.0	-	-	-	-
CBI-6-6-11	Basalt to Andesite	-	-	-	-	-	-	[a]1.9
CBI-6-6-111	Basalt to Andesite	3.1	-	-	-	-	-	-
CBI-6-6-112B	Basalt to Andesite	-	-	-	-	-	-	[b]-3.8

Note: a = disseminated secondary mineral; b = vein mineral; c = previously reported by Potter et al. (2008).
Calculated $\Delta^{18}O$ values are presented in per mill (‰).
Mineral abbreviations, cal - calcite, chl - chlorite, fs - feldspar, hbl - hornblende, qtz - quartz, ser - sericite.

Appendix D. Calculated Temperature and Composition of the Hydrothermal Fluids in Equilibrium with the Mineral Phases Listed in Table 4.1.

Sample	Rock Unit	T (°C)				$\delta^{18}O_{H2O}$ (VSMOW, ‰)				$\delta^{13}C_{CO2}$ (VPDB, ‰)
		qtz-fs	qtz-chl	fs-chl	qtz-cal	qtz-fs	qtz-chl	fs-chl	qtz-cal	cal
Huntington Mountain Pluton										
CBI-8-05-23	Leucogranite	355	398	414	-	1.2	2.3	2.4	-	-
CBI-6-6-81	Leucogranite	352	270	250	-	1.0	-1.8	-2.2	-	-
CBI-6-6-105	Leucogranite	851	241	186	-	5.5	-4.5	-6.0	-	-
CBI-6-6-106	Leucogranite	225	283	306	-	-3.1	-0.5	-0.1	-	-
CBI-6-6-54	Syenogranite	474	206	167	-	1.7	-6.9	-8.2	-	-
CBI-6-6-55	Syenogranite	-	305	174	-	-	-6.2	-9.4	-	-
CBI-8-05-21	Granodiorite	-	402	216	-	-	-2.8	-5.9	-	-
CBI-8-05-22	Granodiorite	-	304	165	-	-	-5.2	-8.7	-	-
CBI-8-05-25	Diorite	-	-	550	-	-	-	1.6	-	-
CBI-8-05-26	Diorite	-	-	400	-	-	-	0.5	-	-
CBI-8-05-27A	Diorite	414	315	292	-	1.0	-1.5	-1.9	-	-
CBI-6-6-56	Diorite	-	-	186	-	-	-	-7.8	-	-
CBI-6-6-82	Diorite	-	-	463	-	-	-	1.9	-	-
CBI-6-6-86	Diorite	-	-	437	-	-	-	2.2	-	-

Appendix D. Calculated Temperatures and Fluid Compositions (continued)

Sample	Rock Unit	T (°C)				$\delta^{18}O_{H2O}$				$\delta^{13}C_{CO2}$
		qtz-fs	qtz-chl	fs-chl	qtz-cal	qtz-fs	qtz-chl	fs-chl	qtz-cal	cal
East Bay Hills Volcanic Suite										
CBI-8-05-30	Rhyolite	249	-	-	-	-0.8	-	-	-	-
CBI-6-6-17	Rhyolite	-	-	-	229	-	-	-	-0.8	-2.9
CBI-6-6-52	Andesite	-78	71	333	-	-73.5	-13.7	-4.8	-	-
CBI-6-6-11	Basalt to Andesite	-	-	-	218	-	-	-	1.2	-3.9
CBI-6-6-111	Basalt to Andesite	108	-	-	-	-13.3	-	-	-	-

The following fractionation factors were used: Friedman and O'Neil (1977) for calcite-H_2O and muscovite(sericite)-H_2O, Matsuhisa et al. (1979) for quartz-H_2O, O'Neil and Taylor (1967) for alkali feldspar-H_2O, and Wenner and Taylor (1971) for chlorite-H_2O.
Mineral abbreviations, cal - calcite, chl - chlorite, fs - feldspar, qtz - quartz.